Advanced Technologies for Energy Savings in Small Cell Networks

Guangpu Yang

Department of Electronic and Electrical Engineering
University of Sheffield

This dissertation is submitted for the degree of
Doctor of Philosophy

November 2020

I would like to dedicate this thesis and everything I do to my family. I would not be who I am today without their love and support.

Declaration

I hereby declare that except where specific reference is made to the work of others, the contents of this dissertation are original and have not been submitted in whole or in part for consideration for any other degree or qualification in this, or any other university. This dissertation is my own work and contains nothing which is the outcome of work done in collaboration with others, except as specified in the text and Acknowledgements. This dissertation contains fewer than 65,000 words including appendices, bibliography, footnotes, tables and equations and has fewer than 150 figures.

Guangpu Yang
November 2020

Acknowledgements

I am thankful to my supervisors Prof. Jie Zhang and Dr. Xiaoli Chu for their academic suggestions and selfless help during my PhD study. I want to especially thank Prof. Jie Zhang, who not only gave me academic guidance, but also a lot of help in life, and also, Dr. Xiaoli chu, who gave me great support for my study.

I want to thank Dr. Zitian Zhang and Dr. Bowei Yang for their valuable suggestions and guidance. Without their precious help, it would not be possible to conduct this research.

I also want to thank all of my colleagues in the Wireless Communications Group, who gave me the opportunity to enjoy a comfortable PhD study.

Last but not the least, I would like to thank my family: my parents, my wife for supporting me spiritually throughout my life.

Abstract

Since small base station (SBS) deployment is one of key technologies in 4G and 5G to meet the explosive increasing traffic demand, the power consumption problem becomes more serious. To reduce the power consumption of cellular networks, two promising technologies were proposed: one is energy efficient SBS deployment, the other is BS sleeping. For the former one, how to identify the number and the locations of SBSs is open research worth investigation. For the latter, when and which SBS is switched on/off are the core issues. Besides, how to guarantee the Quality of Service (QoS) while BSs are switched off also needs to be considered. This thesis tries to answer these two questions by proposing novel algorithms.

In Chapter 3, the SBS deployment problem is investigated, and novel data-driven methods are proposed in different scenarios and different constraints. Based on existing networks, the aim in this scenario is to uncover the blackspots, improve the coverage probability, and minimizing the power consumption. Based on the Twitter data and k-means, the optimal number of SBSs and the tradeoffs between power consumption and coverage probability is investigated and compared with existing method. For a scenario where existing network is not available or non-existent, the aim is to satisfy users traffic requirements, and minimize the power consumption. A reward function is proposed for this work, then the tradeoffs between power consumption and the percentage of served traffic is investigated compared with existing method. The results in this chapter show the superiority of the proposed methods.

In Chapter 4, a joint sleeping control and bandwidth allocation problem is addressed and formulated as a mixed integer non-linear programming (MINLP) problem subject to the transmission rate requirements. The joint optimization problem is then decoupled into two sub-problems: a centralized bandwidth allocation (CBA) sub-problem that minimizes the power consumption of the system by optimizing the allocated bandwidth of the active SBSs; and a centralized sleeping control (CSC) sub-problem that finds the optimal SBS sleeping strategy among all the possible ones. To solve the CSC sub-problem, two different algorithms are proposed based on K-Nearest Neighbor (KNN) and Convolutional Neural Network (CNN), respectively. For the KNN-based algorithm, the effectiveness of the algorithm is

theoretically proven. The performance of proposed algorithm is evaluated in terms of average total power consumption (APC), percentage of unserved traffic (UR), and the complexity. As to CNN-based algorithm, the CSC problem is transformed to a classification problem and solved by a CNN model. For this algorithm, the CNN model is firstly trained by training data, and evaluated by the testing data. The metrics for this algorithm includes APC, UR, complexity, and accuracy. Simulation results in this chapter show the proposed schemes have superior performance compared with existing approaches.

In Chapter 5, a similar problem to Chapter 4 is considered, while a reinforcement learning based mechanism is proposed to solve CSC sub-problem. By regarding the sleeping strategies as arms, mapping the transmission rate requirements to states, and defining the optimal CBA solution corresponding to a sleeping strategy as the arm's reward function, the CSC sub-problem is transformed to a multi-state multi-arm bandit (MSMAB) problem, and a modified Q-learning algorithm is proposed for solving it. The convergence of the modified Q-learning algorithm is theoretically proven, and the computational complexity of proposed algorithm is theoretically analyzed. Finally, numerical results show proposed mechanism has a low computational complexity and can significantly reduce the total energy consumption of all SBSs, subject to the transmission rate requirements compared with existing methods.

List of Publications

Publications

[1] Bowei Yang, Weisi Guo, Bozhong Chen, **Guangpu Yang**, and Jie Zhang. Estimating mobile traffic demand using twitter. *IEEE Wireless Communications Letters*, 5(4):380–383, 2016.

Submitted

[2] **Guangpu Yang**, Xiaoli Chu, Zitian Zhang, Bozhong Chen, and Jie Zhang. Energy Efficient Centralized Sleeping Control and Bandwidth Allocation for Small Base Stations based on Reinforcement Learning. *IEEE Access*

[3] **Guangpu Yang**, Zitian Zhang, Bozhong Chen, Xiaoli Chu, and Jie Zhang. CNN-based Centralized Sleeping Control and Bandwidth Allocation for Small Base Stations. *IEEE Communications Letters*.

[4] Bozhong Chen, Zitian Zhang, **Guangpu Yang**, Xiaoli Chu, and Jie Zhang. Deep Learning Enabled Prediction of Twitter Traffic with a Regional Granularity. *IEEE Communications Letters*.

Table of contents

List of figures

List of tables

List of Abbreviations

3D	3 Dimension
4G	the 4-th Generation
5G	the 5-th Generation
AP	Access Point
APC	Avearge total Power Consumption
ART	Average Running Time
BB	Baseband
BBU	Baseband Unit
BS	Base Station
CBA	Centralized Bandwidth Allocation
CDR	Call Detail Record
CDSS	Cooperative Distributed Sleeping Strategy
CNN	Convolutional Neural Network
CR	Cognitive Radio
CSC	Centralized Sleeping Control
CSS	Centralized Sleeping Strategy
CV	Computer Vision
D2D	Device-to-Device
DBSCAN	Density-Based Spatial Clustering of Applications with Noise
DL	Downlink
DNN	Deep Neural Network
DSS	Distributed Sleeping Strategy
EE	Energy Efficiency
eNB	eNodeB
FBS	Femto Base Station
GSC	Greedy Sleeping Control
HetNet	Heterogeneous Network
i.i.d.	Independent and Identically Distributed

ICT	Information and Communication Technology
ISD	Intersite Distance
KNN	K-Nearest Neighbor
KPI	Key Performance Indicator
LP	Linear Programming
LPN	Low Power Node
LTE	Long Term Evolution
M2M	Machine-to-Machine
MAC	Medium Access Control
MBS	Macro Base Station
MiBS	Micro Base Station
MIMO	Multi Input Multi Output
MINLP	Mixed Integer Non-Linear Programming
ML	Machine Learning
MSMAB	Multi-State Multi-Arm Bandit
NDSS	Non-cooperative Distributed Sleeping Strategy
NLP	Natural Language Processing
NLU	Natural Language Understanding
NP	Non-deterministic Polynomial
OFDM	Orthogonal Frequency Division Multiplexing
OFDMA	Orthogonal Frequency Division Multiple Access
OSC	Optimal Sleeping Control
OSN	Online Social Network
P2P	Peer-to-Peer
PA	Power Amplifier
PBS	Pico Base Station
QoS	Quality of Service
RAN	Radio Access Network
RB	Resource Block
RBS	Relay Base Station
RE	Ready State
RF	Radio Frequency
RNN	Recurrent Neural Network
RRH	Remote Radio Head
SBS	Small Base Station
SCBA	Sleeping Control and Bandwidth Allocation

SCN	Small Cell Network
SE	Spectral Efficiency
SINR	Signal-to-Interference-Plus-Noise Ratio
SL	Sleep State
SON	Self Organising Network
SPPP	Spatial Poisson Point Process
SSC	Strategic Sleeping Control
UA	User Association
UE	User Equipment
UL	Uplink
UR	Unserved Rate
WiMAX	World Interoperability for Microwave Access

Chapter 1

Introduction

Overview

The data demand for the wireless networks is experiencing an explosive growth. According to a Ericsson study [2], the global mobile data traffic is expected to increase by around five times between 2019 and 2025, from 33 exabytes per month in 2019 to 164 exabytes per month in 2025, shown in Fig.1.1. The annual global mobile data traffic in 2025 will reach almost two zettabytes. Furthermore, the number of mobile-connected devices (including machine-to-machine modules) also experienced a rapid increase. It is expected that the number of mobile-connected devices will be three times of global population by 2023 [8]. The increasing data demand and number of mobile devices both bring new challenges to communication networks.

1.1 Background

1.1.1 Evolution of Cellular Networks

In 1983, an analog mobile cell phone system, Advanced Mobile Phone System (AMPS), which is the first-generation (1G) cellular technology, was officially introduced in the America. Analogue circuit-switched technology and Frequency Division Multiple Access (FDMA) were employed in these systems. The frequency bands in 1G was 800-900 MHz. Only voice calls were allowed at that time with a channel capacity of 30KHz and a speed of 2.4kbps. 1G networks had a poor security, poor voice quality, unreliable handover, low traffic capacity.

In 1991, the second-generation (2G) digital cellular networks were commercially launched in Finland. 2G networks were deployed in different parts of the world through various digital technologies, such as Global System for Mobile Communications (GSM) [9], Digital

Advanced Mobile Phone System (D-AMPS) and Interim Standard 95 (IS-95). Based on digital signalling technology, 2G networks offered bandwidths of 30KHz to 200KHz and enabled highly secure voice, text messages (SMS) and multimedia messages (MMS), as well as limited data services at low speeds, up to 64kbps. 2G introduced two new access technologies: Time Division Multiple Access (TDMA) and Code Division Multiple Access (CDMA). Continuous improvement of GSM technology led to the introduction of General Packet Radio Service (GPRS) and Enhanced Data for Global Evolution (EDGE) to provide mobile data services. GPRS and EDGE are also referred to as 2.5G and 2.75G respectively. They enabled data rates up to 144kbps, and allowed users to send/receive e-mail messages and browse the web [10].

Subsequently, the 3GPP developed third-generation (3G) of mobile networks in 2001. 3G have two key tracks, both of which are based on CDMA technology. The first is Universal Mobile Telecommunications Systems (UMTS), and the other is CDMA2000. UMTS is used to migrate the GSM networks to 3G, while CDMA2000 is used for D-AMPS and IS-95 [11]. UMTS employs Wideband CDMA (WCDMA) as the access method and provides peak downlink speeds of up to 2 Mbps. The UMTS network can achieve data rate enhancements through High-Speed Packet Access (HSPA), which can provide peak downlink speeds of up to 14.4 Mbps. As to CDMA2000, it can provide peak downlink and uplink speeds of up to 153 kbps. The CDMA2000 network achieves data rate enhancements through EVolution Data Optimized (EVDO), which can provide peak downlink speeds of up to 14.7 Mbps. The operating frequency range of 3G is 2100MHz and the bandwidth is 15-20MHz. Based on 3G networks, send/receive large emails and texts, video streaming, fast web browsing become available.

The fourth generation (4G) digital cellular network was officially launched in 2008. 4G is designed to provide users with high speed, high capacity and high-quality service while reducing the latency and improving security. Contrary to previous generations, 4G systems do not support traditional circuit-switched telephone service, but rely on the full Internet Protocol (IP). 4G uses Orthogonal frequency-division multiple access (OFDMA) as the access method, and provides a scalable bandwidths of 5–20MHz. There are two important 4G standards: Long Term Evolution (LTE, widely deployed) and World Interoperability for Microwave Access (WiMAX, now obsolete). LTE is a series of upgrades to the existing UMTS technology. When the device is moving, 4G can provide peak downlink speed of up to 100 Mbps. As to low mobility communication scenarios such as stationary or walking, the peak downlink speed will be up to 1 Gbps [12].

5G is the fifth-generation technology standard for broadband cellular networks, which began to be globally deployed in 2019. 5G is expected to significantly increase data transmis-

sion speed, increase connection density, and reduce waiting time [13]. 5G uses the rarely used radio millimeter wave frequency bands in the range of 30 GHz to 300 GHz range and provides a huge unlicensed bandwidth (up to 7 GHz)[14]. 5G uses OFDMA for the access part and provides a peak downlink speed of 10 Gbps, which is more than 10 times faster than 4G. A comparison of the evolutions of cellular network is summarized in Table 1.1.

Table 1.1 Comparison of different generations of cellular networks

Generation	1G	2G	3G	4G	5G
Period	1983-1991	1991-2001	2001-2008	2008-2020	Upcoming
Frequency	800-900MHz	900/1800MHz	1.6-2GHz	2-8GHz	3-300GHz
Bandwidth	30KHz	30KHz-200KHz	5-20MHz	5-20MHz	100MHz/400MHz
Access	FDMA	TDMA/CDMA	CDMA	OFDMA	OFDMA
Peak Speed	2.4kbps	144kbps	14.4Mbps	1Gbps	>10Gbps
Examples	AMPS	GSM, D-AMPS, IS-95	WCDMA, CDMA2000, TD-SCDMA	LTE-A, WiMAX	5G NR

1.1.2 Introduction of Key Technologies in 4G and 5G

OFDMA

OFDMA is a multi-user version of orthogonal frequency-division multiplexing (OFDM). It is a digital transmission method which encodes digital data on multiple carrier frequencies. By allocating a subset of subcarriers to each user, multiple access can be achieved in OFDMA. which makes simultaneous low data rate transmission from multiple users possible.

The basic concept of OFDMA is: The whole channel can be divided into multiple orthogonal sub-channels. High-speed data signals can be converted into parallel low-speed streams. The low-speed streams can be modulated and transmitted on each sub-channel. At the receiver, the streams can be separated by quadrature signals. Since the channel bandwidth is greater than the relevant signal bandwidth of each sub-channel, it can be regarded as flat fading on each sub-channel, which can eliminate inter-symbol interference. And channel equalization also becomes relatively easy since the bandwidth of each sub-channel is only a small part of the original channel bandwidth [15].

MIMO

Multiple input multiple output (MIMO), which has been widely used in 4G, is a term related to Single-Input Single-Output (SISO), which uses a single antenna at the transmitter and

receiver in 3G networks. MIMO uses multiple antennas at both the transmitter and the receiver to form an antenna system with multiple channels between receiving and sending, so that the signals can be transmitted and received through multiple antennas, thereby improving the communication quality [16]. Without increasing spectrum resources and antenna transmission power, it can double the system channel capacity by making full use of space resources.

It is also known as multiple input single outputs (MISO), when multiple antennas are utilized at the transmitter and a single antenna at the receiver. In this way, the transmit diversity gain can be achieved. Similarly, single input multiple output (SIMO) has multiple antennas at the receiver and a single antenna at the transmitter, resulting a receive diversity gain.

MIMO also faces challenges. The correlations between different channel paths in the MIMO system may degrade the achievable capacity and the channel diversity. To overcome this problem, a minimum spacing between the antennas at the transmitter has to be greater than 10 times of the frequency waves, while it has to be greater than a half of the frequency waves at the mobile ends.

NOMA

All current cellular networks implement orthogonal multiple access (OMA) technologies such as FDMA, TDMA, CDMA, etc. The characteristics of the OMA scheme can be summarized as follows. For FDMA implementations, like OFDMA, each user's information is allocated to a subset of orthogonal subchannels [17]. As to TDMA, each user's information is sent in non-overlapping time slots [17], so TDMA-based networks need accurate timing synchronization, which may bring challenges especially in the uplink. In CDMA, orthogonal codes are utilized to modulate data signals from users in the same frequency channel. NOMA is fundamentally different from the above access schemes which provide users with orthogonal access in frequency, time, code, etc. As to NOMA, each user works in the same frequency band and is distinguished by power level at the same time. Superposition coding is utilized in NOMA at the transmitter so that the successive interference cancellation (SIC) receiver can separate the users in the downlink and uplink channels. According to literature [1, 18], NOMA was also proposed to be a candidate for 5G.

A comparison of the spectrum sharing for NOMA and OFDMA is shown in Fig.1.1. It can be seen that different users use different subchannels in OFDMA, while different users can use the same subchannels.

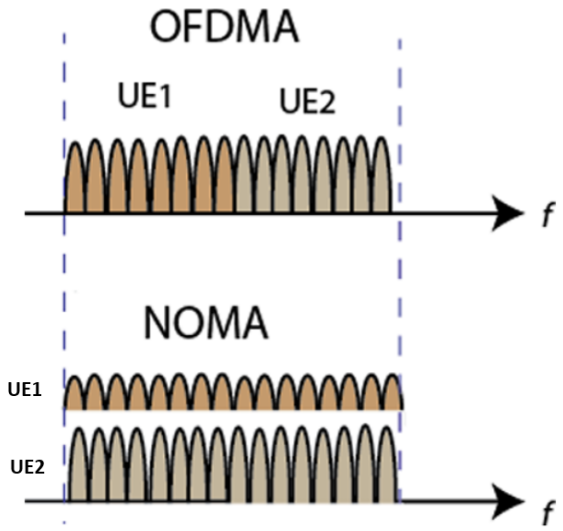

Fig. 1.1 Comparison of OFDMA and NOMA [1].

Massive MIMO

For most MIMO implementations, the BS typically employs only a few (i.e., fewer than 10) antennas, and the corresponding improvement in spectral efficiency is still relatively modest. In this way, massive MIMO were proposed in [19, 20] in order to achieve more dramatic gains, where a lot more antennas, e.g., 100 or more will be equipped with each BS.

There are many advantages for Massive MIMO compared with traditional MIMO. The first one is that it can significantly increase the network capacity due to the increasing number of signal paths resulting from more antennas at the transmitter/receiver. Secondly, with the massive number of antennas at the transmitter, the thermal noise, the effects of fading, and intra-cell interference can all be averaged out, thereby the channel variations decrease and the so-called channel hardening effect appears[21]. Hence, the robustness of massive MIMO is much better than MIMO whose channel varies over time and frequency resulting from small-scale and frequency-selective fading. Thirdly, beamforming will be utilized in Massive MIMO to improve the spectrum efficiency, data rates and latency. Meanwhile, beamforming also enables each antenna to transmit signals only at a low power, thereby increasing energy efficiency and reducing hardware costs.

Since there are so many advantages for massive MIMO, it has been regarded as one of key technologies in 5G.

mmWave

Current wireless networks face a serious problem: More people and devices are consuming more data than ever before, but it is still squeezed on the same radio frequency spectrum that mobile operators always use. This means the bandwidth for everyone is becoming less and less, leading to reduced service speeds and increased connection loss. The problem of global bandwidth shortage has prompted people to explore underutilized millimeter wave (mmWave) spectrum for future cellular networks.

In contrast to the sub-6 GHz frequency bands used in the past for mobile devices, mmWaves are broadcast at frequencies between 30 and 300 GHz. They are called mmWaves because their length varies from 1 to 10 mm, while the length of current radio waves is tens of centimeters. Since this technology can provide up to Gb/s capacity under a huge unlicensed bandwidth (up to 7 GHz), it can be used for high-speed wireless communication [14].

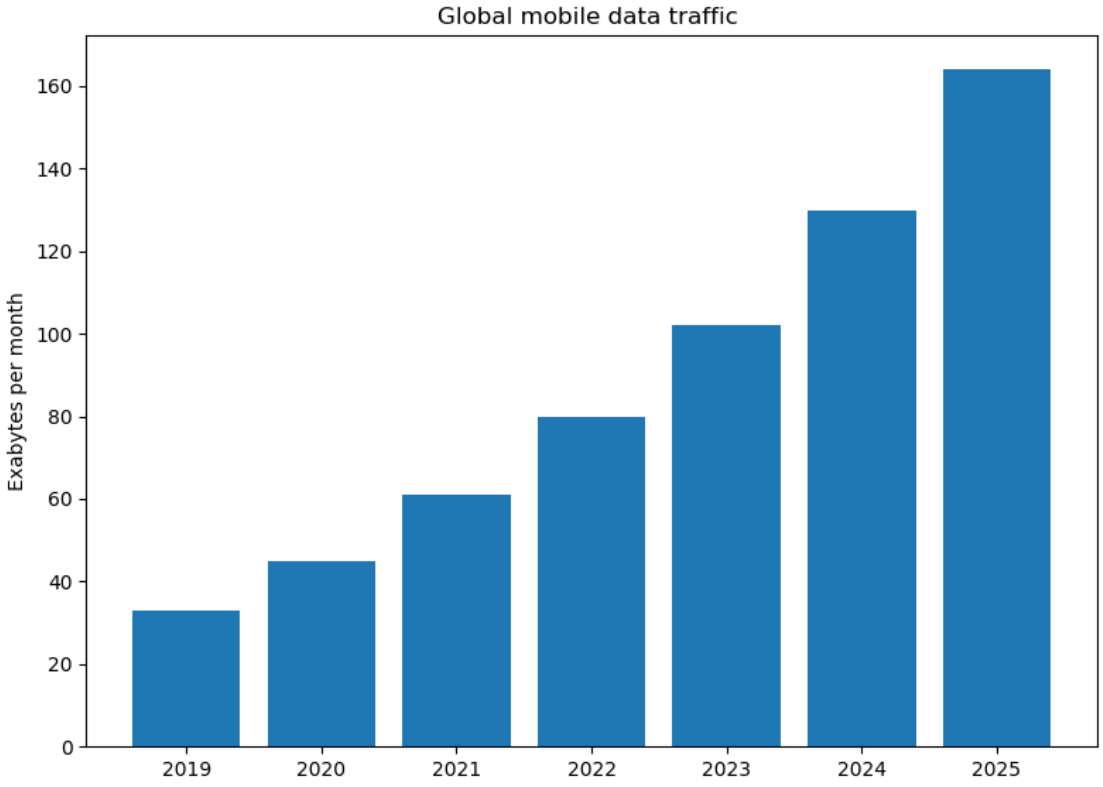

Fig. 1.2 Global mobile data traffic (EB per month) [2]

1.1.3 Heterogeneous network

According to the evolution of communication technology, it can be found mobile operators generally have three methods to improve the capacity and transmission rate: 1) improve the spectral efficiency through coding and modulation in physical layer; 2) increase the spectrum resources; 3) increase the number/density of base stations to improve the transmission rate by shortening the distance between base stations (BSs) and user equipments (UEs), and enlarge the system capacity by frequency reuse. For the first method, the improvements of coding and modulation in physical layer generally means a new generation for cellular network, which may take 10 years or longer. For the second method, the increase of spectrum resources will result to high cost due to the scarcity of spectrum resources and intense competition between mobile operators. Therefore, the third method is the most promising solution for existing networks.

Although deploying macro base stations can increase the system capacity and transmission rate, it faces several challenges: high cost, unbalanced traffic load, poor coverage of edge users, and great energy waste. In this case, LTE standards [22] and WiMAX standards [23] have proposed another solution: based on the existing macro base stations, some low-power nodes (LPNs) can be introduced to expand the system capacity, offload the traffic of hotspots, enhance indoor coverage, improve the quality of service (QoS) of edge users, and improve the energy efficiency. This network architecture composed of macro base stations (MBSs) and low-power nodes (also called small cells/small base stations) is called heterogeneous network (HetNet), while the traditional macro-cellular network is called homogeneous network. For a common HetNet, the MBSs can be used to provide coverage, while small base stations (SBSs) can be used to provide capacity in busy areas such as shopping malls, train stations, and city centers, etc. It is demonstrated that hyper dense HetNets can improve the throughput by 10-100 times [24], and significantly improve the energy efficiency [25–27].

The introductions of different base stations are stated below and summarised in Table 1.2. For ease of description, unless stated, the low power nodes are all referred to as small base stations (SBSs) with respect to MBSs in this thesis.

- MBS: MBS is a high-power BSs that serves conventional cellular networks. MBSs use high transmit power ranging from 5W to 40W to cover large-area macro cells over 30 kilometres [28]. Due to the high transmit power and operating power, air conditioners are usually required for MBSs to cool its surrounding environment to maintain a proper temperature. Considering the huge cost, large sizes, and high-power consumption of MBSs, it is not suitable for large scale MBS deployment. On the other hand, MBSs still have the value of coexisting with future cellular networks due to their

Table 1.2 Characteristics of different base stations

Base Station Type	Transmit Power	Coverage Radius	Scenarios
MBS	43 dBm	$1-35km$	Provide outdoor coverage
PBS	23-30 dBm	$< 300m$	Provide indoor/outdoor coverage and capacity
FBS	20 dBm	$< 50m$	Provide indoor coverage and capacity
RN	30 dBm	$300m$	Provide outdoor capacity and coverage consolidation

wide coverage. MBSs can be used to provide basic coverage in rural areas. Moreover, compared with SBSs, the MBSs require a reduced handover frequency, which has an unparalleled advantage in handling users with high mobility.

- Micro BS and pico BS: Both micro BSs (MiBSs) and pico BSs (PBSs) are simplified MBSs with reduced transmit and operation power, smaller BS size and smaller coverage area. Compared with MiBS, PBS usually provides service for a smaller area (a radius of 200 meters or less) with lower transmit power. However, the differences between them are sometimes unclear. Operators usually carefully plan and deploy them in outdoor or indoor environments with open access to all users. Specifically, for outdoor deployment, the transmit power of PBS ranges from 250 mW to about 2 W, while in indoor situations, it is usually 100 mW or less [28].

- Femto BS: Femto BSs (FBSs) are often used to denote the unplanned indoor nodes which are deployed by consumers according to their needs. The coverage radius of FBSs is 10 to 50 metres, and the transmit power is 100 mW or less [28]. They can be further classified according to whether they allow access to all subscribers. Closed access FBSs only grant access to closed user groups, while the open access FBSs works similarly to PBS. A hybrid method is also possible for which all devices have the access to FBSs, but the designated user group has a higher priority.

- Relay node: The Relay node (RNs) is similar to the PBS, but is usually deployed at the coverage hole or at the edge of a cell to provide coverage consolidation or throughput. The RNs use the air interface spectrum for the wireless backhaul. If the backhaul link and the access link share the same frequency, it will bring challenges to the system. Another method to avoid interference is to use additional dedicated frequencies for wireless backhaul.

1.2 Motivation

1.2.1 Green Communication

To satisfy the explosive growth of traffic demand, mobile operators deployed more and more MBSs, introduced a large number of SBSs, and added supporting facilities such as data centers. According to Global Times, it is estimated that there were approximately 6 million 4G base stations worldwide in 2019 [29], and the number of SBSs is explosively increasing along with the commercial operation of 5G. While providing better service, it also leads to a rapid increase of energy consumption in cellular networks. Research shows that the energy consumption of information and communication technology (ICT) infrastructure is increasing at a rate of 15%-20% per year and accounted for nearly 4% of the total worldwide energy consumption in 2020 [30]. In [31], it has been shown that around 1.4% of global carbon emissions are from cellular networks. On the one hand, the huge energy consumption has brought high costs to cellular operators. On the other hand, the large amount of carbon emissions has a negative impact on the environment, making the greenhouse effect more and more serious. It is of great significance to study how to reduce the energy consumption of cellular networks. This is why green communication has drawn more and more attention recently in both industry and academia. The power proportion for different elements in cellular network is shown in Fig.1.3. It can be found that BSs consume the highest proportion (nearly 60%) of energy in cellular networks [3], while the other elements including mobile switching, core transmission, data center and retail account for approximately 40%. Therefore, optimizing the energy efficiency of BSs and achieving green cellular networks are becoming a necessity to bolster environmental, social and economic sustainability [32, 33].

Generally, there are five technologies to achieve green communication [34]:

- Design and implement new hardware components to improve energy efficiency.
- Optimize the transmission process.
- Introduce renewable energy resources.
- Plan and deploy HetNets.
- Switch off some components of BSs.

The first category aims to improve hardware components (such as power amplifiers) to obtain energy savings [35–38]. Current hardware solutions include high-efficiency power

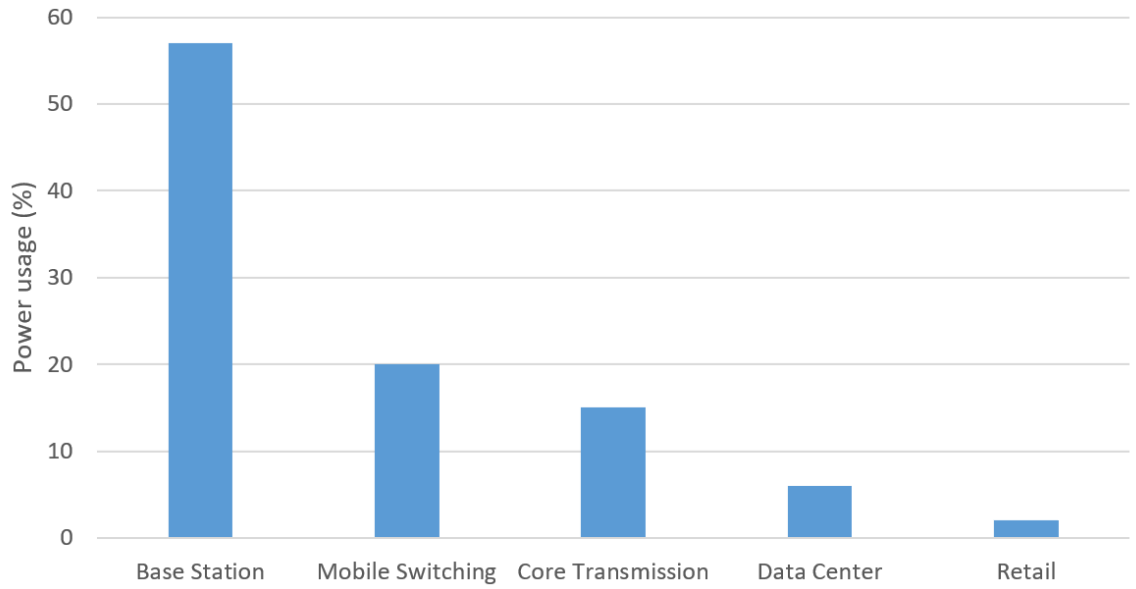

Fig. 1.3 Breakdown of energy consumption in cellular networks (Source: Vodafone [3]).

amplifiers, low-loss antennas, antenna shielding, adaptive sectors, etc. Although these methods can significantly reduce energy consumption, they have the disadvantage of high investment for the hardware replacement and hardware implementation.

As to the second category, renewable energy for power supply has attracted considerable attention from academia and industry in recent years. Compared with the energy widely used at present, such as oil and gas resources that produce greenhouse gases, renewable resources, such as hydropower, wind power and solar power, are sustainable and environmentally friendly [39, 40]. Despite the potential of renewable energy, the safety and stability of renewable energy still face some challenges.

The third category is energy efficiency optimization of wireless transmission, which mainly focuses on physical layer or MAC layer. Current solutions include MIMO technology, cognitive radio, cooperative relay, resource allocation and other technologies[41–47]. This kind of category mainly achieves the purpose of energy saving by improving the utilization of time and frequency, and generally does not need to upgrade the hardware components in the system. These methods need to consider the balance between network energy efficiency and other network performance. Actually, there has been many researches focusing on this field. Various tradeoffs have been studied in the literature, e.g. spectrum efficiency and energy efficiency, bandwidth and energy consumption, and delay and energy consumption [44, 46, 48]. However, since these methods focus on the transmission optimization, the energy savings for this category may be limited.

The fourth category includes microcellular, picocellular and femtocellular network deployment [49–54]. These low-power SBSs serve high-load areas and provide higher data rates by shortening transmission distances. Compared with traditional macrocellular network deployment, one of the main advantages of HetNet deployment is the increased energy efficiency by introducing SBSs [55–57]. However, the deployment of a large number of SBSs still brings additional deployment costs and unexpectable energy consumptions. Therefore, the number and locations of small base stations need to be carefully determined, which motivates the energy efficient BS deployment.

As to the fifth category, BS sleeping is to selectively open and close some components for a period of time (minutes to hours) under some off-peak periods [58–61]. This kind of category usually monitors the network traffic load and then decides whether to switch off (or transfer to sleep mode, also called idle mode or low power mode) or switch on (or transfer to ready mode or active mode) some network elements. The mechanism adopting sleeping mode can avoid unnecessary energy consumption of low-load base stations. The network element involving the sleeping mode can be the power amplifier, the signal processing unit, the cooling device, the entire base station, or the entire network [62]. In most cases, sleeping strategies aim to save energy by selectively shutting down base stations during off-peak periods. The intensive deployment of base stations and random load changes provide strong feasibility for this sleep mode operation.

Although the first three approaches are effective for improving energy efficiency, they have some limitations, such as high investment, unstable, or limited potential. Energy-efficient BS deployment and BS sleeping methods, on the other hand, have great potential for energy savings at the deploying stage and the operating stage of cellular networks. Besides, energy-efficient BS deployment and BS sleeping methods, especially based on social network data and machine learning techniques have not yet been fully investigated. That is why these two categories are the focus of this thesis.

1.2.2 BS deployment

Energy efficient BS deployment is one of key technologies in 4G and 5G, which is promising to uncover blackspots, offload traffic from existing networks, and reduce energy consumption. Existing BS deployment models can be classified as grid based models, stochastic models, and heuristic models, which are summarized below.

- Grid Based Models: Grid based models refer to a class of models where BSs are placed based on 2D grids. The grids can be hexagonal, square, etc. One of the most commonly used grid based models is the hexagonal grid model, which is developed

based on geometrical analysis. Grid based models are widely used by both the industry and the academia to model traditional MBSs for theoretical analysis and simulations [63].

- Stochastic Models: Stochastic models refer to the techniques which employ stochastic geometry to capture the randomness of BS distribution. Stochastic geometry is a mathematical and statistical tool which can provide traceable insights into simulation results [64, 65]. Based on stochastic geometry, the results in simulations generally represent the average over different network realizations. or over multiple BSs or users at different locations. As to a specific BS or user, the results can also be regarded as the expectations weighted by probabilities [64].

- Heuristic Model is a general term for a class of models which determine the locations of BSs by iteratively searching and converging process. Unlike the grid-based models and stochastic models, heuristic models are usually untraceable. Besides, heuristic models generally take environmental conditions into consideration, such as existing networks, user distribution, etc., hence achieve better results in terms of different tradeoffs.

Grid based models and stochastic models were widely used for theoretical analysis computer simulation, network performance prediction, and have achieved remarkable results. However, with the development of communication technologies and the explosive increase of traffic demand, the user distribution, which has an obvious agglomeration phenomenon, has an increasing influence on the BS distribution. These models are not sufficient to capture the traffic demand and the spatial characteristics of BSs in the current cellular networks since these models are based on the assumption that BS is ideal or evenly distributed. It is concluded that SPPP is suitable only in urban and suburban regions but not for dense urban regions [66]. Therefore, the performance of these models for energy efficiency maximization is not good. Heuristic models, on the other hand, can achieve a better performance at the cost of increased complexity. However, existing heuristic models do not consider the accurate user distribution. And the high complexity of existing heuristic models also limits their practicability. In this thesis, these problems are overcame by social network data and machine learning techniques.

1.2.3 BS sleeping

BS sleeping control is widely seen as an effective way to enhance the energy efficiency of mobile networks [41]. For an active BS, about 60% of its energy consumption is due to its

functional modules like the radio frequency (RF) module, the processing module, and the cooling module, etc. [58]. In practice, the distribution of mobile traffic load is extremely uneven in both the temporal and spatial dimensions [67]. Thus, when/where the traffic load is low, the SBS can be set into a 'sleeping' mode by turning off most of the functional modules to reduce the energy consumption [68–70] .

Researchers have proposed various BS sleeping solutions. In [59], the authors proposed two sleeping algorithms for single BS where each single BS decides whether to switch on or off according to its own status. However, due to the lack of coordination between neighboring BSs, these algorithms may degrade the QoS of the network since the BSs in the same region may be switched off at the same time. Neighbor-aware BS sleeping algorithms were proposed in [71–73], where adjacent BSs exchange information and each BS decides its sleeping strategy based on its own and the neighboring BSs' conditions. However, since the information exchange only happens among adjacent BSs, a global optimization cannot be guaranteed in these works. To reach a global optimal sleeping strategy, the authors in [69, 74–76] proposed centralized BS sleeping algorithms, where the BSs in a given region are controlled by a central controller. The controller has the network's global information and determines which BSs are to be switched on or off periodically. Nevertheless, these algorithms are model driven, and their complexity increases significantly as the number of considered BSs expands, which may limit their application in dense networks.

Recent years, the emerging machine learning techniques, including reinforcement learning, deep learning and data analysis are widely used in various fields, and has achieved good performance. Authors in [77, 78] applied reinforcement learning algorithms for BS sleeping, but these approaches have not considered the BS sleeping control jointly with the bandwidth allocation for the active BSs. To the best of author's knowledge, the application of advanced machine learning techniques to energy efficiency BS sleeping is still at a relatively early stage.

In this thesis, different machine learning techniques are introduced to improve the energy efficiency of cellular networks based on BS deployment and BS sleeping, and fill the gaps mentioned above.

1.3 Contributions of the Thesis

In this chapter, the contributions of this thesis are summarised as follows:

- In Chapter 1 and Chapter 2, different energy efficient technologies for green communications are discussed. According to the discussions, it can be found that BS deployment and BS sleeping are promising for energy minimization. The limitations

of existing works for BS deployment and BS sleeping are also discussed in Chapter 2. The high complexity, low accuracy, and relatively poor performance of existing works motivate the author to investigate more efficient methods.

- In Chapter 3, the author propose two novel k-means based SBS deployment methods subject to different constraints based on Twitter data to improve the network performance in terms of power consumption, coverage and capacity. For a HetNet scenario where existing networks provide poor coverage, the proposed algorithm aims to minimize the power consumption while guaranteeing the coverage. For a dense urban scenario, the power consumption can be minimized by proposed algorithm while satisfying the traffic requirements. Simulation results show the performance can be significantly improved by proposed algorithms, with smaller power consumptions and better QoS under different number of BSs.

- In Chapter 4, a joint sleeping control and bandwidth allocation (SCBA) optimization problem is considered, and it is expressed as a mixed integer nonlinear programming problem constrained by the transmission rate requirements. Then the joint optimization problem is decomposed into two sub-problems: the centralized bandwidth allocation (CBA) sub-problem which minimizes the power consumption of the system by optimizing the allocated bandwidth of the active SBSs; the centralized sleeping control (CSC) sub-problem which aims to obtain the optimal SBS sleeping strategy among all possible ones. On the basis of historical datasets, KNN-based algorithm and CNN-based algorithm are proposed to reduce the complexity and achieve good performances. Numerical results show that, compared with other approaches, both algorithms have good performances, and the CNN-based algorithm has a superiority over KNN-based algorithm at the cost of pre-training.

- In Chapter 5, a similar joint SCBA optimization problem is considered. On the basis of few or no historical datasets, Q learning based algorithm is proposed to be trained online. The convergence of the proposed Q-learning algorithm is theoretically analyzed and proved in this chapter. Numerical results for this work confirm the effectiveness of the proposed algorithm with convergence, greater accuracy, smaller energy consumption, greater served rate, and lower computational complexity.

1.4 Structure of the Thesis

The remainder of this thesis is organised as follows:

Chapter 2: Literature Review

In this chapter, an overview of the energy efficiency optimization technologies is given in Sect.2.1, including the introduction of power consumption model of BSs, the traffic patterns and different energy efficient technologies for green communication. In Sect.2.2, the related energy efficient BS deployment strategies are presented, including the grid-based deployment models, stochastic deployment models, and heuristic deployment models. In Sect.2.3, the related energy efficient sleeping strategies are presented, including the distributed sleeping strategies and centralized sleeping strategies. In Sect.2.4, the common used machine learning techniques are introduced, including supervised learning, unsupervised learning, reinforcement learning and deep learning. Finally, the state-of-art related works based on machine learning techniques are introduced In Sect.2.5.

Chapter 3: Data-driven Energy Efficient SBS Deployment

In Chapter 3, data-driven energy efficient SBS deployment methods are investigated. A brief introduction of existing models and the potential of online social network data is given in in Sect.3.1. In Sect.3.2, a HetNet scenario where existing networks provide poor coverage is considered. A data-driven SBS deployment method is proposed to minimize the power consumption while guaranteeing the coverage in this section. The performance evaluation is presented in Sect.3.2.3. Another scenario where existing network is not available or non-existent is discussed in Sect.3.3. The data-driven SBS deployment method proposed in Sect.3.3.2 aims to minimize the power consumption while satisfying the traffic requirements. The performance of proposed method is evaluated in Sect.3.3.3. Finally, a summary of this chapter is given in Sect.3.4.

Chapter 4: Centralized Sleeping Control and Bandwidth Allocation for Small Base Stations Based on KNN and CNN

In Chapter 4, a joint sleeping control and bandwidth allocation problem is introduced and formulated as a mixed integer non-linear programming problem subject to the transmission rate requirements in Sect 4.2. The joint optimization problem is then decoupled into two sub-problems: a centralized bandwidth allocation (CBA) sub-problem that minimizes the power consumption of the system by optimizing the allocated bandwidth of the active SBSs; and a centralized sleeping control (CSC) sub-problem that finds the optimal SBS sleeping strategy among all the possible ones. To solve the CSC sub-problem, two different algorithms based on KNN and CNN are presented in Sect 4.3 and Sect 4.4, respectively. For the KNN-based algorithm, the effectiveness of the algorithm is theoretically proven in Sect 4.3.1, and the

simulation results are given in Sect 4.3.2. As to CNN-based algorithm, the CSC problem is transformed to a classification problem and solved by a CNN model presented in Sect 4.4.1. For this algorithm, the CNN model is firstly trained by training data, and tested by testing data. The comparison of proposed CNN-based algorithm with other approaches, including proposed KNN-based algorithm, are given in Sect 4.4.2. Finally, a summary of this chapter is given in Sect.4.5.

Chapter 5: Energy Efficient Centralized Sleeping Control and Bandwidth Allocation for Small Base Stations based on Reinforcement Learning

In this chapter, the system model and the formulation of the optimization problem is presented in Sect 5.1. Then a reinforcement learning based mechanism is proposed in Sect 5.2. By the transforming the CSC sub-problem to a multi-state multi-arm bandit (MSMAB) problem, a modified Q-learning algorithm is proposed to solve it. The convergence of the modified Q-learning algorithm is theoretically proven. The performance of proposed mechanism is evaluated in terms of various metrics in Sect 5.3. Finally, a summary of this chapter is given in Sect.5.4.

Chapter 6: Conclusions and Future Work

The conclusions of this thesis and the future directions for research are discussed in this chapter.

Chapter 2

Literature Review

Overview

In this chapter, the topics related to energy saving are reviewed. Specifically, an introduction of different energy efficient technologies is provided first, followed by the review of energy efficient BS sleeping strategies, including distributed sleeping strategies, centralized sleeping strategies. Finally, the state-of-art machine learning based related work are presented.

2.1 Review of Energy Efficiency Optimization Technologies

2.1.1 Power Consumption Model

Since BSs accounts for approximately 60% of the total power consumption as shown in Fig. 1.3, a convenient BS power consumption model is required for the simulations of energy reduction researches in different scenarios. Table.2.1. shows different models for different BSs types.

For a base station, the power consumption consists of signal processing, power amplifier, A/D converter, antenna, feeder, power supply, backup battery, cooling etc. Generally, these components can be divided into two parts. The first part is the static power consumption, which is independent of the load situation and is consumed in an idle base station. The second part is the dynamic power consumption, which depends on the load situation. The total power consumption is the sum of these two parts. A simplified block diagram of a BS is shown in Fig.2.1. This diagram can be generalized to different BS types, such as MBS, PBS, FBS, etc.

Table 2.1 Summary of different power models.

Model	Characteristics	References
Ideal MBS model	The BS consumes no power when it is idle.	[69]
Realistic MBS model	The model includes static part and load-dependent dynamic part.	[4, 69, 79–82]
Load-independent SBS model	The power consumptions of BSs are load-independent, and are constant throughout time.	[74, 83]
Load-dependent SBS model	The power consumptions of BSs are load-dependent, and relies on packet size and traffic load.	[84]
General model with sleep mode	The power consumption model is nearly linear, and suitable for different BS types based on different parameters.	[4, 85, 86]

Macro Base Station Power Model

Many models for representing the power consumption of MBSs have been proposed in previous research. In [69], the authors proposed a load dependent power model based on ideal assumptions. This model assumes the power consumption of BS is zero when it is in an idle state, thus the BS only includes load dependent components. The power consumption is formulated as:

$$P_{BS} = \rho P_{TX} \tag{2.1}$$

where ρ and P_{TX} denote the traffic load factor and the transmitted power, respectively.

However, since the power consumption of some components in a MBS is independent with the traffic load, the above model is not realistic. A more sophisticated power consumption model is proposed in [35], which capture captures the power consumption of different components. The formula of this model is given by:

$$P_{BS} = N_{Sector} \cdot N_{PApSec} \cdot (\frac{P_{TX}}{\mu_{PA}} + P_{SP}) \cdot (1 + C_c) \cdot (1 + C_{PSBB}) \tag{2.2}$$

where P_{BS} refers to the total power consumption of BS. N_{Sector} denotes the number of sectors. N_{PApSec} denotes the number of power amplifiers per sector. P_{TX} denotes the transmit power. μ_{PA} refers to the power amplifier efficiency. P_{SP} refers to the power consumption for signal processing. C_c is the cooling loss, and C_{PSBB} is the power supply and battery backup loss.

According to researches [4, 69, 79–82], the model (2.2) can be further simplified to a linear model for convenience. The simplified model can be divided into two parts. The

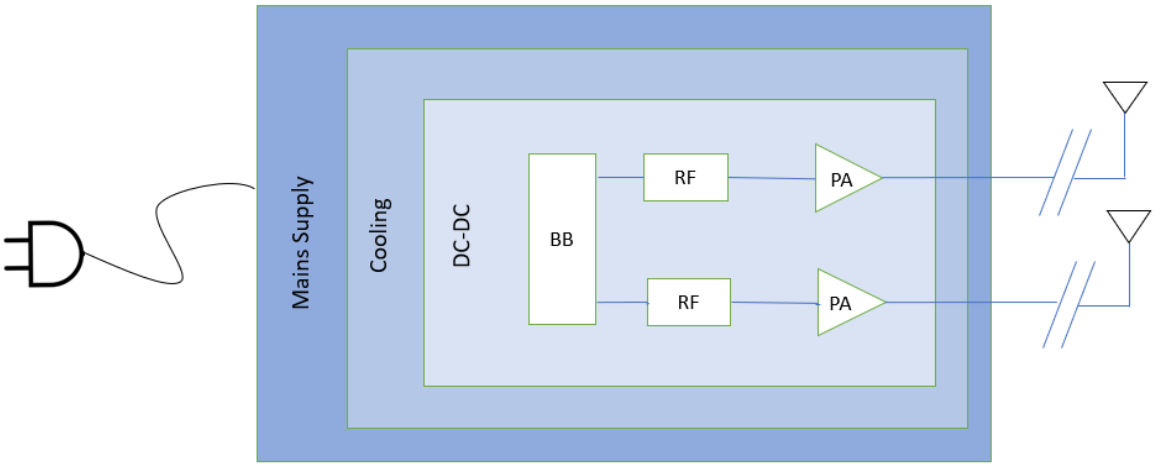

Fig. 2.1 Block diagram of a BS [4]

first part captures the static power consumption which is load-independent. The second part captures the load-dependent power consumption. The linear model is expressed as

$$P_{BS} = \Delta_p \cdot P_{TX} + P_{static} \tag{2.3}$$

where Δ_p refers to the slope of the load dependent power consumption. $\Delta_p \cdot P_{TX}$ denotes the load-dependent dynamic power consumption. P_{static} denotes the load-independent power consumption.

Small Base Station Power Model

In [83], the power consumption model of a SBS is expressed as

$$P_{BS} = P_{mp} + P_{FPGA} + P_{TX} + P_{amp} \tag{2.4}$$

where P_{mp}, P_{FPGA}, P_{TX}, and P_{amp} denote the power consumption of the microprocessor, FPGA, transmitter, and power amplifier. Since the power consumption of each part in (2.4) is constant throughout time, the P_{BS} is a fixed number[74] without any dependence on the cell traffic load.

Experimental results in [84] have illustrated the dependence of the SBS power consumption on the offered load and the data packet size. Hence, the power consumption model for a SBS is given by:

$$P_{BS} = P_{dynamic}(q,s) + P_{static} \tag{2.5}$$

Table 2.2 Parameters for the power models of different BS types

BS type	Δ_p	P_{static} (W)	P_{sleep} (W)
Macro	4.7	780	450
Micro	2.6	112	78
Pico	4.0	13.6	8.6
Femto	8.0	9.6	5.8

where $P_{dynamic}(q,s)$ and P_{static} denote the BS power consumption that relies on the traffic load q (expressed in Mbps) and packet size s (expressed in bytes) and the static power consumption component, respectively.

According to previous research [4, 85, 86], it can be found the relations between cell load and BS power consumption are generally assumed to be linear. By introduce sleep mode, a commonly used power consumption model is given by:

$$P_{BS} = \begin{cases} \Delta_p \cdot P_{TX} + P_{static} \\ P_{sleep} \end{cases} \tag{2.6}$$

where P_{sleep} denotes the power consumption when a BS is switched off. Note that the values of Δ_p, P_{static} and P_{sleep} depend on the BS technology and type. The parameters for different BS types are listed in Table 2.2.

2.1.2 Traffic Pattern

Because of the convergence of user behaviour, the traffic distribution exhibits a strong inhomogeneous character. For example, the total traffic in dense urban area is greatly larger than that in rural areas. According to [5], real traffic profile for one week is presented, shown in Fig.2.2. It can be seen that the traffic load changes periodically within one day or one week. The temporal uneven traffic pattern leads to considerable energy waste in the off-peak periods. Besides, the spatial traffic pattern is also uneven. During the working days, people mainly use mobile phones in urban commercial districts. At night or on weekends, most people are in residential districts. Generally, there are fewer phone calls at night than during the day, but a larger amount of data traffic due to the use of mobile applications, such as social networks, web browsing, video and video chat, etc. Therefore, an accurate and convenient traffic pattern is required to capture the spatial and temporal characteristics of the mobile subscribers and their associated traffic requirements for the simulations of energy reduction researches in different scenarios.

Many studies have been carried out to characterize to the traffic pattern. Generally, the traffic pattern can be characterized in different domains: time domain, and spatial domain. Different models for these two domains will be introduced in this section.

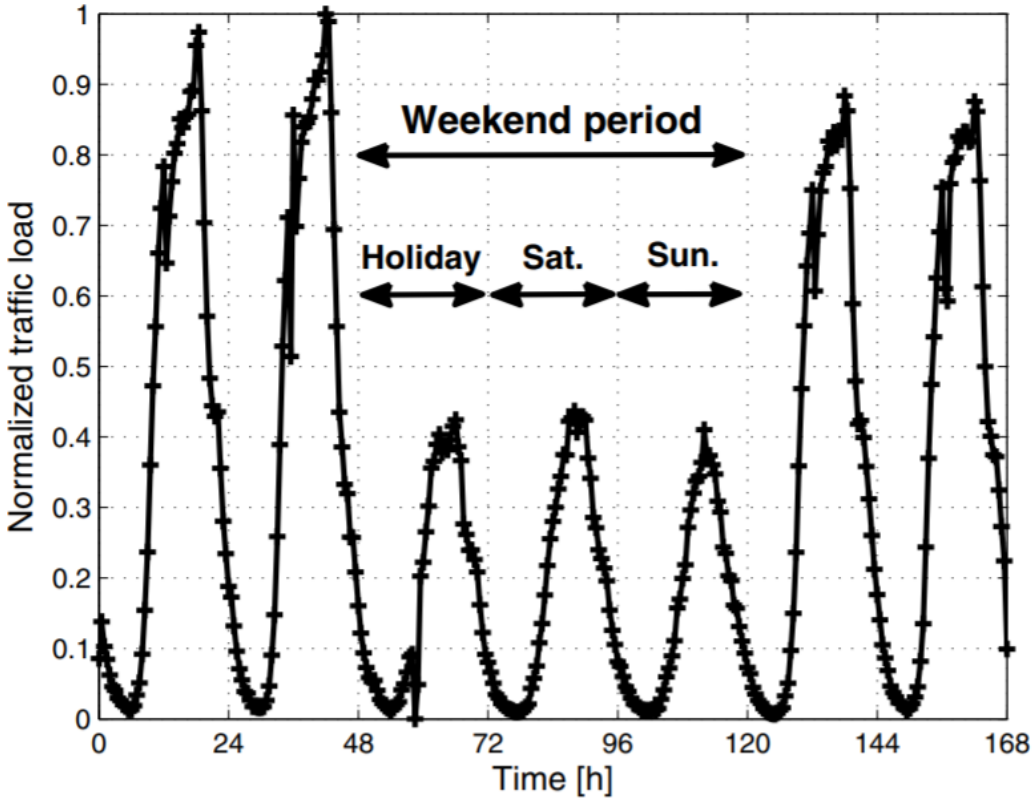

Fig. 2.2 Normalized real traffic load for one week [5]

Temporal Traffic Model

A real traffic profile for one week is presented in Fig.2.2. It can be found the main characteristic of traffic volume in time domain is that it changes with time periodically resulting in low traffic period and high traffic period.

Various methods have been proposed to model the temporal traffic distribution. In [68], the authors propose a trapezoidal model to characterize the daily traffic pattern. With maximum of the model equal to 1 at the peak traffic and different slopes for non-peak one, the proposed model can capture the traffic variation in a day. Since this model is based on ideal assumptions, it is not suitable for long-term traffic distribution modelling. A periodic sinusoidal model is proposed in [87] to represent the traffic profile in multiple days. The different loads in the traffic profile are obtained by adjusting different mean and variance

parameters in the sinusoidal function for the proposed model. Numerical results show this model can achieve a good performance. However, this model is not realistic since it does not take the randomness into consideration. A more practical model is proposed in [88, 89] on the basis of the model in [87]. The authors capture the random fluctuations in the traffic profile by adding a Poisson distributed random process to a periodic sinusoidal model.

Spatial Traffic Model

In spatial domain, the inhomogeneity of traffic distribution can also be captured by different models. Similar to BS deployment, Homogeneous spatial Poisson point process (SPPP) is also widely used to model the users' distribution [90, 91]. The SPPP model can provide tractable insights into theoretical analysis, and it is shown that the SPPP model can capture the randomness of user distribution well. However, along with the development of communication technologies, the agglomeration phenomenon of user behaviour and traffic is becoming more and more obvious. Hence, the SPPP model may be no longer suitable. In [92], an exponential model is proposed to model the traffic density. It is shown that with the decrease of distance from the central urban area, the traffic density increases exponentially based on the traffic data collected in Lisbon and Portugal. In [93], a 2-dimensional Gaussian model is utilized for modelling the user distribution. By adapting the mean values and the standard deviations in this model, the proposed model can output different user distributions, such as hotspot clusters, uniform distribution, etc. The traffic in an urban area is proposed to be modelled by a lognormal distribution in [94]. And in [95], the lognormal model is further verified by comparing with the distribution of real traffic data for different regions. Simulation results show that the lognormal distribution is suitable for spatial traffic modelling.

According to the previous researches, it can be concluded that the uneven spatial characteristics and periodical temporal characteristics of traffic pattern both offer new possibilities for energy efficient solutions, especially for energy efficient BS deployment, and energy efficient BS sleeping.

2.1.3 Energy Efficiency Optimization Technologies

According to the above power consumption model, the energy efficiency optimization technologies can be divided into three categories:

- Improve Δ and P_{static} by designing and implementing new hardware components.
- Reduce P_{TX} by designing energy-aware transmission and resource management strategies.

- Reduce the number or density of base stations in the system through energy efficient BS deployment.
- Reduce the power consumption through BS sleeping.

Energy Efficient Hardware Components

The first category aims to obtain energy savings by improving the energy efficiency of hardware components, such as power amplifiers [36–38, 96, 97], antennas [98, 99], etc.

There are various studies in this field. As to power amplifiers, the authors in [96] employed a breakdown voltage of 27 V to improve GaAs heterobipolar transistors (HBTs). Simulation results show the proposed scheme has a good performance on unthinned wafers. A high voltage InGaP/GaAs HBT technology for 28V operation is reported in [97] with aspect of reliability and device process. In [36], the authors proposed a high-voltage GaAs HBT based power amplifier to achieve linearity and high efficiency. In [37], a high-power Doherty amplifier is proposed to improve the efficiency of a linear amplifier in WCDMA networks. Authors in [38] demonstrate a high linearity and high efficiency power amplifier in a InGaP HBT integrated circuit technology. As to energy efficient antennas, authors in [98] improve the energy efficiency of the networks through antenna sharing, which means distributed radios are coordinated to process transmission. In [99], opportunistic beamforming is employed for dumb antennas to improve the network performance.

Although these methods can reduce energy consumption, they have the disadvantage of high investment for the hardware replacement and hardware implementation. Besides, renewable energy for power supply has attracted considerable attention from academia and industry in recent years. Compared with the energy widely used at present, such as oil and gas resources that produce greenhouse gases, renewable resources, such as hydropower, wind power and solar power, are sustainable and environmentally friendly [39, 40]. Despite the potential of renewable energy, the safety and stability of renewable energy still face some challenges.

Energy Efficient Transmission Optimization

The second category is energy efficiency optimization of wireless transmission, which mainly focuses on physical layer or MAC layer. Current solutions include MIMO technology, cognitive radio, cooperative relay, resource allocation, etc [41–47]. This kind of category mainly achieves the purpose of energy saving by improving the utilization of time and frequency, and generally does not need to upgrade the hardware components in the system. In [42], MIMO and cooperative MIMO based on Alamouti diversity schemes are employed

to minimize the total energy consumption while satisfying given throughput and delay requirements in sensor networks. In [44], the tradeoff between energy efficiency and spectral efficiency, which is named as resource efficiency in this work, is investigated for OFDMA networks. Authors try to maximize the resource efficiency by using water-filling algorithm and provide an upper bound near optimal method to solve the jointly optimization problem. In [45], network cooperation is employed for energy consumption minimization. Simulation results in this work show the effectiveness of proposed cooperation scheme. Besides, the tradeoffs between bandwidth and energy consumption are investigate in [46], while the tradeoffs between delay and energy consumption are studied in [48].

Although the methods for this category is effective for energy savings, this category faces some challenges. According to the discussions, it can be found that the energy efficiency gains are generally obtained at the expenses of the loss of other network performance. Therefore, the balance between energy efficiency and other network performances need to be considered. Besides, the complexity for this kind of category is generally high because of the complicated optimization problem.

Energy Efficient BS deployment

The network deployment includes microcellular, picocellular and femtocellular network deployment [49–54]. These low-power SBSs serve high-load areas and provide higher data rates by shortening transmission distances. Compared with traditional macrocellular network deployment, the main constraint of heterogeneous cellular network deployment is the additional radio jamming brought by a large number of SBSs, which may have a negative impact on the user experience. Meanwhile, the deployment of a large number of SBSs also increases additional deployment costs and energy consumptions. Therefore, the number and locations of small base stations will affect the overall energy consumption and cost of the cellular network. Previous studies have shown that heterogeneous cellular networks have significant gain in energy saving [55–57].

Energy Efficient BS sleeping

BS sleeping is to selectively open and close some components for a period of time (minutes to hours) under some off-peak periods [58–61]. This kind of category usually monitors the network traffic load and then decides whether to switch off (or transfer to sleep mode, also called idle mode or low power mode) or switch on (or transfer to ready mode or active mode) some network elements. The mechanism adopting sleeping mode can avoid unnecessary energy consumption of low-load base stations. The network element involving the sleeping

Table 2.3 Comparison of different energy efficiency optimization technologies

Methods	Examples	Advantages	Limitation	Literature
Hardware components improvements	High-efficiency power amplifiers	Most energy efficient	High cost, difficult implementation	[35–38, 96–99]
Renewable resources	Wind power, solar power	Sustainable, environmentally friendly	Unsafe, unstable	[39, 40]
Radio transmission optimization	Cognitive radio, cooperative relay, resource allocation	Low cost, various applications	Tradeoffs between energy consumption and other performance metrics	[42–47]
Network planning and deployment	HetNet	High potential for energy savings, user-oriented	Additional interference and radio jamming	[49–54].
BS sleeping	Selectively turn on and off some components of a network element	Low cost, easy for testing and implementation	Tradeoffs between energy consumption and other performance metrics	[58–61]

mode can be the power amplifier, the signal processing unit, the cooling device, the entire base station, or the entire network [62]. In most cases, sleeping strategies aim to save energy by selectively shutting down base stations during off-peak periods. The intensive deployment of base stations and random load changes provide strong feasibility for this sleep mode operation.

A summary and comparison between different energy efficiency optimization technologies is given in Table 2.3.

2.2 Review of Energy Efficient BS Deployment

Although the additional deployed BS are able to provide higher data rate, they inevitably incur the increasing the energy consumption. As such, it is imperative to take the energy efficiency into account in the base station deployment stage, thereby reducing energy consumption as well as remaining profitability for network operators. There are various studies working on reducing the energy consumption at the stage of network deployment [63, 70, 86, 90, 100–105]. Generally, the network deployment methods can be categorized into two categories: grid-based models, stochastic models, and heuristic models.

2.2.1 Grid-based BS Deployment Models

Grid based models refer to a class of models where BSs are placed based on 2D grids. The grids can be hexagonal, square, etc. One of the most commonly used grid based models is the hexagonal grid model, which is developed based on geometrical analysis. An example of hexagonal grid model is shown in Fig. 2.3. Grid based models are widely used by both the industry and the academia to model traditional MBSs for theoretical analysis and simulations [63].

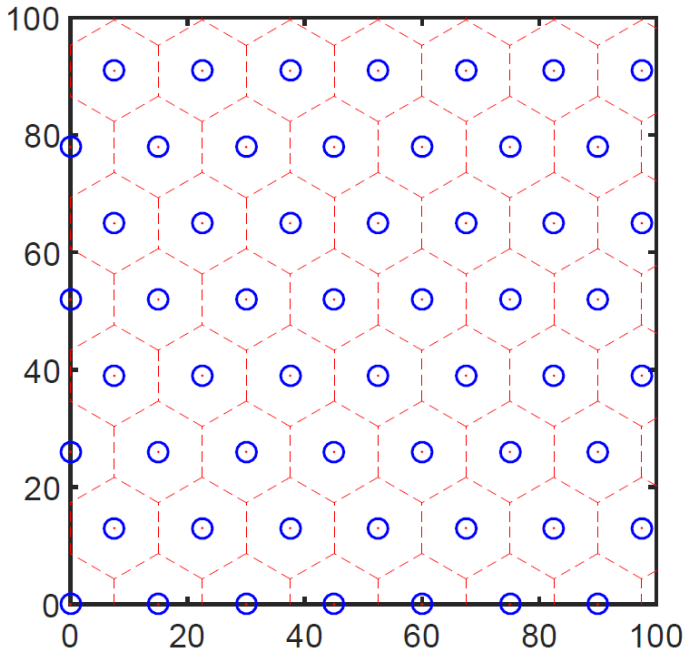

Fig. 2.3 An example of hexagonal grid model.

The benefit of HetNet deployment based on hexagonal grid model is investigated in [102, 103]. It is shown that the proposed model achieves a good performance in terms of different QoS. In [86], the impact of hexagonal grid deployment model is investigated. By deploying different number of SBSs on the existing MBS network, the energy consumption and the capacity are evaluated. Simulation results show the large gain of power savings can be obtained when the traffic load is relatively low. Unlike only considering peak traffic load, the authors in [104] take the traffic variation process into consideration and minimize the energy consumption by a grid based model. Numerical results show the proposed model has superiority over other models. A framework called TANGO is proposed in [70]. In this work, hexagonal grid structure and cell zooming are employed to maximize the energy efficiency of the network while guaranteeing the coverage threshold. In [105], the tradeoff between the system performance and energy efficiency by deploying femtocell in macrocell networks

was investigated. In this work, the macrocell networks was modelled by hexagonal grids, while the femtocells were dropped based on uniform distribution.

The results in the aforementioned papers are mainly based on Monte Carlo simulations by using regular hexagonal grid models. However, the grid models were based on ideal assumptions, which cannot sufficiently capture the randomness in the spatial distribution of BSs, especially for the SBSs such as PBSs and FBSs. To fill the gap, stochastic geometry theory is introduced in cellular networks for network modelling. It is proved that stochastic deployment models are close to that in actual networks[90].

2.2.2 Stochastic BS Deployment Models

Stochastic models refer to the techniques which employ stochastic geometry to capture the randomness of BS distribution. An example of stochastic model is shown in Fig.2.4. Stochastic geometry is a mathematical and statistical tool which can provide traceable insights into simulation results [64, 65]. Based on stochastic geometry, the results in simulations generally represent the average over different network realizations. or over multiple BSs or users at different locations. As to a specific BS or user, the results can also be regarded as the expectations weighted by probabilities [64]. Compared with grid based models, stochastic models usually have a better performance and can characterize more general cellular networks since it can capture the randomness in spatial distribution.

The most commonly used stochastic models is spatial Poisson point processes(SPPP) model [106]. Considering a 2D Euclidean plane $\mathbb{R}$, and a bounded open or closed (or more precisely, Borel measurable) region B of the plane. The number of points N in this region $B \subset \mathbb{R}$ is a random variable, denoted by $N(B)$. The expectation of $N(B)$ can be expressed as:

$$E[N(B)] = \lambda A(B) \tag{2.7}$$

where $A(B)$ denotes the area of the region B. λ denotes a Poisson factor, and $N(B)$ follows Poisson distribution with the intensity $\lambda A(B)$.

The probability of k points existing in region B is thus given by:

$$P_r(N(B) = k) = \frac{(\lambda A(B))^k}{k!} e^{-\lambda A(B)} \tag{2.8}$$

In [90], the authors proposed a tractable homogeneous Poisson point process (PPP) based algorithm to model BS deployment. By comparing with grid based algorithm, it is shown that the proposed algorithm can better capture dense BS deployment in future networks. This work was extended in [107] to optimal BS density design for cellular network planning

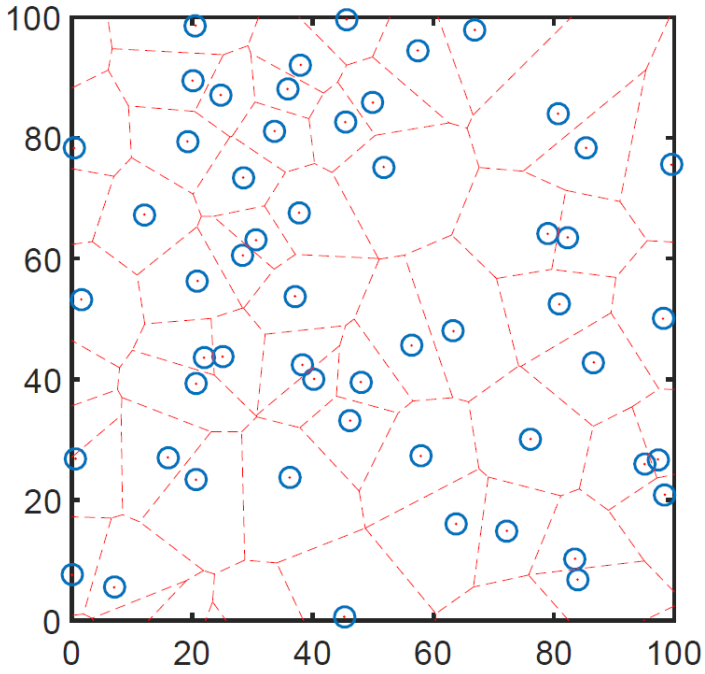

Fig. 2.4 An example of stochastic model.

and dynamic BS sleeping. The study in [80] investigated the energy efficiency of cellular networks by jointly considering homogeneous PPP model and BS sleeping. In [91], the authors investigated the performance of HetNets in terms of coverage probability based on stochastic model, while in [108], the outage probability is evaluated for a stochastic model. In [109], the distributions of the two-tier BSs are modelled by PPPs, and the performance of energy efficiency is addressed but without considering the traffic variation. The authors in [110] developed a K-tier HetNet model whereby the locations of BSs of each tier are assumed to form a homogeneous PPP. The authors in [111] analyzed the minimal BS density with service outage constraint to minimize the network energy cost in HetNets based on PPP model. The authors in [112] investigated the impact of BS deployment, especially BS density on energy efficiency in ultra dense HetNets using the stochastic geometry theory. Simulation results confirm the accuracy and superiority of the proposed model over other algorithms in terms of energy efficiency maximization. The relationship between the QoS and the power consumption was discussed in [113], and the simulations were based on a sum of multiple 2D normal distributions for the femtocell networks. Results showed that the network deployment combining with femtocells offers high QoS and low power consumption.

Based on aforementioned researches, it can be found stochastic BS deployment models can capture the randomness of BS distribution, and provide a tractable insights for simulations and analysis. However, with the development of communication technologies and the

explosive increase of traffic demand, the user distribution, which has an obvious agglomeration phenomenon, has an increasing influence on the BS distribution. Therefore, these models are not sufficient to capture the traffic demand and the spatial characteristics of BSs in the current cellular networks since these models are based on the assumption that BS is uniformly distributed. Heuristic BS deployment models were thus developed in this situation.

2.2.3 Heuristic BS Deployment Models

Heuristic Model is a general term for a class of models which determine the locations of BSs by iteratively searching and converging process. Unlike the grid-based models and stochastic models, heuristic models are usually untraceable. Besides, heuristic models generally take environmental conditions into consideration, such as existing networks, user distribution, etc., hence achieve good results in terms of different tradeoffs.

The authors in [114] aim to minimize the total energy consumption by jointly optimizing the transmit power and micro BS deployment while guaranteeing the area spectral efficiency. Numerical results show the proposed algorithm can achieve a good performance in terms of energy savings. A heuristic BS deployment model is proposed in [115]. In this work, a specific number of BSs is initialized to be located at pre-selected locations, then the locations of BSs are iteratively updated to minimize the outage of the network. Simulation results show that the proposed model works sufficiently well for the testing scenarios. In [116], the authors proposed a heuristic BS deployment method over the existing MBSs to find the appropriate locations of SBSs among the candidates by iteratively choosing the candidates which provides the highest gain in terms of energy efficiency. In [117], a heuristic co-deployment algorithm of micro and macro BSs based on the inhomogeneous spatial traffic modelling was proposed to improve the performance of energy efficiency. The idea of the algorithm is that some SBSs are deployed for providing sufficient capacity with lower power consumption if the MBS cannot satisfy all the traffic demand around it. The authors in [118] proposed a heuristic small cell planning scheme considering different traffic states to maximize the energy efficiency while satisfying the QoS requirements according to the predefined candidate locations for base stations (BSs) in a geographical area.

According to the researches above, it can be found heuristic models can be used to identify potential locations for additional BSs which provide highest gain of the network performance. Compared with grid-based models and stochastic models, heuristic models can achieve a better performance since they take environmental conditions into consideration, such as existing networks, user distribution.

Table 2.4 Comparison of different types of BS deployment strategy

Type	Grid-based Models	Stochastic Models	Heuristic Models
Tractability	Traceable	Traceable	Untraceable
Performance	Poor	Medium	Good
Scenarios	MBS deployment, basis for other simulations	MBS/SBS deployment, theoritical analysis	SBS deployment, maxmize network performance
Literature	[63, 70, 86, 90, 100–105]	[64, 65, 80, 90, 91, 108–113]	[114–118]

2.2.4 Summary

As presented in previous sections, a lot of literature about BS deployment models are reviewed. By categorizing the BS deployment models into grided-based, stochastic and heuristic ones, the characteristics of them are analyzed and compared in Table 2.4. Generally, grided-based models are the simplest models since they assume the BSs are evenly distributed in grids. However, the actual spatial distribution of BSs contains randomness according to realistic conditions, especially for SBSs. Thus, grid-based models are no longer suitable for SBS deployment modelling. Stochastic models, on the other hand, are introduced to fill the gap. These models can capture the randomness of BSs based on the assumption that BSs are uniformly distributed. Besides, stochastic models can provide tractable analytical results and insights for theoretical analysis, which is very important for academia. However, with the development of communication technologies and the explosive increase of traffic demand, the user distribution, which has an obvious agglomeration phenomenon, has an increasing influence on the BS distribution. In this situation, heuristic models, which take environmental conditions into consideration, such as existing networks, user distribution, etc., are introduced. Generally, the complexity of heuristic models is higher, and the results are untraceable. On the other hand, the performance of heuristic models is much better than grid-based models and stochastic models. Note that these three types of BS deployment models can be utilized together for different tier of networks.

2.3 Review of Energy Efficient BS Sleeping Strategies

For network elements involving sleep mode (mainly base stations), they may reside in two states at any given time:

- Ready state (RE): In this state, the network element does not perform energy-saving function, and network element operate normally with all hardware components turned on.
- Sleep state (SL): In this state, some hardware components of the network element are either operated in low-power modes or completely shut down.

It should be noted that the control part of the element will remain active in SL state to ensure the network element can be quickly switched to the RE state when necessary. Based on the above states, a complete sleeping strategy includes two basic processes:

- Sleep Activation: In this process, some hardware components of the network element are either operated in low-power modes or completely shut down, thus achieving the purpose of energy saving. As a result, specific network elements transfer to SL state.
- Sleep Deactivation: In this process, all hardware components in the network element are turned on. As a result, specific network elements transfer from SL state to a RE state.

Researchers have done quite a lot of work on BS sleeping strategies. Based on the controller for sleeping operation in the network, the sleeping strategies are divided into two categories: distributed sleeping strategies (DSS) and centralized sleeping strategies (CSS), in this thesis.

2.3.1 Distributed Sleeping Strategies

Distributed sleeping strategies, also named decentralized sleeping strategies, refer to the sleeping strategies that the sleeping operation of a BS is determined by its own. According to whether BS cooperates with other BSs, the DSS can be further divided into non-cooperative distributed sleeping strategies (NDSS) and cooperative distributed sleeping strategies(CDSS).

Non-cooperative Distributed Sleeping Strategies

NDSS, also called single base station sleeping strategies, refers to a group of sleeping strategies that BSs do not cooperate or exchange information with neighbouring BSs. BSs make the decision of switching on or off by its own status. There are many researches about NDSS considering different tradeoffs or scenarios [59, 119–125].

In [59], the authors jointly optimize power matching and sleeping control considering the energy-delay tradeoffs of the communication system. three sleeping control schemes

are proposed to minimize a cost function which combines the average delay and the power consumption. For each sleeping scheme, the authors give several interesting results about when and where the sleeping scheme can be used for energy saving. In [119], the authors study sleeping control method considering the balance between energy consumption and mean response time, and propose a hysteretic sleep structure. In [120], the authors minimize the total power consumption by jointly optimizing the sleeping control and transmit power for a single BS subject to the delay requirement. The power consumption and delay performance of the proposed algorithm is evaluated based on transmit power and sleeping threshold. In [121], queueing models are utilized to characterize the overall delay and energy consumption for a sleeping BS. Total power consumption considered in this paper includes static power, transmit power, and switch-over power rather than only transmit power, and the overall delay consists of transmission delay and queueing delay. In [122], hysteretic sleep structure and three typical wake-up schemes are considered, and an energy minimization problem based on sleeping strategy subject to delay requirements is proposed. In this paper, the counting or detection cost of a BS during the sleep mode is considered. The works mentioned above mainly focus on the tradeoffs between delay and energy consumption, and homogeneous networks.

In [123], the authors propose a 3-D model based sleeping strategy to minimize the energy consumption of the system. In this work, the sleeping probability of a single small cell is subject to average connection ratio and rate constraints. Different depths sleep mode are introduced in [124]. In this paper, the authors optimize energy efficiency with 'bits/joule' as the metric based on a heterogeneous cellular network model under either a strategic sleeping policy or a random sleeping policy. In [125], according to if any users exist in the coverage of the BS, a two-stage (light and deep) base station sleeping strategy is proposed. The performance of the proposed strategy are evaluated by the average power consumption, the average traffic delay, and the average deep sleeping rate.

Since the BSs make the decisions about switching ON/OFF based on its own status, and the traffic of sleeping BSs will not be offloaded by other BSs for all the existing works mentioned above, the overall network performance cannot be guaranteed, i.e. it is possible that all BSs in a region go to sleep state, leading to a great reduced network performance. Thus, queueing theory and delay tolerable networks are mainly considered for NDSS, and the switching ON/OFF for NDSS is generally activated by certain threshold of number of users or traffic in the queue.

Cooperative Distributed Sleeping Strategies

To improve the network performance reduction problem in NDSS, CDSS are introduced. Generally, CDSS refers to a group of sleeping strategies where the traffic load of sleeping BSs will be served by other active BSs, including BSs in the same tier or different tier. For the implementation of CDSS, extra signalling and information exchange are necessary between cooperative BSs to achieve a good performance. Without information exchange, the network performance can still not be guaranteed because of the same reason for NDSS. Thus, BSs in CDSS generally not only consider its own status, but also consider their neighbors status when they make decisions about switching ON/OFF. Specifically, a BS will only be switched OFF if its traffic load can be served by other active BSs. Based on different types of exchange information, load-aware sleeping strategies where the sleeping operation of a BS is determined on the traffic load of itself and its cooperative BSs [126–130], and distance-aware sleeping strategies where the switching operation of a BS is decided according to their distances to the MBS or UEs [131, 132] are studied in many existing works. In recent years, there has been many researches about CDSS considering different metrics or tradeoffs [133–140, 107, 141–143, 80, 104, 144, 145].

In [133], the authors propose a cooperative sleeping strategy where the macro BS will serve the traffic when micro BS goes to sleep state. The tradeoffs between power consumption and delay are investigated in this paper. In [134], the authors propose two sleeping strategies (random and repulsive strategy) for a hyper-cellular network, where the traffic of sleeping SBSs are served by macro BSs. It is obtained that 50% SBSs can be turned off for the given traffic pattern. In [135, 136], the energy efficiency is optimized by jointly considering SBS sleeping and transmission power management for MBS based on traffic prediction. In [137], the authors propose a traffic prediction based sleeping strategy using Markov Decision Process (MDP) in femtocell networks. The tradeoffs between the energy consumption and blocking probability are investigated in this paper. In [138], sleeping strategies based on different cases of traffic load and user localization information are proposed at flow-level using Markov Decision Process (MDP). The tradeoffs between energy consumption and QoS are investigated in this paper. In [139], the authors consider a separation architecture for the control plane and data plane, and propose a probabilistic sleeping strategy for data base stations to minimize the power consumption by jointly optimizing the sleeping probability and spectrum resource allocation.

All the existing works mentioned above are so called vertical offloading [134], which are based on multi-tier HetNets. For these algorithms, the traffic of sleeping SBSs are served by MBSs. Specifically, a SBS decides to sleep only if its traffic can be handled by MBSs. In

contrast, the algorithms where the traffic of sleeping SBSs are served by neighboring SBSs in the same tier are called horizontal offloading [134], which is discussed in the following part.

In [140], a load based sleeping strategy is proposed based on a separation architecture where the data plane and control plane are separated, and energy gain is investigated as the metrics. In [107], the authors aim to minimize energy consumption by optimizing the BS densities for two-tier HetNet. In this paper, it is shown that by deploying SBSs with sleep mode, the energy consumption can be reduced by 75% compared with tradition macrocellular network. In [141], the authors propose two sleeping strategies, including centralized and decentralized, based on the network traffic. The tradeoffs between energy saving and coverage guarantee are demonstrated. In [142], the authors present two sleeping strategies for which the BS sleeping operation is based on the traffic threshold and the received BS interference level. In [143], a sleeping strategy is proposed to minimize the power consumption subject to certain blocking probability requirements. In [80], the authors aim to maximize the energy efficiency by jointly considering BS sleeping and SBS deployment in different scenarios. And the sleeping strategy in [104] is proposed while the BS deployment is jointly considered based on the whole traffic variation rather than the peak traffic load only. In [144], the authors propose dynamic sleeping strategies based on a simplified traffic model for three different UMTS scenarios. The performance of proposed strategies is evaluated based on different constraints including propagation, link-budget, quality of service guarantees, and electromagnetic exposure. The proposed sleeping strategy in [145] tries to maximize the energy saving by matching the traffic demand with the offered capacity in a flexible manner based on the exchange information about load and coverage.

To summarize, CDSS is regarded as a promising technology for self-organizing networks (SON). Generally, it has a better performance for energy savings without degrading the QoS compared to NDSS. However, the complexity for CDSS is increased because more information is considered for decision-making.

2.3.2 Centralized Sleeping Strategies

Compared with DSS, the decision of BSs' switched ON/OFF in CSS is determined by a central controller rather than itself. By collecting the global information in a region at a given time, a central controller, which can be integrated with a BS, core network, or standalone, analyzes and decides which BS to be switched ON/OFF. Since the global information in the region are fully analyzed, the CSSs have the advantage to reach a global optimum instead of a local optimum for CDSS. Extra signalling between the central controller and controlled BSs are necessary for this type of sleeping strategy. Many researches about CSS considering different system models and metrics are proposed in recent years [73–75, 146–155].

In [73], the authors propose a traffic-aware centralized sleeping strategy associated with clustering problems to maximize the energy savings and show the superiority of the proposed algorithm in low-load situation. In [74], a core network controlled sleep strategy is proposed to minimize the energy consumption of the network. The performance of the proposed algorithm is evaluated with adjusted MBS configuration. In [75], a novel user association scheme for which users are connected to BSs with maximal energy-efficiency rather than maximal RSRP, and a centralized sleeping strategy which minimizes the total power consumption of the network while guaranteeing traffic requirements and ensuring coverage are proposed. In [76], energy minimization problem with multi-objective are investigated in OFDMA networks. The combinatorial optimization problem in this paper is proposed to be solved by a genetic algorithm in a centralized way.

User association and sleeping strategy are jointly optimized for two-tier open access femto networks in [146]. The sleeping strategies of femtocells in this work were controlled by a central femtocell management system. In [147], the authors take the state stability which is defined as the number of state transitions for BSs into consideration and propose a specific centralized sleeping strategy to balance the BS state stability and the energy consumption. A sleeping strategy based on centralized RAN architecture is proposed in [148]. The potential of centralized RAN architecture for energy saving is also investigated in this paper. Also based on centralized RAN, the authors in [149] propose a BBU (baseband unit)-RRH (remote radio head) switching algorithm in a centralized way to minimize the energy consumption. In [150], the authors try to minimize the energy consumption while guaranteeing the coverage based on associated BS sleeping and cell expansion. Then, both centralized and distributed sleeping strategies are proposed and compared in this work. In [151], a QoS aware user association scheme handled by the core network is proposed. Then a heuristic algorithm is proposed considering the tradeoffs between QoS and energy saving. An offline-optimized centralized sleeping strategy that considers the balance between the energy consumption and QoS is proposed in [152]. In [153], load based sleeping strategies, including centralized and distributed strategy, are proposed for delay-tolerant 5G networks considering the tradeoffs of energy consumption and average throughput.

Besides the above researches for radio access networks, centralized sleeping strategies can also be used for cognitive radio network [154], wireless sensor networks [155], etc.

To summarize, CSS is a promising technology for energy consumption minimization under various scenarios. Since the global information is collected and analyzed for decision-making, the performance of it is significant for various tradeoffs, whereas the computation complexity is high.

Table 2.5 Comparison of different types of BS sleeping strategy

Type	NDSS	CDSS	CSS
Interaction overhead	None	High	Medium
Performance	Poor	Medium	Good
Complexity	Low	Medium	High
Literature	[59, 119–125]	[80, 104, 107, 133–145]	[73–75, 146–155]

2.3.3 Summary

As presented in previous section, a lot of literature are reviewed. By categorizing the sleeping strategies into centralized and distributed ones according to whether the BS sleeping operation is controlled by itself, the characteristics of them are analyzed and compared in Table 2.5. Generally, NDSS has the lowest computation complexity, since it only considers the information from itself. Meanwhile, the performance of this type of sleeping strategy is relatively poor because it may cause coverage holes when multiple BSs in the same region go to sleep state at the same time. CDSS, on the other hand, is an improved technology to improve the network performance during BS sleeping period by offloading the traffic of sleeping BSs to other active BSs. To guarantee a better performance, information exchange between cooperative BSs are necessary which leads to extra signalling. Besides, the complexity increases compared with NDSS since a lot more information from cooperative BSs need to be analyzed. For CSS, BS sleeping operation is controlled by a central controller, which can be standalone, or integrated with existing network elements, such as core network, MBSs. The central controller in this type of sleeping strategy collects the global information from its controlled BSs and determines how many and which BSs can be switched OFF by analyzing the global information. Thus, the computation complexity for CSS will be high when the number of the BSs handled by a central controller is large. On the other hand, since the information exchange is not required for CSS, it has a lower interaction overhead compared to CDSS [150]. Besides, the performance for CSS is generally the best, since it can reach a global optimum rather than local optimum in CDSS.

2.4 Machine Learning Techniques

As the era of big data arrives, machine learning (ML) [156] has attracted more and more attention from academia and industry. Tom M. Mitchell gave a widely quoted definition of machine learning in his book [157] by: “A computer program is said to **learn** from experience E with respect to some class of tasks T and performance measure P, if its performance at

tasks in T, as measured by P, improves with experience E." According to the definition of machine learning, the experience E, also known as training data, is acquired for the learning process. Based on the learning process, the machines can acquire new knowledge or update existing knowledge like human beings.

The development process of ML is generally divided into three stages:

- First stage(mid-1950s to the mid-1970s): During this period, people tried to control computers to complete a series of logical reasoning functions through software programming, thus making the computer have a certain degree of intelligent thinking ability as human beings. The representative work at this stage includes: Samuel's checkers player, which is the world's first successful self-learning programs and now known as reinforcment learning, the invention of perceptron [158] which is the foundation of neural network (NN) and support vector machine(SVM), automatic differentiation (AD) which is corresponding to the modern version of backpropagation (BP). Despite many exciting discoveries in this period, the results in this period were far from meeting people's expectations. Researchers began to believe that a large amount of prior knowledge is necessary for making machines intelligent. Besides, several fundamental limits that could not be overcome at that time were encountered in late 1970s, including limited computer power[159], common sense knowledge and reasoning[160], intractability and the combinatorial explosion[161], etc. Thus, it went to the first AI winter.

- Second stage(mid-1980s-late-1980s): In this period, people tried to use the rules extracted from their own thinking to "teach" computers to execute decision-making mechanism. The representative work at this stage is various expert systems, the discovery of Hopfield networks (a type of recurrent neural network) [162], and the proposition of backpropagation (also known as the reverse mode of automatic differentiation)[163]. However, these expert systems always face the problem of sparse knowledge, that is, in the face of endless knowledge and information, people cannot summarize the rules that are foolproof. Therefore, the idea of autonomous learning by machines naturally surfaced.

- Last stage(late-1980s-present): Due to the emergence of big data and hardware GPU during this period, machine learning has broken away from the bottleneck period. Machine learning has begun to develop explosively and has become an independent and popular subject which has been applied to various fields. Various machine learning algorithms are constantly emerging, and deep learning are further developed.

According to the definition of machine learning, the experience E, also known as training data, is acquired for the learning process. Machine learning is generally divided into supervised learning and unsupervised learning according to whether there is artificial labelling of the training data. In addition, the reinforcement learning and deep learning are regarded as independent branches of machine learning in this work due to their rapid development.

2.4.1 Supervised Learning

For supervised learning, the training data is labelled, which can be data categories, data attributes and feature point locations, etc. These labels are used as the expected results for machines to continuously correct the predicted results. The specific process for a supervised learning method with a large number of labelled data is: 1) predict results based on given model and given parameters; 2) compare the predicted results with the expected results; 3) update the parameters of the model based on the comparison results, then to step 1. The process will repeat until converge. Finally, a model with certain robustness to achieve the ability of intelligent decision-making will be generated. Typical algorithms of supervised learning include regression, K Nearest Neighbors (KNN), Support Vector Machine (SVM), etc.[164].

Regression

In statistics, regression refers to a statistical analysis method that determines the relationships between two or more variables. According to the type of dependent variables, regression can be further divided into linear regression, and logistic regression.

- **Linear regression**: In this method, the dependent variable is continuous, the independent variables can be continuous or discrete, and the property of the regression line is linear. For more than one independent variables, it can also be called multiple linear regression [165], while it is called simple linear regression when the number of independent variables is one. Linear regression models are usually fitted by least squares approach to establish a relationship between dependent variable and one or more independent variables. Generally, linear regression is widely used for prediction or forecasting [166].

- **Logistic regression**: In this method, the dependent variable is discrete (usually binary), the independent variables can be continuous or discrete. For a implementation of binary logistic regression, a sigmoid function can be added to a linear regression, thus transfer

continuous results to a binary one. Generally, logistic regression is widely used for classification in various fields [167].

Since the principle of regression is quite basic, it has been the foundation of many other machine learning techniques, such as convolution neural network.

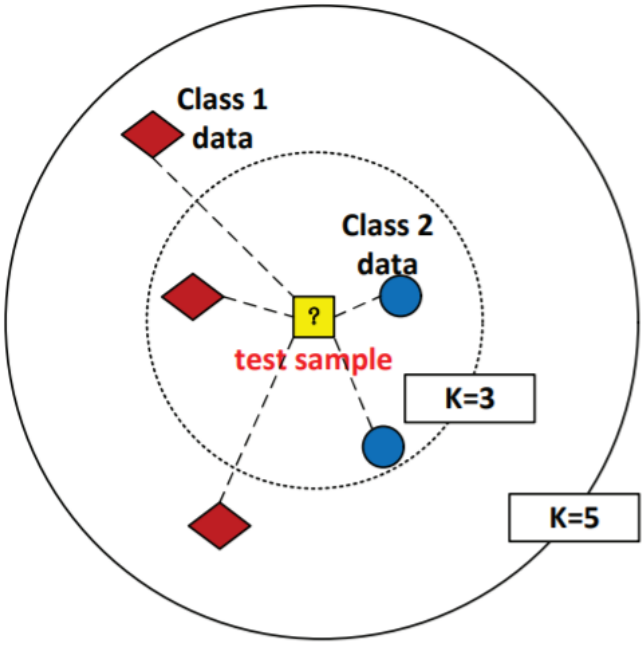

Fig. 2.5 An illustration of the KNN model [6]

K Nearest Neighbors

K Nearest Neighbor (KNN) algorithm is a nonparametric lazy learning algorithm for classification and regression. It does not need to make assumptions about data distribution. In KNN classification, the output is a class label which can be obtained by the most common class label of its K nearest neighbors through voting. An example of KNN classification is shown in the Fig 2.5. If $K = 1$, then the class of the test sample will be the class of its nearest neighbor. When $K = 3$, the label of the test sample in Fig 2.5 will be 2, since there are two samples of class 2 in its K-neighborhood. Similarly, when $K = 5$, the label of the test sample in Fig 2.5 will be 1. As to KNN regression, the output of the test sample will be a value which can be obtained by the average of the values of k nearest neighbors. Consider that the nearer samples have a greater influence on the test sample, the KNN algorithm can be modified by adding a weight factor which is inversely proportional to the distances between

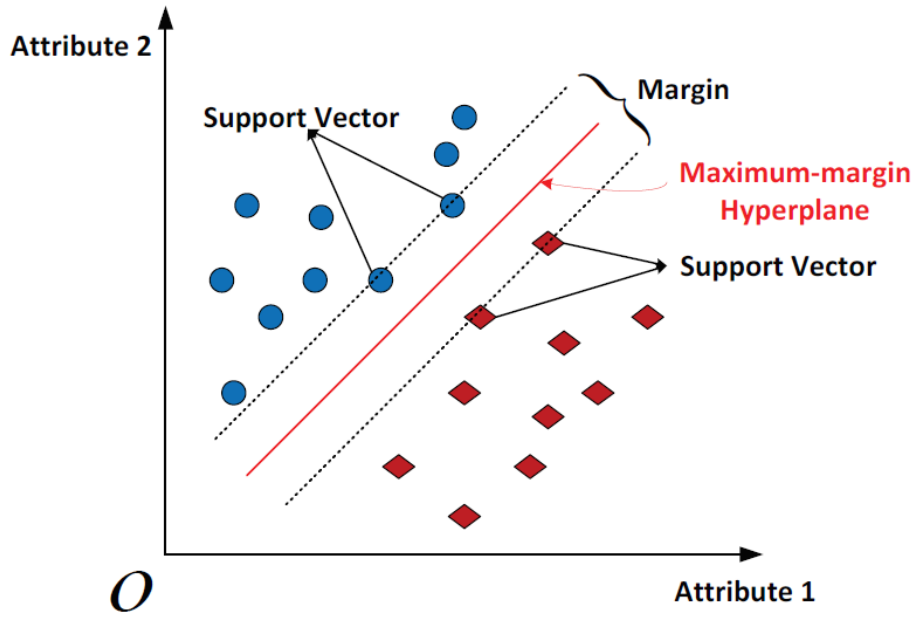

Fig. 2.6 An illustration of a basic SVM model [6]

the neighbors and the test sample. Meanwhile, parameter K is the most important factor in KNN, which can significantly affect the performance of KNN algorithm [168].

Support Vector Machine

The basic model of Support Vector Machine (SVM) is a linear classifier whose purpose is to separate data points into p-dimensional vectors using $p-1$ hyperplanes, which is illustrated in Fig. 2.6. The best hyperplane is called maximum margin hyperplane which results in the maximum distance or margin between two given classes. However, datasets in the original space are usually not linearly separable. To classify the non-linear datasets, kernel functions, such as Gaussian kernels or polynomials can be employed to transform the original space to a higher dimensional space. More details about SVM can be found in [169].

2.4.2 Unsupervised Learning

Contrast to supervised learning, unsupervised learning [170] refers to a group of machine learning techniques where the training data is unlabelled. Unsupervised learning is mainly used to find or capture the unknown patterns in training data without need of manual intervention. A typical algorithm of unsupervised learning is clustering which includes k-means, density-based spatial clustering of applications with noise (DBSCAN), etc.

k-means clustering

k-means clustering is a popular data analysis method based on vector quantization. It is developed originally from signal processing. Given a set of observations $(x_1, x_2, ..., x_n)$, where each observation is a d-dimensional real vector, *k*-means is aiming to divide the n observations into k clusters $C = \{c_1, c_2, ..., c_k\}$ so that the minimization of the within-cluster sum of squares (WCSS) [171] can be got. The WCSS formula is shown below:

$$\min \sum_{i=0}^{k} \sum_{x \in c_i} ||x - \mu_i||^2 \tag{2.9}$$

where μ_i is the mean of observations in cluster c_i .

In *k*-means algorithm, k centroids are firstly initialized to define clusters by randomly selecting from the n observations. Then, each observation is allocated to a particular cluster when it is closest to that cluster's centroid. After the allocation, the k centroids are updated by the means of the observations in different clusters. The k centroids will converge and reach the best by iteratively executing allocation process and updating process.

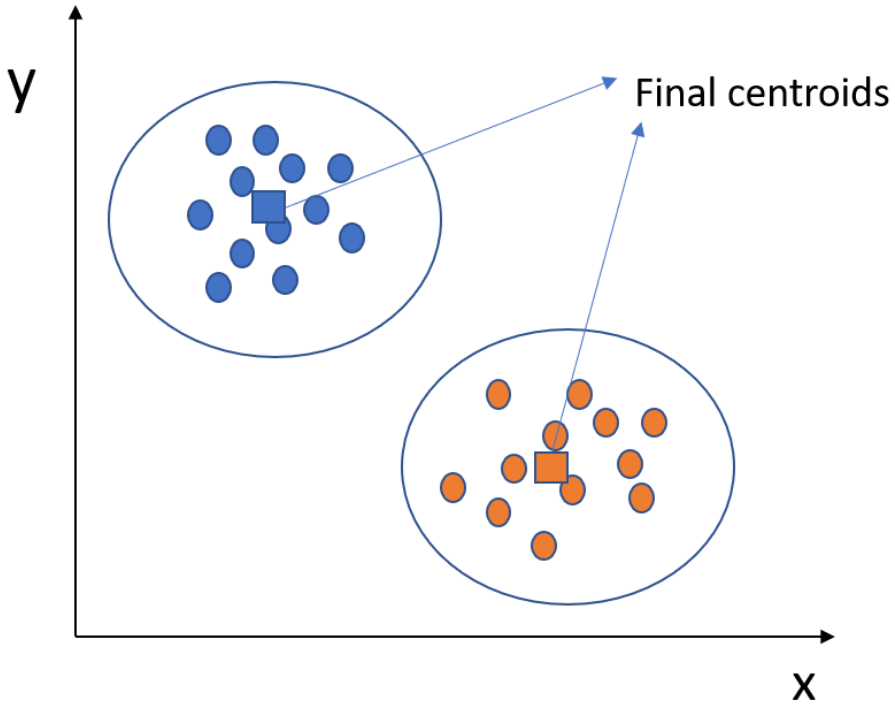

Fig. 2.7 An example of *k*-means algorithm

DBSCAN clustering

Similar to k-means algorithm, DBSCAN is another common clustering algorithm proposed in 1996 [172]. Compared with k-means, DBSCAN is a clustering algorithm based on density rather than spatial extent. The basic concept of DBSCAN is: given a set of points in some space, it groups points that are closely packed together (points with many nearby neighbours), marking as outlier points that lie alone in low-density regions (whose nearest neighbours are too far away). There are three inputs in DBSCAN algorithm, including database and two adjustable parameters: distance eps and minpoints $MinPts$.

For the purpose of DBSCAN clustering, the input database can be classified into three categories: core points, boundary points and noise points following the below rules:

- A point a is a core point if there are at least $MinPts$ points within distance eps from point a including itself. The distance eps represents the radius of the neighbourhood from a. And those points within distance eps from point a are called to directly density-reachable from a.
- Given a path $p_1,...,p_i,...,p_n$ with $p_1 = a$ and $p_n = b$, point b is said to be density-reachable from point a if each p_{i+1} is directly density-reachable from p_i. And each p_i must be core points except point b. If point b isn't a core point, it is said to be a boundary point.
- A point c is said to be a noise point if it is not density-reachable from any other points.

The aim of DBSCAN algorithm is to find the largest dataset of density-reachable points. An example of those points is shown as follows:

Given the distance $eps = 3$, $MinPts = 3$, and dataset $D = \{o, p, q, s, m, p_1, p_2, m_1, m_2, s_1\}$. The neighbourhood of point p is $\{m, p, p_1, p_2, o\}$. The neighbourhood of point m is $\{m, q, p, m_1, m_2\}$. The neighbourhood of point q is $\{q, m\}$. The neighbourhood of point o is $\{o, p, s\}$. The neighbourhood of point s is $\{o, s, s_1\}$.

Then the core points in dataset D is $\{p, m, o, s\}$ (point q isn't a core point since the number of points in its neighbourhood is smaller than eps); Point m is directly density-reachable from point p since it is contained in the neighbourhood of point p and point p is a core point; Point q is density-reachable from p because point q is directly density-reachable from point m and point m is directly density-reachable from point p. An example of DBSCAN algorithm is shown in Fig.2.8.

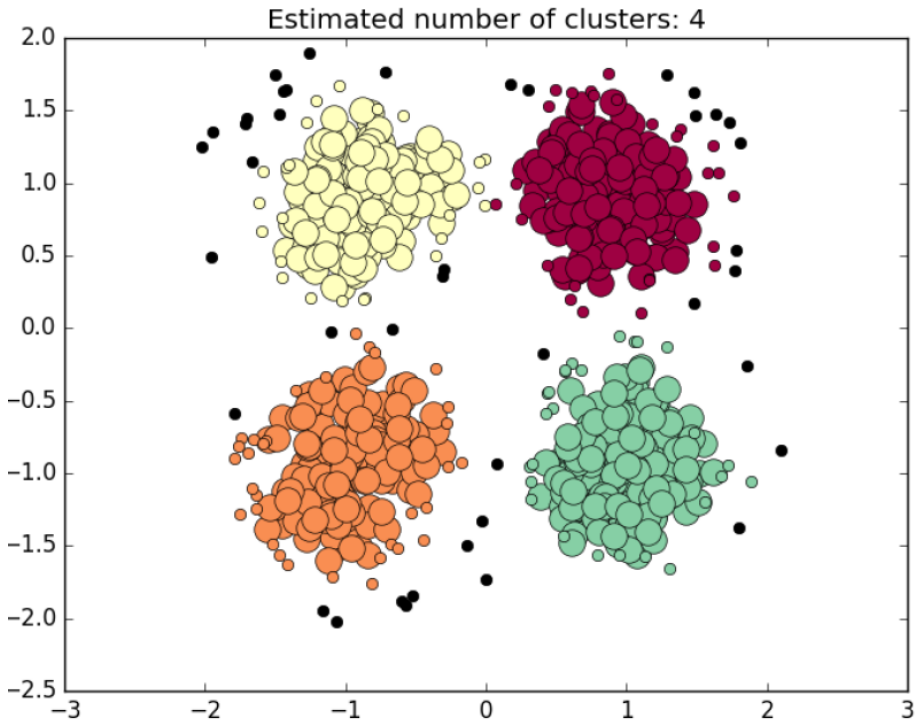

Fig. 2.8 An example of DBSCAN algorithm

2.4.3 Reinforcement Learning

Reinforcement learning [7] is a group of machine learning techniques which simulate the learning process of human beings. A basic diagram of reinforcement learning is illustrated in Fig.2.9. For reinforcement learning, an agent can learn by trial and error through interacting with the environment. Specifically, the agent observes a state s from the environment and takes an action a based on the accumulated knowledge from historical learning and a specific action selecting policy. After the action a is carried out, the environment will give the agent a reward r, then go to the new state. After enough iterations, the agent can learn which action is the best for a specific state to achieve a goal, such as maximizing the instantaneous reward in this iteration or the accumulative rewards in some future successive iterations. Typical algorithms for reinforcement learning include Q-learning, actor-critic, etc.

Q-learning

One of the most commonly adopted reinforcement learning algorithms is Q-learning. In iteration t, the agent observes the state S_t from the environment, and takes an action A_t based on the accumulated knowledge from historical iterations and a specific action selecting policy. After the action A_t is carried out, the environment will be transformed into a new state S_{t+1},

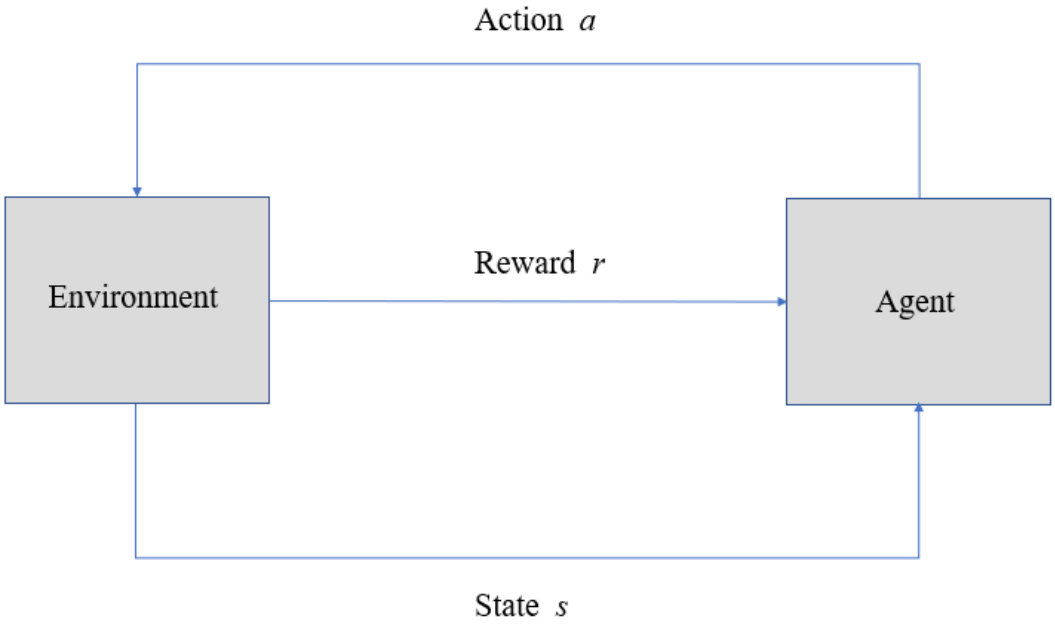

Fig. 2.9 A basic diagram of reinforcement learning[7].

and give the agent a reward R_{t+1}, which may be affected by the state transformation and action adopted by the agent. After enough iterations, the agent can learn which action is the best for a specific state to achieve a goal, such as maximizing the instantaneous reward in this iteration or the accumulative rewards in some future successive iterations. The key concept of Q-learning is a Bellman equation for Q value iteration update, using the weighted average of the old value and the new information:

$$Q^{new}(s_t,a_t) \leftarrow Q^{old}(s_t,a_t) + \alpha * (r_t + \gamma \cdot \max_a Q(s_{t+1},a) - Q^{old}(s_t,a_t)) \tag{2.10}$$

where r_t is the reward received when moving from the state s_t to the state s_{t+1}, and α ($0 < \alpha \leq 1$) and γ is the learning rate and discount factor, respectively.

Note that $Q^{new}(s_t,a_t)$ is the addition of three factors:

- $(1-\alpha)Q^{old}(s_t,a_t)$: the current value weighted by the learning rate. Values of the learning rate near to 1 made faster the changes in Q.
- αr_t: the reward $r_t = r(s_t,a_t)$ is obtained if action a_t is taken when in state s_t (weighted by learning rate).

- $\alpha\gamma\max_a Q(s_{t+1},a)$: the maximum reward that can be obtained from state s_{t+1} (weighted by learning rate and discount factor).

More details about Q learning can be referred to [7]. In addition, to handle continuous state spaces, fuzzy Q learning can be used [173].

2.4.4 Deep Learning

Deep learning [7] was a development of neural network at first. In recent years, with the introduction of supervised learning and unsupervised learning, deep learning has been used to refer various machine learning models based on multi-layer network structures, through which more complex functional relationships can be realized. Generally, deep learning takes the original observation data as input, and carries out step-by-step feature extraction and transformation through the multi-layer model to realize more effective feature representation. On this basis, a shallow model, such as Softmax classifier, multi-layer perceptron (MLP) neural network, SVM, etc., is often connected at the last layer to achieve better classification performance. Deep learning has been applied to various fields including computer vision (CV), pattern recognition, natural language processing (NLP), etc. Typical models for deep learning include deep neural networks (DNN), recurrent neural networks (RNN) and convolutional neural networks (CNN). In the field of energy efficiency optimization, deep learning is often associated with reinforcement learning, forming deep reinforcement learning [174–176], to reduce the training complexity of traditional reinforcement learning models.

Deep Neural Network

Deep neural network (DNN) is a neural network with multiple layers between the input and output layers, shown as Fig. 2.10. The basic component of a DNN is a neuron corresponding with weights for the input and an activation function for the output. The input in DNN is transformed from the input layer to hidden layers, and then to output layer. There is no direct connection between two non-adjacent layers, while the adjacent layers are fully connected. It means any neurons in layer i must be connected to any neurons in layer $i+1$. Take a neuron in layer $i+1$ as an example. The input for this neuron can be expressed as:

$$z = \sum w_i x_i + b \tag{2.11}$$

where x_i denotes the output from neurons in layer i, and w_i refers to the corresponding weights. b is a bias.

Since (2.11) is a linear equation, activation functions, such as tanh, Relu, etc., are applied to model complex non-linear relationships. Thus, the output of this neuron can be represented by $\sigma(z)$. For the parameter optimization, backpropagation together with different gradient descent (GD) methods such as Adam, Momentum, etc. can be employed [177].

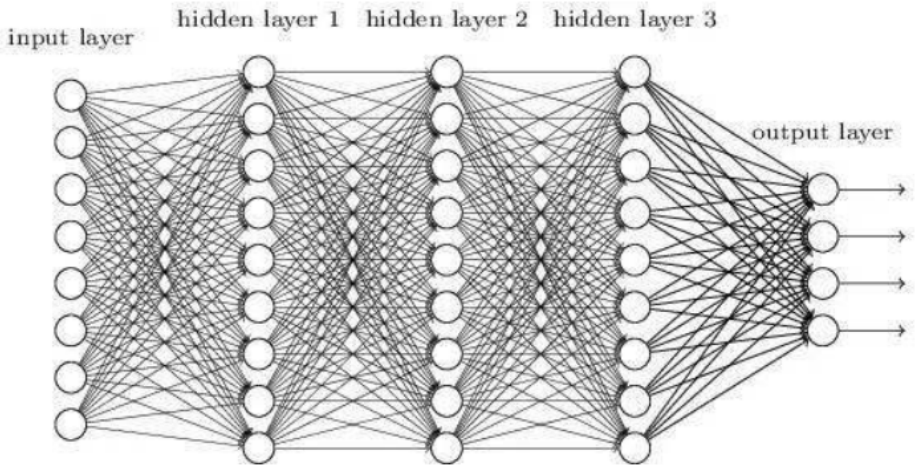

Fig. 2.10 The architecture of a DNN [7].

Convolutional Neural Network

CNN is a class of deep neural network which is particularly suitable for learning tasks with large dimensions of input features. Due to the deep neural network structure and the sharing of neuronal connection weights, CNN can capture the complex dependencies at different levels from input features and significantly reduce the complexity in training process.

An illustration of CNN is shown in Fig.2.11. the CNN consists of convolutional layers, pooling layers, and a fully connected hidden layer. In each convolutional layer, convolution filters are used to produce feature maps for each input map of this layer. Convolutional layer is followed by a pooling layer, which reduces the dimensions of feature maps by sub-sampling them with pooling kernels, in order to combat overfitting as well as shorten the training complexity. By stacking convolutional layers and pooling layers alternately, the CNN can learn rather complex models based on progressive levels of abstraction. Finally, a fully connected hidden layer is used to transform the final feature maps into the output vector. Different from dense layers in DNNs that learn global patterns of the input, convolutional layers can learn local patterns. Meanwhile, CNNs can learn spatial hierarchies of patterns.

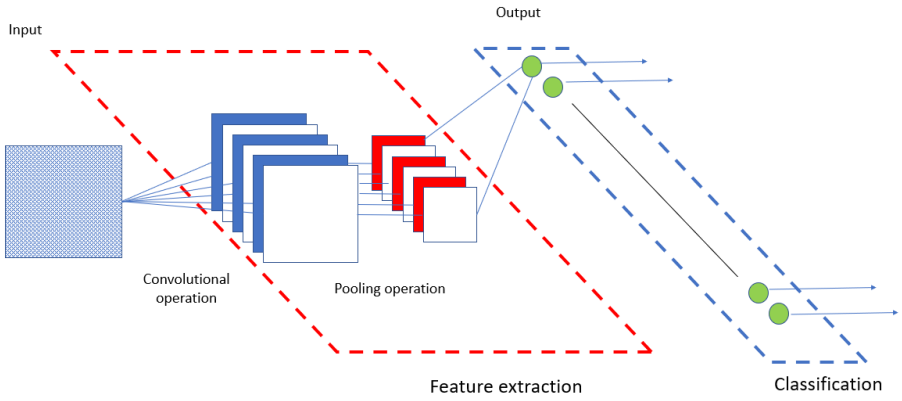

Fig. 2.11 The architecture of a CNN.

Recurrent Neural Network

Recurrent Neural Network (RNN) refers to a class of feedforward neural networks which have memories. RNN is called recurrent since it executes the same function for each data input and the output of the past one computation. The output of the current computation will then be copied and entered into the next computation process. An unrolled architecture of RNN is given in Fig. 2.12. First, it takes the X_0 from the input sequence and then it outputs h_0. Then the input for the next step is X_1 and h_0. Similarly, h_1 and X_2 will be the inputs for the third step.

The formula for the adjacent steps can be expressed by:

$$h_{t+1} = \sigma(h_t, X_{t+1}) \tag{2.12}$$

where σ refers to an activation function.

Compared with other neural networks, the inputs of RNN are related to each other. Unlike DNN and CNN, RNNs are capable of remembering, which makes them applicable to deal with the sequence datasets, such as speech recognition, handwriting recognition, etc.

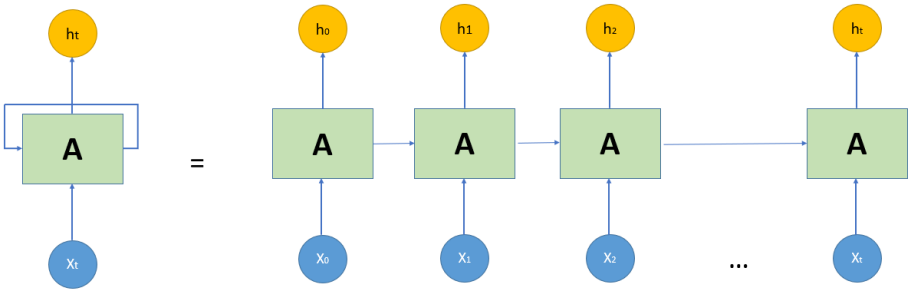

Fig. 2.12 The architecture of a RNN.

2.5 State-of-Art Machine Learning Based Energy Efficient Strategies

The applications of machine learning have spread to many fields, such as expert system, automatic reasoning, natural language processing (NLP), natural language understanding (NLU), pattern recognition, computer vision (CV), intelligent robots and other fields. As to communication fields, machine learning also gives researchers a chance to re-think about the original problems, such as the network optimization problems, and improve the network performance because of their capability for solving complex problems without explicit programming. As shown in a survey[6], plenty of applications of machine learning have been applied to wireless networks such as for resource management, backhaul management, spectrum management, power control, BS sleeping, etc., and have led to significant improvement on the network performance. Specifically, the energy efficient researches based on machine learning techniques will be discussed in this section.

2.5.1 Machine Learning Based BS Deployment Strategies

In [178], the relationship between online social network data and realistic traffic demand is investigated. A log-linear relationship between Twitter activity level (Tweets/s) and the traffic load (kbps) is obtained in this paper. The high correlation between Twitter data and traffic load makes prediction and estimation of traffic demand using Twitter data available, which may be quite useful for energy efficient SBS deployment, and proactive network optimization. In [179], authors investigated the received signal power of users in HetNet, and proposed a DBSCAN based SBS deployment method. Simulation results in this work show the proposed algorithm has a better performance compared with other existing approaches. In [180], the authors firstly propose a machine learning based model to predict the received signal strength (RSS), then optimizes the coverage performance of BS deployment through heuristic models. Based on the well-trained ML models, the number of deployed BSs can be minimized while satisfying the coverage constraint.

Recent years, aerial base station (ABS) has drawn more and more attention, since it can assist existing networks, and it is flexible for various emergency scenarios. As to ABSs, the energy efficient placement is one of the key issues. In [181], the authors proposed a multi-agent Q-learning-based algorithm to determine the optimal positions of the ABSs based on the locations of the users. In this algorithm, multiple ABSs act as agents to find optimal actions by interacting with environment and learning from their mistakes. Numerical results in this work show the proposed algorithm can significantly improve the network performance.

In [182], a deep reinforcement learning (DRL) method was proposed for ABSs placement. In this work, the coverage bitmap which capture the spatial correlation between ABSs and users is used as the state, while the propagation conditions are used as the environment. By interacting with the environment, the agent effectively learns how to place ABSs in order to maximize the reward. Numerical results show that the proposed approach significantly improves the performance in complex environment. Authors in [183] proposed a Q-learning based algorithm for ABS placement, user mobility is taken into account. Simulation results show proposed algorithm can find the optimal ABS placement in discrete environments and significantly improve the QoS.

2.5.2 Machine Learning Based BS Sleeping Strategies

In [184], a k-means-based SBS sleeping strategy is proposed to maximize the energy efficiency of the network. By dividing the SBSs into clusters based on the load and location, the cost function involving energy efficiency and flow level performance is minimized by proposed sleeping strategy. Simulation results show the superiority of the algorithm over other conventional methods. In [185], k-means is used to partition users into clusters at the first stage depending on the corresponding RSRQ values. The results will be entered into Q-learning algorithm as the system state to obtain the optimal BS sleeping strategies. Simulation results show the proposed algorithm has a better performance in terms of energy saving and QoS with the help of k-means, compared with the algorithms without k-means.

In [186], the authors take the transition cost between ON and OFF into account and propose a Q-learning based sleeping strategy. For this algorithm, the actions are defined by pairs of lower user threshold and upper user threshold to avoid frequent transition between ON and OFF. The performance shows that the energy consumption including the cost for transition can be reduced by this algorithm. The authors propose an actor-critic learning based BS sleeping strategy in [187]. By defining the traffic load of BSs as states, defining BSs' status of sleeping as actions, the proposed algorithm can minimize the overall energy consumption and achieve a better performance compared with other algorithms after it has converged. In [188], a Q-learning based sleeping strategy is proposed to minimize the energy consumption. For this algorithm, the state is defined as a tuple which involves the number of active BSs and the number of users, while the actions are defined as BSs' status of sleeping. Numerical results confirm the effectiveness of the proposed algorithm when it has converged. In [189], distributed Q-learning based sleeping strategy is proposed to maximize the energy efficiency for an energy harvesting small cell network. The proposed algorithm considers a tuple of BS load, the battery level and energy harvested as state, and the sleeping operation of a BS as action. Simulation results show the proposed algorithm can gain higher energy

efficiency and greater throughput. In [190], the authors proposed a Q-learning based sleeping strategy for K-tier heterogeneous networks. In this work, the MBSs were assumed to be always active, while the SBSs went to sleep when there are no active users. Numerical results show the proposed algorithm can improve the energy efficiency while maintaining network capacity and coverage probability. An online reinforcement learning algorithm without need of training phase was proposed in [191] to maximize energy saving. In this work, the proposed algorithm can continuously adapt to the changing network traffic, thus decide which action to take. Numerical results showed that proposed algorithm can significantly improve the energy saving without degrading QoS.

In [175], a deep Q-network based sleeping strategy is proposed to maximize the energy efficiency based on un-quantized systems state vectors or high-dimensional raw observations. Since deep learning techniques are employed to improve Q-learning in deep Q-network, the performance of proposed algorithm outperforms the traditional Q-learning algorithm. Authors in [176] propose a deep actor-critic learning based sleeping strategy which aims to minimize the energy consumption without degrading the QoS. The results in this paper show the proposed algorithm has higher computational efficiency and energy efficiency compared with existing methods.

2.5.3 Summary

As presented in previous sections, a lot of literature about machine learning based energy efficient BS deployment and BS sleeping are reviewed. The characteristics of them are analyzed and compared in Table 2.6. According to the discussions, it can be found that how to energy-efficiently deploy BSs is an open issue. To the best of author's knowledge, utilizing machine learning techniques for energy efficient BS deployment is still at a relatively early stage. Various algorithms of machine learning have not been investigated for energy efficient BS deployment. Recent years, with the availability to online social network data, the clustering algorithms can offer another perspective to the BS deployment problem since it is quite suitable for dealing with multiple dimensional locating. In this thesis, the author investigates the potential of k-means algorithm for energy efficient BS deployment since k-means is based spatial extent with low complexity. It should be noted that other clustering algorithms and even other machine learning techniques may also be promising, which worth of further investigation.

As to energy efficient BS sleeping, it can be concluded that reinforcement learning has been widely used. However, the aforementioned literature are mostly based on offline train phase, which may not be practical for realistic scenarios. Besides, the system states for these works are generally based on traffic load, which is not suitable for BS sleeping process due

to the variations caused by the sleeping BSs. Meanwhile, many models of deep learning have not been investigated for energy efficient BS sleeping, such as CNN, which are also worth of investigation.

Table 2.6 Summary of machine learning based energy efficient strategies

Scenario	Machine Learning Techniques	Characteristics	Literature
Traffic load prediction	Regression	A log-linear relationship between Twitter activity level (Tweets/s) and the traffic load is obtained, which form the basis of BS deployment	[178]
SBS deployment	DBSCAN	Propose a DBSCAN based SBS deployment method based on the results in [178]	[179]
BS deployment	Multiple techniques	An integrated machine learning algorithm and herustic method is proposed to minimize the number of deployed BSs	[180]
ABS placement	Q-learning	A multi-agent Q-learning-based algorithm was proposed based on the locations of the users.	[181]
ABS placement	Deep reinforcement learning	The proposed algorithm maximize the reward by interacting with environment which is represented by propagation conditions.	[182]
ABS placement	Q-learning	Take user mobility into consideration.	[183]
BS Sleeping	k-means	Maximize the energy efficiency of the network based on the load and location.	[184]
BS Sleeping	k-means and Q-learning	The results of k-means are entered into Q-learning algorithm as the system state to obtain the optimal BS sleeping strategies.	[185]
BS Sleeping	Q-learning	The cost for transition between ON/OFF is taken into account	[186]
BS Sleeping	Actor-critic learning	Traffic load of BSs are regarded as states.	[187]
BS Sleeping	Q-learning	The state is defined as a tuple which involves the number of active BSs and the number of users.	[188]
BS Sleeping	Q-learning	Energy harvesting is considered.	[189]
BS Sleeping	Q-learning	Sleeping strategy for K-tier heterogeneous networks	[190]
BS Sleeping	Reinforcement learning	An online reinforcement learning algorithm without need of training phase	[191]
BS Sleeping	Deep Q-network	Based on unquantized systems state vectors or high-dimensional raw observations.	[175]
BS Sleeping	Deep actor-critic learning	Minimize the energy consumption without degrading the QoS	[176]

Chapter 3

Data-driven Energy Efficient SBS Deployment

Overview

SBS deployment is one of key technologies in 4G and 5G, which is promising to uncover blackspots, and offload traffic from existing networks. However, existing models, like SPPP model, hexagonal grid model, are not suitable to capture the spatial characteristics of SBSs in dense urban regions. In this chapter, data-driven energy efficient SBS deployment methods are proposed based on k-means. These methods aim to minimize the total power consumption of the system subject to different constraints, i.e., the coverage, and the traffic demand. Moreover, two different network models, i.e., HetNet, SCN, are used, respectively. Simulation results show that the proposed SBS deployment method is energy-efficient to provide coverage and provide traffic, compared with SPPP model.

3.1 Introduction

The system performance for a cellular network is intensively influenced by the spatial characteristics of base stations (BSs). To characterize the spatial distribution, many interesting models were proposed including spatial Poisson point process (SPPP) model, traditional hexagonal grid model, etc. These models were widely used for theoretical analysis computer simulation, network performance prediction, and have achieved remarkable results. However, with the development of communication technologies and the explosive increase of traffic demand, the user distribution, which has an obvious agglomeration phenomenon, has an increasing influence on the BS distribution. Therefore, these models are not sufficient

to capture the traffic demand and the spatial characteristics of BSs in the current cellular networks since these models are based on the assumption that BS is ideal or evenly distributed.

According to [66], it is concluded that SPPP is suitable only in urban and suburban regions but not for dense urban regions. Since the dataset in that work is only collected from a mobile operator in one city of China, the generality of this conclusion needs to be considered. Therefore, the spatial characteristics of London BSs is analyzed based on a dataset in 2012. Based on the analysis, similar results are obtained. The detailed analysis is shown in **Appendix A**. The reason why SPPP is suitable in urban and suburban regions but not for dense urban regions is because the number of SBSs is considerable in dense urban regions, but small in urban and suburban regions. Therefore, more precisely, SPPP model is suitable for MBS deployment, which is mainly used to provide coverage, but not for SBS deployment, which is mainly used to provide traffic.

With the rapid development of mobile technologies, various online social networks (OSN) are available on mobile phones. Massive data have been produced in daily life [192, 193]. According to a statistics accounting, the monthly active users for the two most commonly used social networks, i.e. Twitter and Facebook, are more than 310 million and more than 1.7 billion, respectively. There have been several studies for analyzing social network data, which are mainly focus on information predicting, the hot degree of online topics, and correlation between different social networks [193, 194]. Very few works about social networks focus on BS deployment. Actually, online social networks, such as the Facebook and Twitter, usually contains accurate GPS information, which has a great significance for BS deployment. By comparing the data structures for Facebook and Twitter, it can be found Twitter data has a relatively simpler structure than Facebook [193]. In other words, it is more convenient to collect and analyze the data from Twitter, which is of great significance at the early stage of the research.

A typical data collected from Twitter contains GPS (longitude, latitude), upload date, the text, etc. That information can provide network operators with a chance to understand and improve the network performance in another way. Compared with traditional Call Detail Record(CDR) data based network optimization, the OSN data have the following advantages: 1) it is operator-neutral, providing operators chances to understand the potential customers; 2) it contains text information, which can used for event prediction, blackspots identification [195]; 3) it contains accurate GPS information which can be used for BS deployment, and traffic demand prediction [178].

According to previous research [178], a log-linear relationship between Twitter activity level (Tweets/s) and the traffic load (kbps) is obtained. The high correlations between Twitter data and traffic load gives the feasibility of Twitter data based SBS deployment method. In

this chapter, the author proposes data-driven energy efficient SBS deployment methods to minimize the total power consumption guaranteeing the QoS of users. Different scenarios, HetNet, and small cell network (SCN), are considered subject to different constraints.

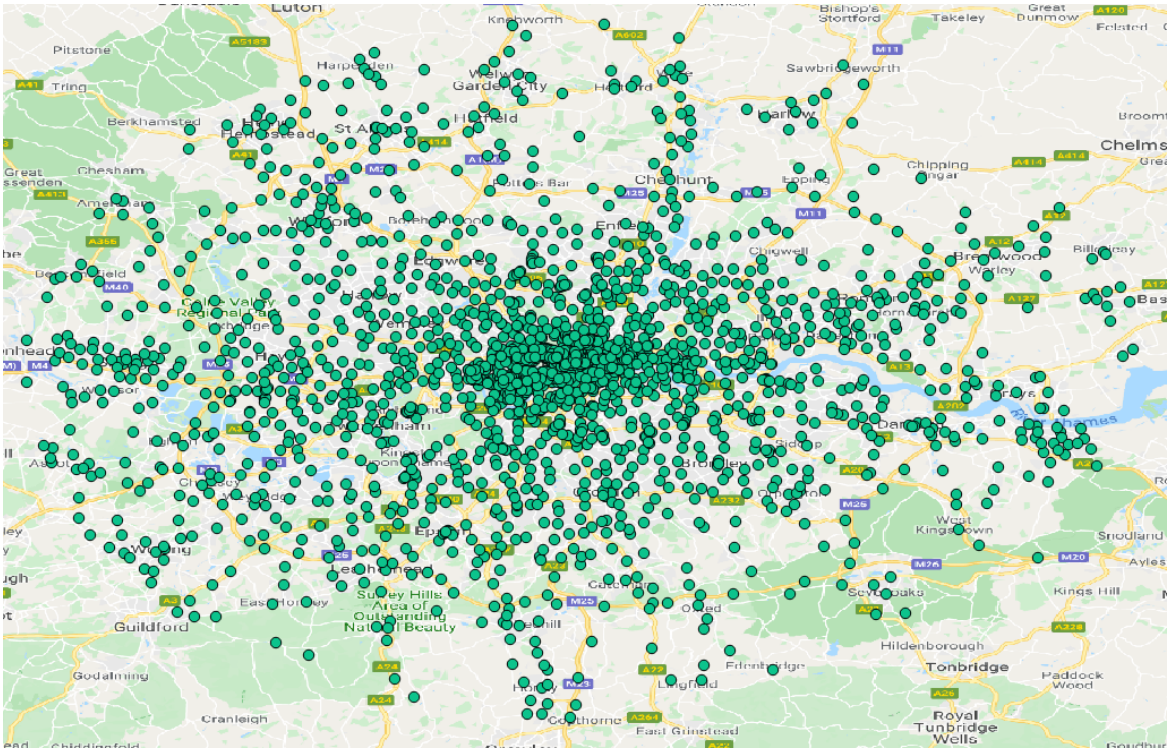

Fig. 3.1 Actual BSs deployment in London depicting dense urban (red), urban (blue) and suburban regions (black).

3.2 SBS Deployment for Energy-Coverage Tradeoffs

In this section, a HetNet scenario of Greater London is considered. Two datasets are utilized:

- **Base Station Data**: An operator's BS location information in 2012 for London, shown in Fig.3.1.
- **Online Social Network Data**: Twitter data over a period of 2 weeks in 2012 for London, shown in Fig. 3.2.

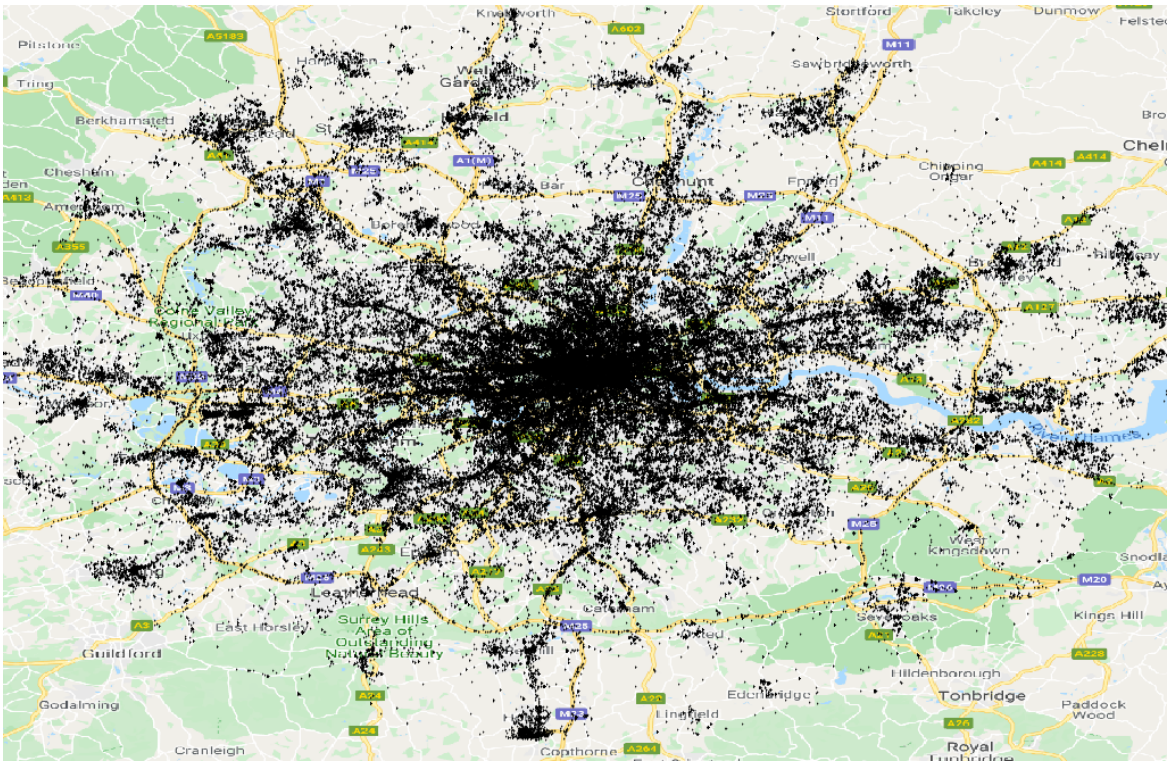

Fig. 3.2 Twitter data distribution in London

3.2.1 System Model and Problem Formulation

System model

Consider the existing network contains N_M MBSs and N_{Mi} Micro Base Stations (MiBSs). M users is simulated by Twitter data based on its location information. Suppose N_S SBSs are needed to be further deployed to uncover the blackspots in the scenario. Assume the BSs in the same tier have the same transmit power, denoted by PTX_M, PTX_{Mi}, and PTX_S, respectively. For analytical tractability, the total number of BSs in this scenarios is denoted by N, and the whole BSs are indexed by $[1,...,N]$, where the first N_M in the index denote MBSs, the last N_S in the index denote SBSs, and the others denote MiBSs.

The received power (dBm) of user j from BS i can be calculated as:

$$PRX_{i,j} = PTX_i + GTX_i - L_{tx} - L_p - L_m + GRX_j - L_{rx} \tag{3.1}$$

where PTX_i (dBm) denotes the transmit power of BS i. GTX_i and GRX_j (dBi) denote the transmitter antenna gain and receiver antenna gain, respectively. L_{tx} and L_{rx} (dB) denotes transmitter losses and receiver losses, respectively. L_m (dB) denotes other losses, including body loss, fading margin, penetration loss, etc. L_p (dB) denotes the path loss.

There are various propagation models for mobile communication [196], including Okumura et al. Model, Hata Model, etc. In this section, COST-231-Walfisch-lkegami Model is employed to calculate the path loss, which is given by:

$$L_p = \begin{cases} 42.6 + 26log(d_{i,j}) + 20log(f), & d \leq 20m \\ L_0 + max\{0, L_{rts} + L_{msd}\}, & d > 20m \end{cases} \tag{3.2}$$

where $d_{i,j}$ (km) denotes the distance between BS i and user j. f refers to the frequency band. The detail information about COST-231-Walfisch-lkegami Model is shown in **Appendix B**.

The maximum received power for a typical user j is then given by:

$$RX_j = \max_i PRX_{i,j} \tag{3.3}$$

Problem Formulation

The total power consumption of the system is given by:

$$P_{total} = \sum_i^N PTX_i + P_{static} \tag{3.4}$$

where P_{static} denotes the static power consumption of a SBS including the power consumption of signal processing, battery backup and power supply, cooling etc. It is assumed that the static power consumption for each SBS is the same.

The coverage probability is defined as:

$$\Pr[RX_j > R_s] = \Pr[\max_i PRX_{i,j} > R_s] \tag{3.5}$$

where R_s denotes the receiver sensitivity. It should be noted that this model is for link budgeting only (ignore fading).

Subject to a certain coverage probability threshold, the author aims to find the best deployment of SBSs (smallest number of SBSs) to minimize the total power consumption. The optimization problem can be formulated as:

$$\begin{aligned} & \arg\min_N P_{total} \\ \text{s.t.} \quad & Pr[RX_j > R_s] > \rho \end{aligned} \tag{3.6}$$

where (3.6) is the objective of the optimization problem, which aims to minimize the total power consumption of the network guaranteeing the coverage probability. The constraint denotes that coverage probability should be greater than a certain threshold ρ. It should be noted that the larger ρ is, the better coverage performance is expected.

3.2.2 Proposed SBS Deployment Method

The optimization problem in (3.6) is hard to solve, since the possible number of SBSs is discrete and the locations of SBSs in spatial domain are continuous. To address this problem, the received power of users based on existing network are firstly evaluated according to (3.2). For a given receiver sensitivity R_s, the coverage probability and users suffering from poor coverage can be obtained. Since k-means can divide the observations or points into k clusters based on the principle that each point is allocated to the cluster with the nearest mean, it is an appropriate method for SBS deployment in this work by efficiently analyzing geographic location information. The author proposes a heuristic k-means based SBS deployment algorithm to determine the number and the locations of SBSs.

The pseudo code of proposed algorithm is given in **Algorithm 1**. Given the locations of users $\mathbb{M}$ and existing BSs $\mathbb{B}$, the receiver sensitivity R_s, coverage probability threshold ρ and the maximum number of iterations N_{max}, the first step in **Algorithm 1** is to evaluate the received power of users based on existing BSs according to (3.3). Then the users suffering from poor coverage can be identified as $\mathbb{U} = \{u^1, ..., u^{j^*}, ..., u^m\} \in \mathbb{M}$ with u^{j^*} satisfying $RX_{u^{j^*}} < R_s$. Step 3 - step 4 for this algorithm are to initialize a small number of SBSs k_{init} and initialize the count number of iterations n with zero, respectively. While $n < N_{max}$, k-means will be employed to determine the locations of k_{init} SBSs in each iteration from Step 6 to Step 16. Step 6 - Step 8 are used to initialize k-means algorithm. In Step 6, the k_{init} was initialized as k in this iteration. Step 7 initializes $C = \{c^{(1)}, ..., c^{(j^*)}, ..., c^{(m)}\}$ to store the index cluster number of user u^{j^*}, $c^{(j^*)} \in \{1, ..., i, ..., k\}$. Step 8 initializes k centroids as $X = \{x^1, ..., x^i, ..., x^k\}$, which are randomly choose from $\mathbb{U}$. From step 10 to step 12, each user is allocated to a particular cluster when it is closest to that cluster's centroid. Then the k centroids are updated with the mean of users in each cluster by step 13 - step 15. Step 10 - step 15 will be repeated until k centroids reach the best. Then the locations of k SBSs can be obtained. Given the locations of k SBSs and existing BSs, the users suffering from poor coverage is identified in step 17. Then the coverage probability P_r^k is calculated based on (3.7). It will be estimated that if P_r^k is smaller than the coverage probability threshold or not in step 19. If smaller, k_{init} and n will be updated by $k_{init} + 1$ and $n + 1$, respectively. Then the algorithm will go to step 6 and repeat the steps until P_r^k is greater than the coverage

Algorithm 1 Proposed algorithm for SBS deployment

Input: The dataset of users $\mathbb{M}$; the dataset of existing BSs $\mathbb{B}$; the parameters for (3.1), receiver sensitivity R_s, coverage probability threshold ρ, the maximum number of iterations N_{max}.

Output: The minimal number and locations of SBSs.

Evaluate the received power of users based on existing BSs according to(3.3)
Identify the set of users suffering poor coverage by $\mathbb{U} = \{u^1, ..., u^{j^*}, ..., u^m, \} \in \mathbb{M}$, each user u^{j^*} satisfying $RX_{u^{j^*}} < R_s$.
Initialize the number of SBSs k_{init}.
Initialize the count number of iterations n with zero.
while $n < N_{max}$ **do**
  $k = k_{init}$
  Initialize $C = \{c^{(1)}, ..., c^{(j^*)}, ..., c^{(m)}\}$ to store the index cluster number of user u^{j^*}, $c^{(j^*)} \in \{1, ..., i, ..., k\}$.
  Initialize k centroids by $X = \{x^1, ..., x^i, ..., x^k\}$, which are randomly choose from $\mathbb{U}$.
  repeat
    for $j^* = 1$ to m **do**
      $c^{(j^*)} := \arg\min_i \left\| u^{j^*} - x^i \right\|$;
    end for
    for $i = 1$ to k **do**
      $u^{j^*} := \dfrac{\sum_{j^*=1}^{m} I\{c^{(j^*)} = i\} \cdot u^{j^*}}{\sum_{j^*=1}^{m} I\{c^{(j^*)} = i\}}$;
    end for
  until Minimize the within-cluster sum of squares (WCSS) for the k clusters.
  Identify users suffering from poor coverage based on existing BSs and the k SBSs.
  Calculate the coverage probability P_r^k based on (3.7).
  if $P_r^k < \rho$ **then**
    $k_{init} = k_{init} + 1$
    $n = n + 1$
  else
    return the k SBSs
  end if
end while

Table 3.1 Parameters for SBS deployment based on energy-coverage tradeoffs

Parameter	Symbol	Value
Area of region	R	$5.8km \times 6.4km$
Frequency band	f	2100 MHz
MBS transmitted power	PTX_M	43 dBm
MiBS transmitted power	PTX_{Mi}	38 dBm
SBS transmitted power	PTX_S	23 dBm
User distribution		Twitter distribution
Propagation model		Cost 231 WI model
Gain of MBS antenna	GTX_M	18 dBi
Gain of MiBS antenna	GTX_{Mi}	5 dBi
Gain of SBS antenna	GTX_S	0 dBi
MBS height	h_M	30 m
MiBS height	h_{Mi}	3m
SBS height	h_S	3m
Average building height	h_{roof}	18m
Mobile height	h_m	1.5m
Average building separation	b	25m
Average street width	w	12.5m
Angle of incidence	φ	90°
Gain of mobile antenna	GRX	0 dBi
Transmitter loss	L_{tx}	6 dB
Other losses	L_m	18 dB
Receiver loss	L_{rx}	0 dB
Receiver sensitivity	R_s	-90 dBm

probability threshold or $n = N_{max}$. The minimal number and locations of SBSs can thus be obtained by Step 23.

3.2.3 Testing and Results

An urban region ($5.8km \times 6.4km$) is chosen as the scenario in this work. There are 23 BSs, including 18 MBSs and 5 MiBSs, respectively, and 6919 users simulated by Twitter data in this scenario, shown in Fig.3.3. The parameters used in this section is given in Table 3.1. Similar simulations are applied to suburban region and dense urban region, the experimental results were shown in **Appendix C**.

Fig.3.4 (a) shows the heatmap of the received power for users in the region based on existing BSs. Fig.3.4 (b) shows the probability density function (PDF) of received power. According to Fig.3.4 (b), 11.53% of the users are suffering from poor coverage since their

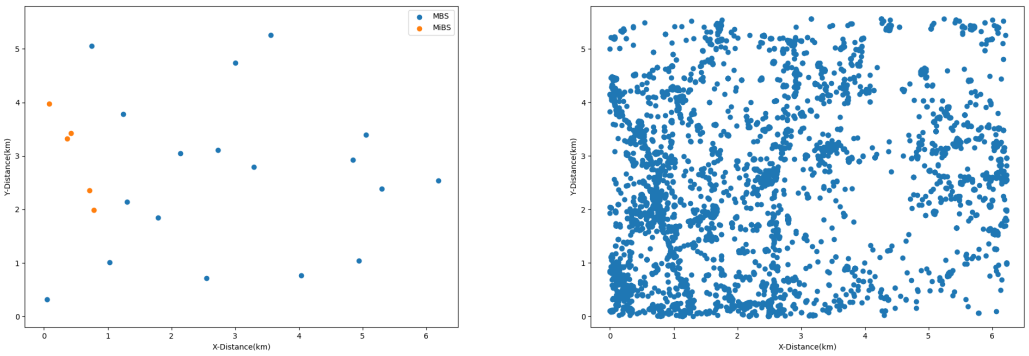

(a) (b)

Fig. 3.3 (a)MBSs and MiBSs in the region. (b) Users in the region.

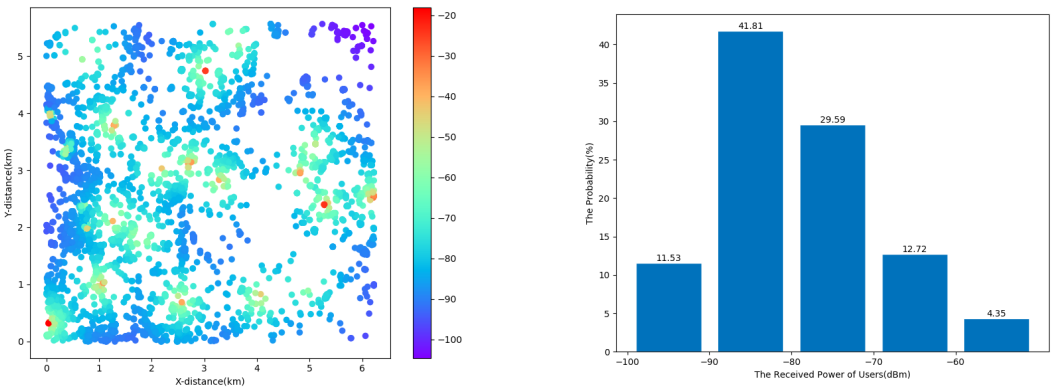

(a) (b)

Fig. 3.4 (a)The heatmap of the received power (dBm) of users. (b) The PDF of the received power.

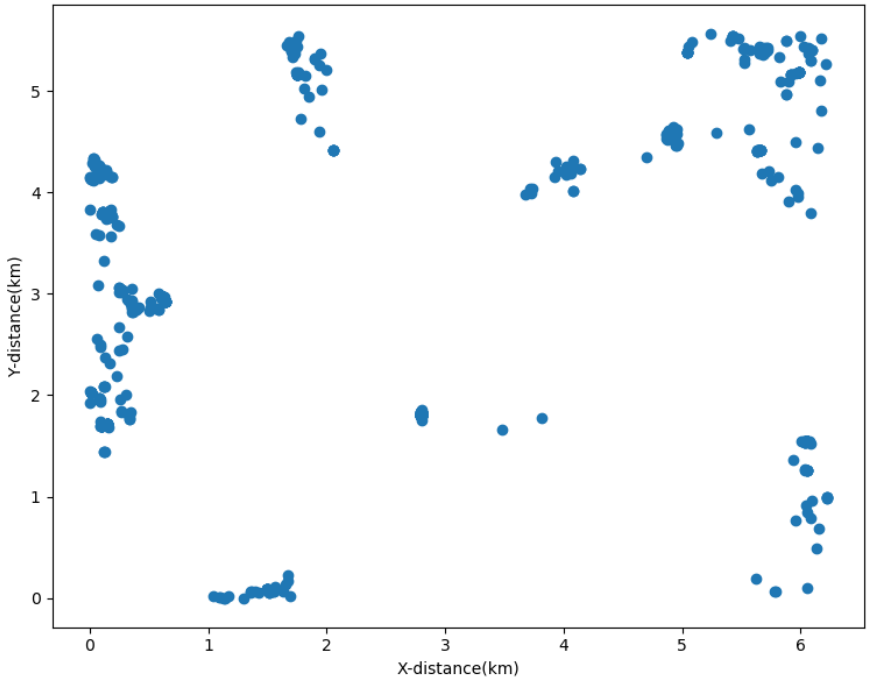

Fig. 3.5 Users suffering from poor coverage.

received power is below the receiver sensitivity, which is given by -90 dBm in this work. The distribution of the users suffering from poor coverage, referred to as poor users, is given in Fig.3.5. To improve the network performance, several SBSs need to be deployed.

Based on the poor users shown in Fig.3.5, k-means is employed for SBS deployment. To evaluate the performance of proposed SBS deployment method, a SPPP model is employed for comparison. The metrics of these two models are based on the coverage probability, Pr, which is calculated by (3.7), and the power consumption for the same coverage probability threshold. Notably, the density λ in SPPP model is calculated based on K which is the input of k-means based algorithm and represents the number of SBSs, and the area of the region B.

Fig.3.7 presents the coverage probability Pr of the proposed model and SPPP model under different value of K. It can be seen that as the number of SBSs increases, the Pr of the proposed model increases rapidly and gradually converges to 100% percent when K is greater than 95, while the Pr of SPPP model does not change much when K is smaller than 38, and experiences an irregular fluctuation after that. This phenomenon is caused by the randomness in SPPP model, and is consistent with the analyses in **Appendix A**.

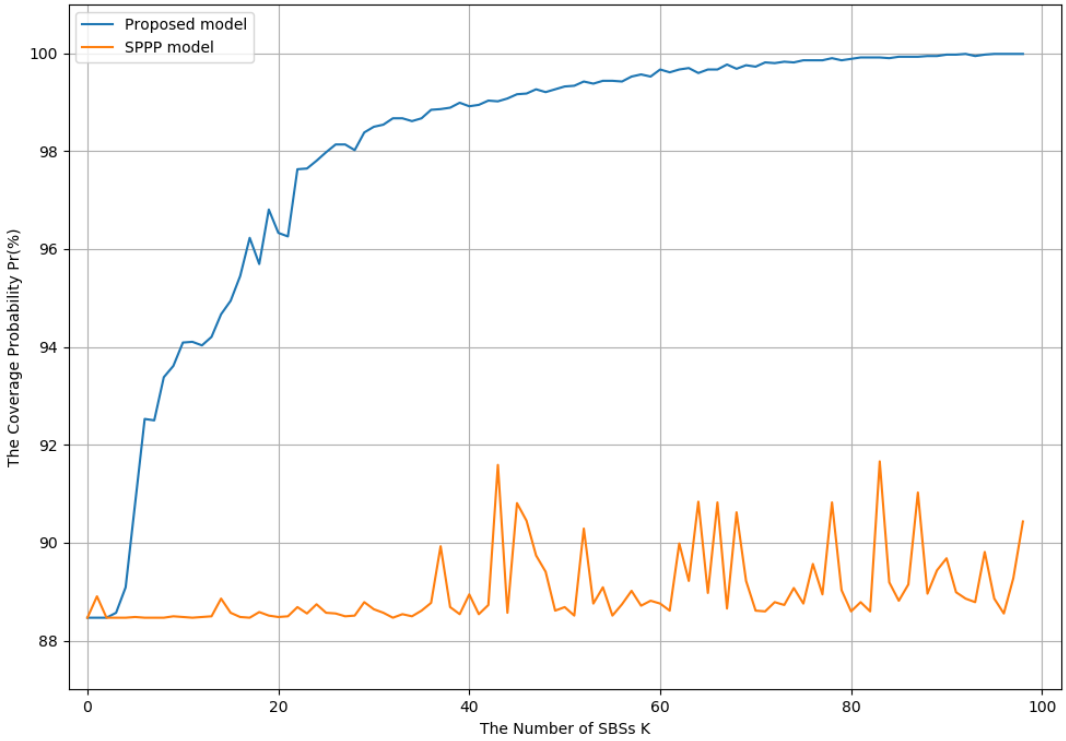

Fig. 3.6 Comparison of coverage probability for two models under different number of SBSs.

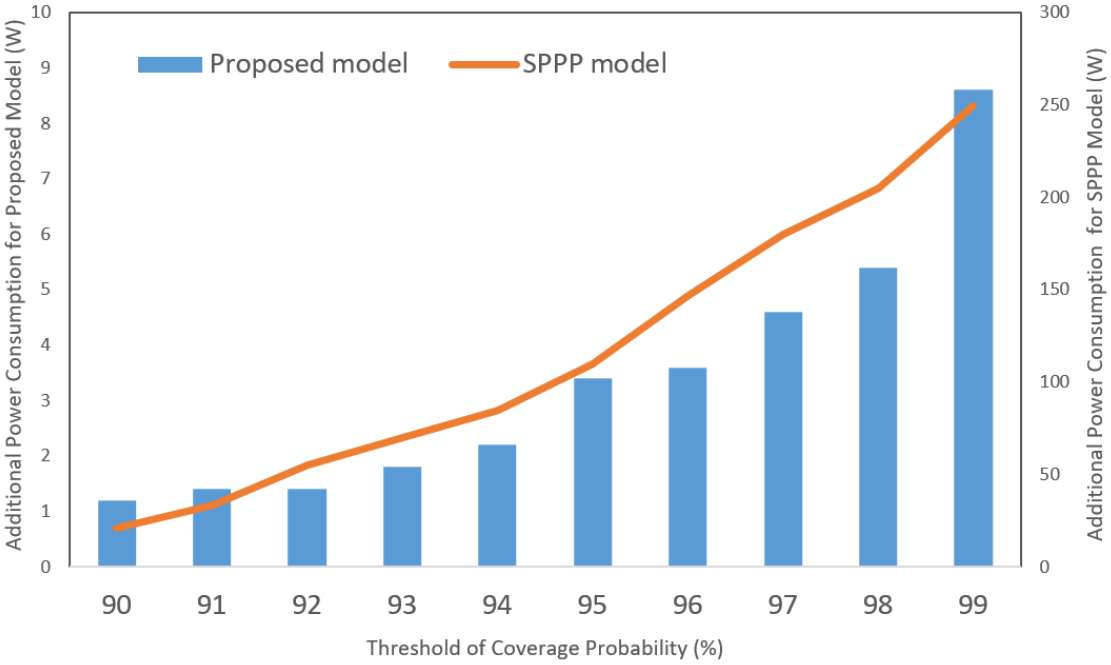

Fig. 3.7 Comparison of the additional power consumption for two models under different coverage probability threshold.

$$Pr = \frac{The\ \ number\ \ of\ \ users\ \ whose\ received\ power\ greater\ than\ R_s}{The\ total\ number\ of\ users\ in\ this\ region} \tag{3.7}$$

The additional power consumption of the SBSs under different coverage probability threshold ρ is shown in Fig.3.7. Since the sleep mode is not considered in this work, the total power consumption of a SBS is represented by its transmit power for simplicity. It can be seen that as coverage probability threshold ρ increases from 90% to 99%, the additional power consumption for two models have a similar growth trend. But the additional power consumption for SPPP model is almost 30 times of that of proposed model under the same ρ. Notably, for a typical coverage probability threshold, 95%, the additional power consumption for the proposed model is 3.4 W, while it is 109.8W for SPPP model.

3.2.4 Conclusion

In this section, the author formulates the power consumption minimization problem subject to the coverage probability, and propose an energy-efficient heuristic SBS deployment algorithm based on k-means and Twitter data. Numerical results show that, compared with existing SPPP model, the coverage probability can be significantly improved under the same number of SBSs, and the power consumption can be significantly reduced by almost 30 times under the same coverage probability threshold.

3.3 SBS Deployment for Energy-Traffic Tradeoffs

3.3.1 System Model and Problem Formulation

System model

In this section, an orthogonal frequency division multiple access (OFDMA) radio access network (RAN), where N SBSs cover a region $\boldsymbol{B}$ is considered. Similar to the previous section, the users in the region are simulated by Twitter data based on its location information, which is denoted by M. Transmission rate requirement of user j is denoted by r_j. According to coordinated multiple point (CoMP), it is assumed that each SBS may serve the transmission rate requirements of different users while each user may also be served by multiple SBSs simultaneously. Note that the detailed optimization about CoMP is out of scope for this work. Assume the transmission power per unit bandwidth of each SBS is fixed as P_{tx} and SBSs use the same downlink frequency band with the same bandwidth of BW. Considering the worst interference scenario that all the SBSs are transmitting data using the same spectrum resources and will generate interference to each other, the signal to interference plus noise ratio (SINR) for a type user j from SBS i can be formulated as:

$$SINR_{i,j} = \frac{PRX_{i,j}}{\sum\limits_{k=1,k\neq i}^{N} PRX_{k,j} + \sigma^2} \tag{3.8}$$

where $PRX_{i,j}$ (W) denotes the received power of user j from SBS i, which can be calculated based on (3.1). It should be noted that a unit conversion is needed since the unit of $PRX_{i,j}$ in (3.1) is dBm, while it is watt in (3.8). And this model is for link budgeting only (ignore fading). $\sum\limits_{k=1,k\neq i}^{N} PRX_{k,j}$ denotes the interference generated by other SBSs, and σ^2 denotes the noise.

Assume the bandwidth allocated from SBS i to user j is $bw_{i,j}$. The transmission rate between SBS i and user j is given by $t_{i,j}$, shown as:

$$t_{i,j} = bw_{i,j} \cdot \log_2(1 + SINR_{i,j}) \tag{3.9}$$

Based on power consumption model proposed in [4], the power consumption of a BS is a linear function of the load, which is given by:

$$P_i = P_0 + P_{tx} \cdot \sum_{j=1}^{M} bw_{i,j} \tag{3.10}$$

where P_0 denotes the static power consumption of a SBS, including the power consumption of radio frequency (RF) circuit, processing, cooling etc. $\sum_{j=1}^{M} bw_{i,j}$ denotes the overall occupied bandwidth of SBS i. Since P_{tx} is the transmit power density over the whole bandwidth, the last term denotes the load-dependent dynamic power consumption of an SBS.

The total power consumption of the N SBSs can be expressed as:

$$P_{total} = \sum_{i=1}^{N} P_i \tag{3.11}$$

Problem Formulation

In this section, the author aims to minimize the total power consumption of the network subject to the transmission rate requirements of M users. The optimization problem can be formulated as:

$$\begin{aligned} &\underset{N,d_{i,j},bw_{i,j}}{\arg\min}\ P_{total} \\ \text{s.t.} \quad &\text{C1: } \sum_{j=1}^{M} bw_{i,j} \leq BW, \quad \forall i \in \{1,...,N\} \\ &\text{C2: } \sum_{i=1}^{N} t_{i,j} \geq r_j, \quad \forall j \in \{1,...,M\} \\ &\text{C3: } bw_{i,j} \geq 0, \quad \forall i,j \end{aligned} \tag{3.12}$$

where C1 is a constraint of the available bandwidth of each SBS. C2 is a constraint to guarantee the transmission rate requirements of users, which is relevant to N and $d_{i,j}$. C3 denotes that the allocated bandwidth from any SBS to any user is non-negative. Since the objectives in this problem contain not only the number and the location of SBSs, but also the bandwidth allocation between SBSs and users, (3.12) is a mixed integer non-linear programming (MINLP) problem containing both discrete and continuous variables, which is NP-hard to solve.

3.3.2 Proposed SBS Deployment Method

Since the optimization problem in (3.12) is arduous to solve and bandwidth optimization is required for a given number of SBSs, the joint optimization problem can be decoupled into a bandwidth allocation (BA) sub-problem which minimizes the power consumption for a given

SBS deployment; and a SBS deployment (SD) sub-problem that finds the optimal number and locations of SBS to satisfy the transmission rate requirements of users.

BA Sub-problem

The BA sub-problem tries to find the optimal solution of variables $bw_{n,m}$ ($n = 1,...,N, m = 1,...,M^2$) to minimize the total power consumption for the given number and locations of SBSs. Subject to transmission rate requirements of M users, this sub-problem can be formulated as:

$$\begin{aligned} &\arg\min_{bw_{i,j}} P_{total}, \\ \text{s.t.} \quad &\text{C1, C2, C3} \end{aligned} \tag{3.13}$$

For the BA sub-problem, the following Corollary is given.

Corollary 1. *The problems in* (3.13) *are linear programming problems, which can be solved in polynomial time by many existing software tools.*

Proof:

As to (3.13), it can be re-written as (3.14) according to (3.10). Transparently, when the number and locations of SBSs are given, the objective function of problem (3.13) is a linear function of $bw_{i,j}(i = 1,...,N, j = 1,...,M)$

$$\begin{aligned} \arg\min_{bw_{i,j}} P_{total} &= \arg\min_{bw_{i,j}} \sum_{i=1}^{N} (P_0 + P_{tx} \cdot \sum_{j=1}^{M} bw_{i,j}) \\ &= \arg\min_{bw_{i,j}} \sum_{i=1}^{N} (P_{tx} \cdot \sum_{j=1}^{M} bw_{i,j}) \end{aligned} \tag{3.14}$$

Transparently, C1 and C3 are linear inequalities about $bw_{i,j}$. According to (3.9), C2 can be re-written as:

$$\begin{aligned} &\sum_{i=1}^{N} t_{i,j} \geq r_j, \quad \forall j \in \{1,...,M\} \Rightarrow \\ &\sum_{i=1}^{N} bw_{i,j} \cdot \gamma_{i,j} \geq r_j, \quad \forall j \in \{1,...,M\} \end{aligned} \tag{3.15}$$

where each $\gamma_{i,j} = \log_2(1 + SINR_{i,j})$ is a constant according to (3.8).

Thus, C2 is also a linear inequality about $bw_{i,j}$ for a given SBS deployment. Therefore, (3.13) is a LP problem about $bw_{i,j}$, which can be solved in polynomial time by many existing software tools.

SD Sub-problem

To solve the SD sub-problem, a heuristic k-means based algorithm is proposed to find the optimal number and the locations of SBSs. The pseudo code of the proposed algorithm for SD sub-problem is given in **Algorithm 2**.

Given the locations of users $\mathbb{M} = \{u^1, ..., u^j, ..., u^M\}$ and the transmission rate requirements of users $\mathbb{T}$, the first two steps for this algorithm are to initialize a relatively large number of SBSs k_{init} and initialize two clusters N and L to store the number and locations of SBSs, respectively. While $k_{init} > 0$, k-means will be employed to determine the locations of k_{init} SBSs in each iteration from Step 4 to Step 14. Step 4 - Step 6 are used to initialize k-means algorithm. In Step 4, the k_{init} was initialized as k in this iteration. Step 5 initializes $C = \{c^{(1)}, ..., c^{(j)}, ..., c^{(M)}\}$ to store the index cluster number of user u^j, $c^{(j)} \in \{1, ..., i, ..., k\}$. Step 6 initializes k centroids as $X = \{x^1, ..., x^i, ..., x^k\}$, which are randomly choose from $\mathbb{M}$. From step 8 to step 10, each user is allocated to a particular cluster when it is closest to that cluster's centroid. Then the k centroids are updated with the mean of users in each cluster by step 11 - step 13. Step 8 - step 13 will be repeated until k centroids reach the best. Then the locations of k SBSs can be obtained. Given the locations of k SBSs, it will be estimated that if the k SBSs can satisfy users' traffic requirements or not in step 15. If possible, the k_{init} will be updated by $k_{init} - 1$, and the k SBSs will be stored in clusters N and L. Then the algorithm will go to step 4 and repeat the steps until $k_{init} = 0$ or the k SBSs cannot satisfy users' traffic requirements. Finally, the minimal number and locations of SBSs can be obtained by Step 23 and 24.

The pseudo code of the overall algorithm is given in **Algorithm 3**. The first 15 steps are almost the same as those in **Algorithm 2** except step 2. In **Algorithm 3**, step 2 is to initialize a cluster P to store the total power consumption of SBSs. After the locations of k SBSs are obtained, it will be estimated that if the k SBSs can satisfy users' traffic requirements or not in step 15. If possible, the corresponding BA sub-problem for the k SBSs will be solved based on (3.13), and $bw^k_{i,j}$ will be obtained in step 16. Then the total power consumption P^k_{total} for the k SBSs will be calculated based on (3.11) in step 17. P^k_{total} will then be stored in cluster P, and k_{init} will be updated by $k_{init} - 1$. Then the algorithm will go to step 4 and repeat the steps until $k_{init} = 0$ or the k SBSs cannot satisfy users' traffic requirements. Finally, the minimal power consumptions of SBSs can be obtained by Step 24.

Algorithm 2 Proposed algorithm for SD sub-problem

Input: The locations of users $\mathbb{M} = \{u^1, ..., u^j, ..., u^M\}$; the transmission rate requirements of users $\mathbb{T}$; the parameters for (3.1).

Output: The minimal number and locations of SBSs.

Initialize the number of SBSs k_{init}.
Initialize clusters N and L to store the number and locations of SBSs, respectively.
while $k_{init} > 0$ **do**
  $k = k_{init}$
  Initialize $C = \{c^{(1)}, ..., c^{(j)}, ..., c^{(M)}\}$ to store the index cluster number of user u^j, $c^{(j)} \in \{1, ..., i, ..., k\}$.
  Initialize k centroids by $X = \{x^1, ..., x^i, ..., x^k\}$, which are randomly choose from $\mathbb{M}$.
  repeat
    for $j = 1$ to M **do**
      $c^{(j)} := \arg\min_i \left\| u^j - x^i \right\|$;
    end for
    for $i = 1$ to k **do**
      $u^j := \dfrac{\sum_{j=1}^{M} I\{c^{(j)} = i\} \cdot u^j}{\sum_{j=1}^{M} I\{c^{(j)} = i\}}$;
    end for
  until Minimize the within-cluster sum of squares (WCSS) for the k clusters.
  if the k SBSs can satisfy users' traffic requirements **then**
    $k_{init} = k_{init} - 1$
    $N \leftarrow k$
    $L \leftarrow X_k$
  else
    break
  end if
end while
$N_{min} = \min N$.
$L_{min} = X_{N_{min}}$.

Algorithm 3 Overall algorithm for SBS deployment

Input: The locations of users $\mathbb{M} = \{u^1, ..., u^j, ..., u^M\}$; the transmission rate requirements of users $\mathbb{T}$; the parameters for (3.1).

Output: The minimal power consumptions SBSs.

Initialize the number of SBSs k_{init}.
Initialize a cluster P to store the total power consumption of SBSs.
while $k_{init} > 0$ **do**
  $k = k_{init}$
  Initialize $C = \{c^{(1)}, ..., c^{(j)}, ..., c^{(M)}\}$ to store the index cluster number of user u^j, $c^{(j)} \in \{1, ..., i, ..., k\}$.
  Initialize k centroids by $X = \{x^1, ..., x^i, ..., x^k\}$, which are randomly choose from $\mathbb{M}$.
  repeat
    for $j = 1$ to M **do**
      $c^{(j)} := \arg\min_i \left\| u^j - x^i \right\|$;
    end for
    for $i = 1$ to k **do**
      $$u^j := \frac{\sum_{j=1}^{M} I\{c^{(j)} = i\} \cdot u^j}{\sum_{j=1}^{M} I\{c^{(j)} = i\}};$$
    end for
  until Minimize the within-cluster sum of squares (WCSS) for the k clusters.
  if the k SBSs can satisfy users' traffic requirements **then**
    Solve the corresponding BA sub-problem in (3.13), and obtain $bw_{i,j}^k$
    Calculate the total power consumption P_{total}^k for the k SBSs based on (3.11).
    $P \leftarrow P_{total}^k$
    $k_{init} = k_{init} - 1$
  else
    break
  end if
end while
$P_{min} = \min P$.

Table 3.2 Parameters for SBS deployment based on energy-traffic tradeoffs

Parameter	Symbol	Value
Area of region	B	$200m \times 200m$
Frequency band	f	2100 MHz
SBS static power	P_0	38 dBm
SBS transmitted power	P_{tx}	23 dBm
User distribution		Twitter distribution
Propagation model		Cost 231 WI model
Gain of SBS antenna	GTX_S	0 dBi
SBS height	h_S	3m
Average building height	h_{roof}	18m
Mobile height	h_m	1.5m
Average building separation	b	25m
Average street width	w	12.5m
Angle of incidence	φ	90°
Gain of mobile antenna	GRX	0 dBi
Transmitter loss	L_{tx}	6 dB
Other losses	L_m	18 dB
Receiver loss	L_{rx}	0 dB
Transmission rate requirements	r	10-100 kbps

3.3.3 Testing and Results

In this work, a dense urban region ($200m \times 200m$) with 1797 users distributed in this scenario is considered, shown in Fig.3.8. The parameters used in this section is given in Table 3.2. It is assumed that users in this scenario have the same transmission rate requirements, given by r.

Based on the users shown in Fig.3.8, and a given number for SBSs, k-means is employed for SBS deployment. To evaluate the performance of proposed SBS deployment method, a SPPP model is employed for comparison. Notably, it is possible that the BA sub-problem has no feasible solution for the SBS deployment given by a specific algorithm. In the situation where constraint C2 cannot be satisfied, (3.13) is modified to a best-effort solution

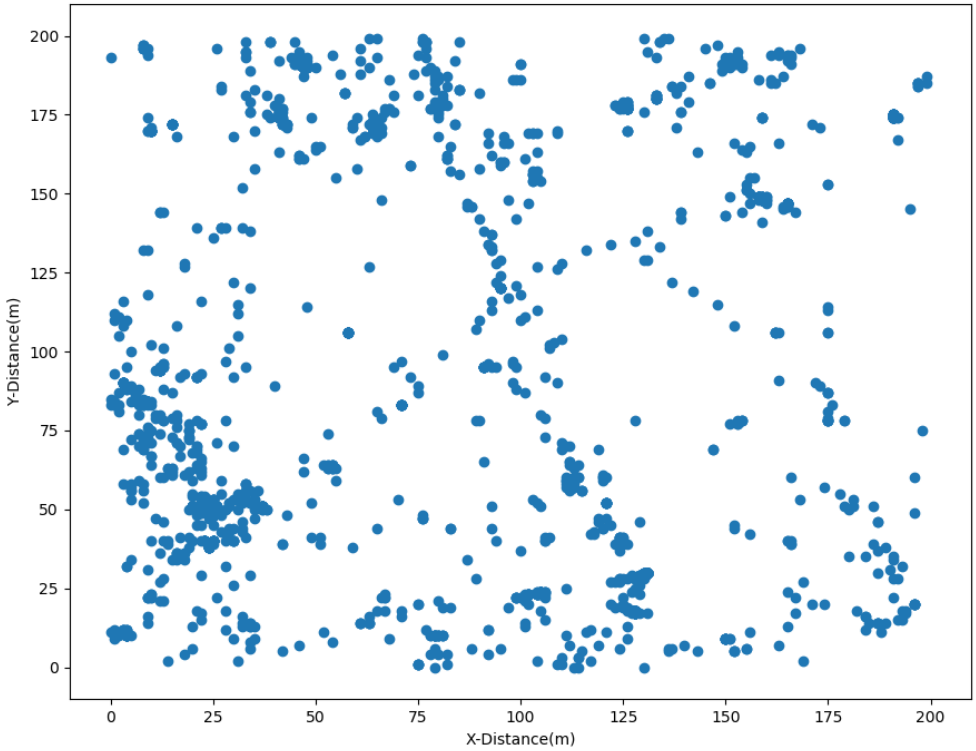

Fig. 3.8 Users in the region.

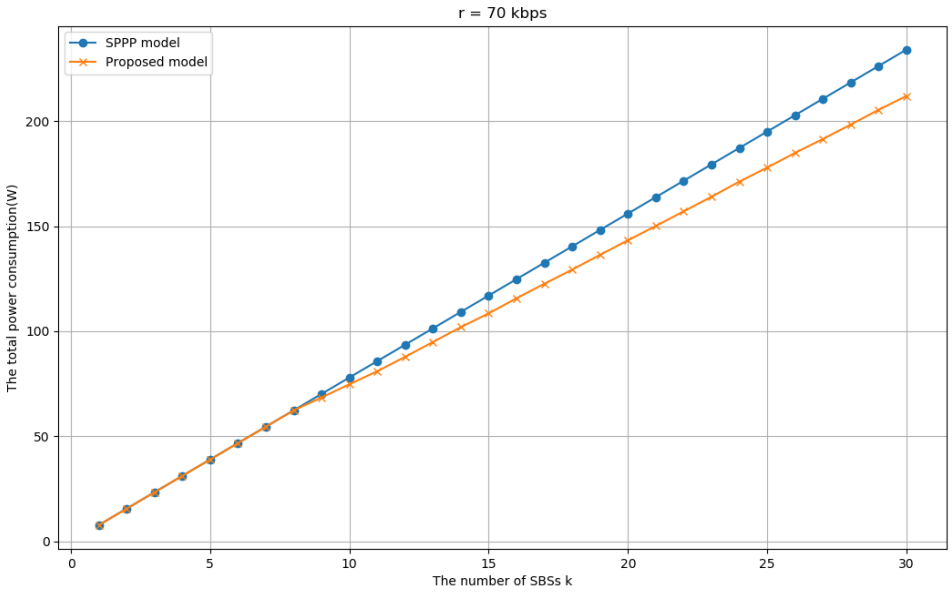

Fig. 3.9 Comparison of the total power consumption for different algorithms under different number of SBSs.

to maximize the served traffic, given by (3.16).

$$\begin{aligned} &\arg\max_{bw_{i,j}} \sum_{j=1}^{M}\sum_{i=1}^{N} t_{i,j} \\ &\text{s.t.} \qquad \text{C1, C3} \end{aligned} \tag{3.16}$$

For a specific transmission rate requirement, and a specific SBS deployment, the total power consumption can be calculated as:

$$PC = \begin{cases} \min\limits_{bw_{i,j}} P_{total}, & \text{if C2 is satisfied} \\ N \cdot (P_0 + P_{tx} \cdot BW), & \text{if C2 is not satisfied} \end{cases} \tag{3.17}$$

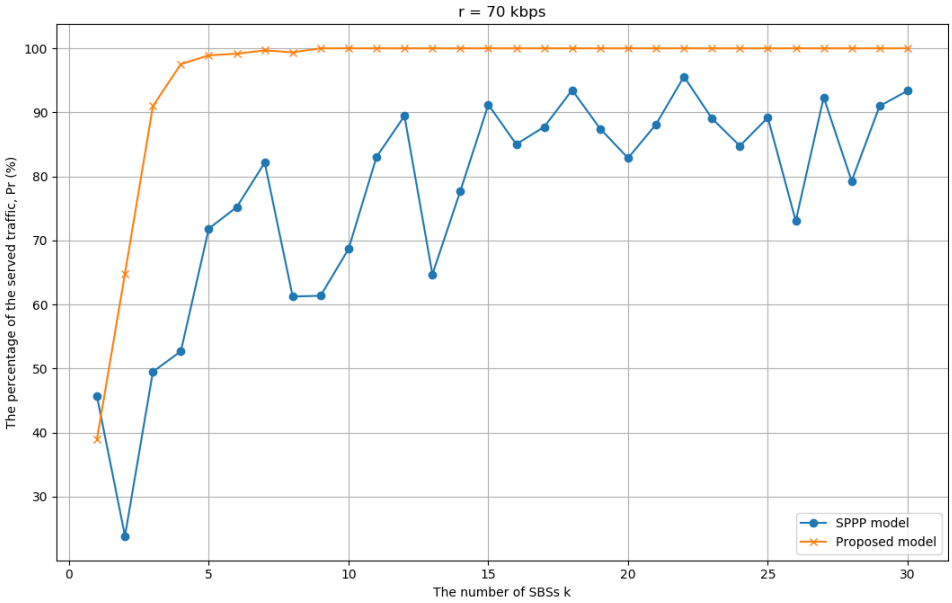

Fig. 3.10 Comparison of the percentage of served traffic for different algorithms under different number of SBSs.

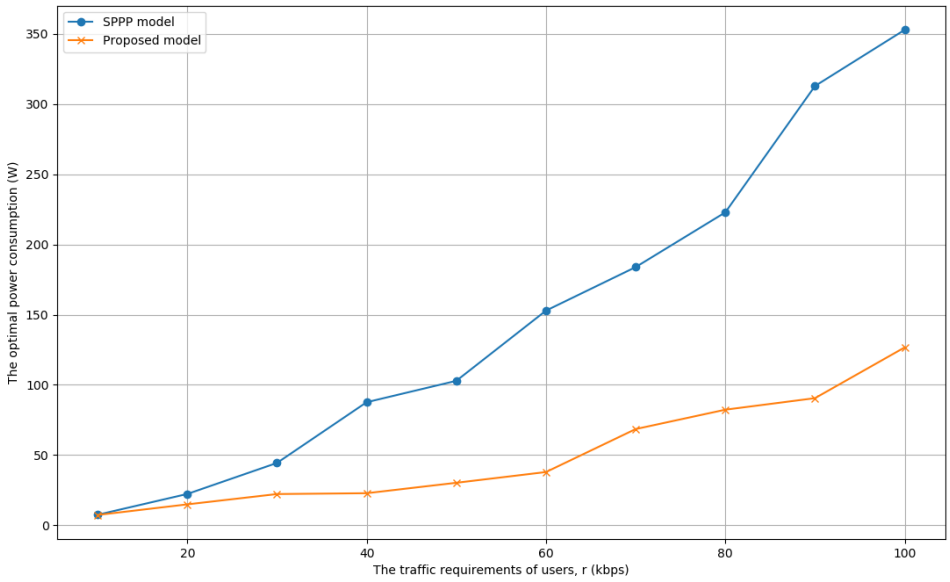

Fig. 3.11 Comparison of the optimal power consumption for different algorithms under different traffic requirements.

And the percentages of served traffic over the total traffic (referred to as the served rate, SR) can be calculated as:

$$SR(\%) = \begin{cases} 100\%, & \text{if C2 is satisfied} \\ \dfrac{\max\limits_{bw_{i,j}} \sum\limits_{j=1}^{M} \sum\limits_{i=1}^{N} t_{i,j}}{\sum\limits_{j=1}^{M} r_j} \times 100\%, & \text{if C2 is not satisfied} \end{cases} \tag{3.18}$$

Fig.3.9 shows the comparison of total power consumption for different algorithms under different number of SBSs with $r = 70kbps$. It can be seen that with $r = 70kbps$, the total power consumption for the proposed model and SPPP model both increase as the number of SBSs increases. Besides, the total power consumption of proposed model will always be equal to or smaller than that of SPPP model under the same number of SBSs.

Fig.3.10 shows the comparison of the percentage of served traffic for different algorithms under different number of SBSs with $r = 70kbps$. The percentage of served traffic is calculated by (3.18). It can be seen that as k increases, the percentage of served traffic for proposed model increases rapidly, and reaches 100% when $k \geq 9$. As to SPPP model, it can be seen that it has a similar trend with some fluctuations caused by its randomness. It should be noted that when $k \geq 2$, the percentage of served traffic for proposed model will always be greater than that of SPPP model under the same number of SBSs.

The comparison of the optimal power consumption for different algorithms under different traffic requirements is shown in Fig.3.11. The optimal power consumption refers to the minimal power consumption to satisfy the total traffic requirements. It can be seen that as the traffic requirements r increases, the optimal power consumptions for both models increase. For any given traffic requirements r, the optimal power consumption for the proposed model is always smaller than that of SPPP model , which is consistent to the previous analysis.

3.3.4 Conclusion

In this paper, the author formulates a tradeoffs between power consumption and percentage of served traffic and proposes a data-driven SBS deployment algorithm based on k-means. Numerical results show that, compared with existing SPPP model, the power consumption can be significantly reduced under the same number of SBSs, the optimal power consumption for proposed model will always be smaller than that of SPPP model under the same traffic requirements.

3.4 Summary

In this chapter, existing models and the potential of OSN data are briefly introduced at first. The performance of SPPP model in different scenarios, i.e., dense urban, urban, suburban, are evaluated in **Appendix A**. Then, two different data-driven SBS deployment methods are proposed subject to different constraints. For the first method, the author aims to minimize the total power consumption in a HetNet subject to a coverage probability threshold. It can be obtained that the coverage probability can be significantly improved under the same number of SBSs, and the power consumption can be significantly reduced under the same coverage probability threshold by the proposed method compared with SPPP model. For the second method, a tradeoff between the power consumption and the percentage of served traffic is investigated. The author thus aims to minimize the power consumption in a SCN. The performance of the algorithm is evaluated in various scenarios. Simulation results show that the power consumption can be significantly reduced under the same number of SBSs, the optimal power consumption for proposed model will always be smaller than that of SPPP model under the same traffic requirements. For the future work, the sleeping mode will be considered for further power consumption reduction.

Chapter 4

Centralized Sleeping Control and Bandwidth Allocation for Small Base Stations Based on KNN and CNN

Overview

The deployment of small base stations (SBSs) has led to the rising power consumption of mobile networks. In this section, a centralized sleeping control and bandwidth allocation (SCBA) problem for multiple SBSs controlled by a central controller to minimize the total power consumption is studied. Subject to the transmission rate requirements, the optimization problem is formulated as a mixed integer non-linear programming (MINLP) problem and addressed by decoupling into two sub-problems: a centralized bandwidth allocation (CBA) sub-problem that minimizes the power consumption by optimizing the bandwidth allocation of the active SBSs; and a centralized sleeping control (CSC) sub-problem that finds the optimal sleeping strategy among all the possible ones. It is proven that the CBA sub-problem is a linear programming (LP) problem which can be solved by many existing software tools. Two different methods, based on k-nearest-neighbor (KNN) and convolutional neural network CNN, respectively, are proposed to solve the CSC sub-problem. Simulation results show that the proposed schemes have superior performance compared with existing approaches in terms of complexity, power consumption, and the percentage of unserved traffic (referred to as unserved rate).

4.1 System Model

Consider an orthogonal frequency division multiple access (OFDMA) radio access network (RAN) where N SBSs covering a region $\boldsymbol{B}$ and these SBSs are controlled by a central controller. The SBSs are fixed and randomly distributed following a homogeneous Poisson point process. Region $\boldsymbol{B}$ is further divided into $M \times M$ grids, which are small enough so that different mobile users in the same grid are assumed to have equal distances from an arbitrary SBS. Since the downlink traffic is much higher than the uplink one in usual multimedia communications [197], this work focuses on the downlink transmission. The RAN works in time intervals and the central controller has the global information. At the beginning of each time interval, the central controller collects the knowledge about transmission rate requirements in $M \times M$ grids during this time interval and then controls the N SBSs to switch on/off as well as allocates the bandwidth to the active SBSs in a centralized way. Transmission rate requirements generated in region $\boldsymbol{B}$ are assumed to be entirely served by the N SBSs.

4.1.1 Received SINR and Achievable Rate at the Grid End

For analytical tractability, it is assumed that users in each grid see the same external-interference environment and have a constant spectral noise power density of σ^2. It is also assumed that the SBSs use the orthogonal downlink frequency band with the same bandwidth of BW [198], and the transmission power per unit bandwidth of each SBS is fixed as P_{tx}. Each SBS may serve the transmission rate requirements in different grids while the transmission rate requirement generated in a single grid can be simultaneously served by multiple SBSs. The sleeping state of SBS n is denoted by $a_n \in \{0,1\}$, and $bw_{n,m}$ denotes the bandwidth allocated from SBS n to grid m. The signal to interference plus noise ratio (SINR) at grid m from SBS n can be formulated as:

$$SINR_{n,m} = \frac{a_n \cdot P_{tx} \cdot g_{n,m}}{\sigma^2} \tag{4.1}$$

where $g_{n,m}$ denote the channel power gains from SBS n to grid m. In this work, the Rayleigh fading channel model is considered. $g_{n,m}$ is calculated as: $g_{n,m} = d_{n,m}^{-\alpha} \cdot |h_{n,m}|^2$, where $d_{n,m}$ is the distance between SBS n and grid m, α ($\alpha > 2$) is the path loss exponent, $h_{n,m}$ denotes the complex Gaussian channel coefficients following $h \sim CN(0,1)$.

The expected data transmission rate provided by SBS n to grid m is calculated according to Shannon's theory:

$$t_{n,m} = bw_{n,m} \cdot \mathbb{E}_{h_{n,m}}[\log_2(1 + SINR_{n,m})] \tag{4.2}$$

4.1.2 Power Consumption Model

Based on power consumption model proposed in [4], the power consumption of an SBS can be expressed as:

$$P_n = \begin{cases} P_0 + P_{tx} \cdot \sum_{m=1}^{M^2} bw_{n,m} & \text{if } a_n = 1 \ , \\ P_s & \text{if } a_n = 0 \ . \end{cases} \tag{4.3}$$

where P_0 denotes the static power consumption of an active SBSs, including the power consumption of radio frequency (RF) circuit, processing, cooling etc. $\sum_{m=1}^{M^2} bw_{n,m}$ denotes the overall occupied bandwidth of SBS n. Since P_{tx} is the transmit power density over the whole bandwidth, the $P_{tx} \sum_{m=1}^{M^2} bw_{n,m}$ denotes the load-dependent dynamic power consumption of a SBS. P_s denotes the power consumption of an SBS when it is in sleep state.

The total power consumption of the N SBSs is thus given by:

$$P_{total} = \sum_{n=1}^{N} \{a_n \cdot (P_0 + P_{tx} \cdot \sum_{m=1}^{M^2} bw_{n,m}) + (1 - a_n) \cdot P_s\} \tag{4.4}$$

4.1.3 Traffic Model

The transmission rate requirements in $M \times M$ grids are simulated by lognormal distribution [95] as shown in (4.5). To capture the traffic distribution in the region, different σ and μ are used to reflect the spatial characteristics of traffic demand and the average traffic load

condition in the region, respectively. For each pair of μ and σ, TW samples are generated.

$$R(\mu,\sigma) = lognrnd(\mu,\sigma,[TW, M\times M]) \tag{4.5}$$

4.2 Problem Formulation and Solution

4.2.1 Problem Formulation

In this work, the author aims to minimize the total power consumption of the system subject to the transmission rate requirements in the $M \times M$ grids. Given the transmission rate requirements r_m in each grid m, the joint optimization problem can be formulated as:

$$\begin{aligned} &\arg\min_{a_n, bw_{n,m}} P_{total} \\ \text{s.t.} \quad &\text{C1: } \sum_{m=1}^{M^2} bw_{n,m} \le a_n \cdot BW, \quad \forall n \in \{1,...,N\} \\ &\text{C2: } \sum_{n=1}^{N} t_{n,m} \ge r_m, \quad \forall m \in \{1,...,M^2\} \\ &\text{C3: } a_n \in \{0,1\}, \quad \forall n \in \{1,...,N\} \\ &\text{C4: } bw_{n,m} \ge 0, \quad \forall n,m \end{aligned} \tag{4.6}$$

C1 is a constraint of available bandwidth of each SBS. C2 is a QoS constraint to satisfy the transmission rate requirements in each grid. C3 denotes that each SBS can either be active or sleeping, while C4 denotes that the allocated bandwidth from any SBS to any grid is non-negative. Obviously, (4.6) is a mixed integer non-linear programming (MINLP) problem containing both discrete and continuous variables, which is NP-hard to obtain the global optimal solution.

4.2.2 Problem Solution

Since the bandwidth allocation is required for active SBSs only, the original optimization problem in (4.6) can be decoupled into two sub-problems: a centralized bandwidth allocation (CBA) sub-problem that minimizes the power consumption by optimizing the bandwidth allocation of the active SBSs, which can be solved by linear programming (LP); and a centralized sleeping control (CSC) sub-problem that finds the optimal SBS sleeping strategy among all the possible ones, which can be solved by KNN or CNN, shown in the Sect 4.3 and Sect 4.4, respectively. Then by coupling the solutions of CSC and CBA, the overall power consumption minimization in the system can be obtained.

Solution of the CBA Sub-problem

The CBA sub-problem tries to find the optimal solution of variables $bw_{n,m}$ ($n = 1,...,N, m = 1,...,M^2$) to minimize the total power consumption for a given sleeping strategy of the N SBSs. Subject to transmission rate requirements in $M \times M$ grids, this sub-problem can be formulated as:

$$\begin{aligned} & \arg\min_{bw_{n,m}} P_{total} \\ \text{s.t.} \quad & \text{C1, C2, C4} \end{aligned} \tag{4.7}$$

To solve the CBA sub-problem, the following corollary is given:

Corollary 1. *The problem* (4.7) *is a LP problem, which can be solved in polynomial time by many existing software tools.*

Proof:

According to (4.4), (4.7) can be re-written as:

$$\begin{aligned} \arg\min_{bw_{n,m}} P_{total} &= \arg\min_{bw_{n,m}} \sum_{n=1}^{N} \{a_n \cdot (P_0 + P_{tx} \cdot \sum_{m=1}^{M^2} bw_{n,m}) + (1 - a_n) \cdot P_s\} \\ &= \arg\min_{bw_{n,m}} \sum_{n=1}^{N} (a_n \cdot P_{tx} \cdot \sum_{m=1}^{M^2} bw_{n,m}) \end{aligned} \tag{4.8}$$

Transparently, when $a_n, (n = 1, ..., N)$ is given, the objective function of problem (4.7) is a linear function of $bw_{n,m}, (n = 1, ..., N, m = 1, ..., M^2)$.

According to (4.2), C2 can be re-written as:

$$\begin{aligned} &\sum_{n=1}^{N} t_{n,m} \geq r_m, \quad \forall m \in \{1, ..., M^2\} \Rightarrow \\ &\sum_{n=1}^{N} bw_{n,m} \cdot \gamma_{n,m} \geq r_m, \quad \forall m \in \{1, ..., M^2\} \end{aligned} \tag{4.9}$$

where each $\gamma_{n,m} = \mathbb{E}_{h_{n,m}}[\log_2(1 + SINR_{n,m})]$ is a constant which can be calculated as:

$$\gamma_{n,m} = \int_{\Psi_n} \log_2(1 + \frac{a_n \cdot P_{tx} \cdot d_{n,m}^{-\alpha} \cdot |h_{n,m}|^2}{\sigma^2}) dh_{n,m} \tag{4.10}$$

where Ψ_n denote the ranges of $h_{n,m}$.

Thus, C2 can be transformed into a linear inequality about $bw_{n,m}$ when a_n $(n = 1, ..., N)$ are given. Meanwhile, C1 and C4 are also linear inequalities about $bw_{n,m}$.

Therefore, the problem (4.7) is a LP problem about $bw_{n,m}$, which can be solved in polynomial time by many existing software tools.

4.3 KNN-based Centralized Sleeping Control and Bandwidth Allocation Scheme

4.3.1 KNN-Based Solution of the CSC Sub-problem

In this section, KNN is employed to handle the CSC sub-problem. For the convenience of representation, the author uses $\mathbb{A} = \{A^1, ..., A^i, ..., A^{2^N}\}$ to denote the set of all possible sleeping strategies, where i is used to represent the index of sleeping strategy. For a specific sleeping strategy A^i, the sleeping choices of all the N SBSs are contained, given by $A^i =$

$[a_1^i, ..., a_n^i, ..., a_N^i]$. The index of this sleeping strategy is expressed by:

$$i = \sum_{n=1}^{N} a_n \cdot 2^{n-1} + 1 \tag{4.11}$$

For the KNN algorithm, the distance between two samples of transmission rate requirements $R^k = [r_1^k, ..., r_m^k, ..., r_{M^2}^k]$ and $R^l = [r_1^l, ..., r_m^l, ..., r_{M^2}^l]$ is defined as:

$$D_{k,l} = \max_m \left| r_m^k - r_m^l \right| \tag{4.12}$$

Lemma 1. *Assume sleeping strategy A^i is the optimal sleeping strategy for sample R^k, which means $P_{total}^k(A^i) - P_{total}^k(A^{i'}) = \omega \leq 0, \forall A^{i'} \in \mathbb{A} \setminus A^i$. Assume R^k and R^l simultaneously have feasible solutions or not to the CBA sub-problem for any given action, then $P_{total}^l(A^i) \leq P_{total}^l(A^{i'}), \forall A^{i'} \in \mathbb{A} \setminus A^i$, when the distance between R^k and R^l is small enough.*

Proof:

For any sample of transmission rate requirements, the optimal solution of the CBA sub-problem can be obtained if it exists. If the samples of transmission rate requirements R^k and R^l do not have feasible solution for the CBA sub-problem, the transmission rate requirements cannot be satisfied. Thus, this situation is not considered in this work.

If both of them have feasible solution for the CBA sub-problem, the optimal solution can and only can be obtained when the equality is established according to the characteristics of linear programming. Therefore, the optimal solutions of R^k and R^l for action A^i will satisfy:

$$\begin{aligned} \sum_{n=1}^{N} bw_{n,n}^{k,i} \cdot \gamma_{n,m}^i &= r_m^k, \quad \forall m \in \{1, ..., M^2\} \\ \sum_{n=1}^{N} bw_{n,m}^{l,i} \cdot \gamma_{n,m}^i &= r_m^l, \quad \forall m \in \{1, ..., M^2\} \end{aligned} \tag{4.13}$$

According to the definition of distance between two samples in (4.12),

$$\begin{aligned}\left|r_m^k - r_m^l\right| &= \left|\sum_{n=1}^{N} bw_{n,m}^{k,i}\cdot\gamma_{n,m}^{i} - \sum_{n=1}^{N} bw_{n,m}^{l,i}\cdot\gamma_{n,m}^{i}\right| \\ &= \left|\sum_{n=1}^{N}(bw_{n,m}^{k,i} - bw_{n,m}^{l,i})\cdot\gamma_{n,m}^{i}\right| \\ &= \left|\sum_{n=1}^{N} bw_{n,m}^{\Delta,i}\cdot\gamma_{n,m}^{i}\right| \le D_{k,l}, \quad \forall m\in\{1,...,M^2\}\end{aligned} \tag{4.14}$$

Thus,

$$\left|\sum_{n=1}^{N} bw_{n,m}^{\Delta,i}\right| \le \frac{D_{k,l}}{\min\limits_{n}\gamma_{n,m}^{i}}, \quad \forall m\in\{1,...,M^2\} \tag{4.15}$$

where each $\gamma_{n,m}^{i}$ is a constant according to (4.10) and $bw_{n,m}^{\Delta,i} = bw_{n,m}^{k,i} - bw_{n,m}^{l,i}, \quad \forall n,m.$

Consider that both samples of transmission rate requirements have an optimal solution, then substitute (4.4) to the problem,

$$\begin{aligned}&\left|P_{total}^{k}(A^i) - P_{total}^{l}(A^i)\right| \\ &= \left|\left\{\sum_{n=1}^{N}[a_n\cdot(P_0 + P_{tx}\cdot\sum_{m=1}^{M^2} bw_{n,m}^{k,i}) + (1-a_n)\cdot P_s]\right\}\right. \\ &\qquad\left. - \left\{\sum_{n=1}^{N}[a_n\cdot(P_0 + P_{tx}\cdot\sum_{m=1}^{M^2} bw_{n,m}^{l,i}) + (1-a_n)\cdot P_s]\right\}\right| \\ &= P_{tx}\cdot\left|\sum_{n=1}^{N} a_n\cdot(\sum_{m=1}^{M^2} bw_{n,m}^{k,i} - \sum_{m=1}^{M^2} bw_{n,m}^{l,i})\right| = P_{tx}\cdot\left|\sum_{m=1}^{M^2}\sum_{n=1}^{N} a_n\cdot bw_{n,m}^{\Delta,i}\right|\end{aligned} \tag{4.16}$$

To find the boundary of $\left|P^k_{total}(A^i) - P^l_{total}(A^i)\right|$, (4.17) is given:

$$\begin{aligned}\left|P^k_{total}(A^i) - P^l_{total}(A^i)\right| &= P_{tx} \cdot \left|\sum_{m=1}^{M^2}\sum_{n=1}^{N} a_n \cdot bw^{\Delta,i}_{n,m}\right| \\ &\leq P_{tx} \cdot \left|\sum_{m=1}^{M^2}\sum_{n=1}^{N} bw^{\Delta,i}_{n,m}\right| \leq P_{tx} \cdot \sum_{m=1}^{M^2} \frac{D_{k,l}}{\min\limits_{n} \gamma^i_{n,m}} = f_{A^i}(D_{k,l})\end{aligned} \tag{4.17}$$

Thus, $f_{A^i}(D_{k,l})$ is a linear function of $D_{k,l}$ and the coefficients are dependent on the parameters calculated by (4.10). As $D_{k,l}$ approaching zero, $f_{A^i}(D_{k,l})$ will approach zero.

For any other action $A^{i'}$, similar results can be obtained. Then,

$$\begin{aligned}&\left|P^k_{total}(A^i) - P^l_{total}(A^i)\right| \leq f_{A^i}(D_{k,l}) \Rightarrow \\ -f_{A^i}(D_{k,l}) \leq P^k_{total}(A^i) - P^l_{total}(A^i) &\leq f_{A^i}(D_{k,l}) \Rightarrow \\ P^k_{total}(A^i) - f_{A^i}(D_{k,l}) \leq P^l_{total}(A^i) &\leq P^k_{total}(A^i) + f_{A^i}(D_{k,l})\end{aligned} \tag{4.18}$$

Similarly, it can be obtained that

$$-P^k_{total}(A^{i'}) - f_{A^{i'}}(D_{k,l}) \leq -P^l_{total}(A^{i'}) \leq -P^k_{total}(A^{i'}) + f_{A^{i'}}(D_{k,l}) \tag{4.19}$$

Therefore,

$$\begin{aligned}P^l_{total}(A^i) - P^l_{total}(A^{i'}) &\leq P^k_{total}(A^i) - P^k_{total}(A^{i'}) + f_{A^i}(D_{k,l}) + f_{A^{i'}}(D_{k,l}) \\ &= \omega + f_{A^i}(D_{k,l}) + f_{A^{i'}}(D_{k,l})\end{aligned} \tag{4.20}$$

Therefore, as long as the distance $D_{k,l}$ between R^k and R^l is small enough satisfying that $\omega + f_{A^i}(D_{k,l}) + f_{A^{i'}}(D_{k,l}) \leq 0$, the optimal action for R^l will be the same as that of R^k.

Based on **Lemma.1**, a KNN-based centralized sleeping control method is proposed. The pseudo code of the proposed method for CSC sub-problem is given in **Algorithm 4**. Given historical dataset $\mathbb{H} = \{H^1, ..., H^\theta, ..., H^\Theta\}$ and the test sample R^δ, the first three steps for

this algorithm are to initialize the number of k and initialize two clusters C_d and C_k to store the distances and the labels of k nearest neightbors, respectively. Step 4 - Step 7 are used to calculate the distances between the test sample and every sample in historical dataset based on (4.12). After going through all the historical samples, the distances are stored in cluster C_d. Step 8 then sort the distances in cluster C_d. Step 9 obtain the k nearest neightbors in the sorted cluster C_d, and store the labels of the k nearest neightbors in cluster C_k. Then the label which appears most often in cluster C_k will be outputted as the predicted result in step 10.

Algorithm 4 KNN-based algorithm for the CSC sub-problem

Input: The historical dataset $\mathbb{H} = \{H^1, ..., H^\theta, ..., H^\Theta\}$; the test sample R^δ.
Output: The predicted sleeping strategy $Pred^\delta$
1: Initialize the number of k.
2: Initialize a cluster C_d to store the distances.
3: Initialize a cluster C_k to store the labels of k nearest neightbors.
4: **for** $\theta = 1$ to Θ **do**
5: $\quad D_{\theta,\delta} = \max_m \left| h_m^\theta - r_m^\delta \right|$
6: $\quad C_d \leftarrow D_{\theta,\delta}$
7: **end for**
8: Sort the cluster C_d
9: Obtain the k nearest neighbors, and store the labels in C_k.
10: $Pred^\delta = \text{mode}(C_k)$

The overall KNN-based algorithm is given in **Algorithm 5**. The first 10 steps are the same as those in **Algorithm 4**. After the predicted sleeping strategy for the test sample is obtained in Step 10, it will be estimated that if the sleeping strategy $Pred^\delta$ can satisfy users' traffic requirements or not in step 11. If possible, the corresponding CBA sub-problem for sleeping strategy $Pred^\delta$ will be solved based on (4.7), and $bw_{i,j}^k$ will be obtained. Then the total power consumption P_{total}^k for the sleeping strategy $Pred^\delta$ will be calculated based on (4.4) in step 13, and be outputted in step 14. If the predicted sleeping strategy $Pred^\delta$ cannot satisfy users' traffic requirements, the algorithm will break in step 16.

Suppose large enough dataset is available, and each sample in the dataset is labeled by the index of its optimal sleeping strategy, denoted by $\mathbb{H} = \{H^1, ..., H^\theta, ..., H^\Theta\}$, and H^θ is a M^2-dimensional vector. This dataset is called historical dataset in this work. For a specific sample of transmission rate requirements, KNN-algorithm will identify k nearest samples in the historical dataset based on the distance calculated by (4.12). Then the prediction result of this specific sample is given as the label which appears most often for the k nearest neighbors.

Algorithm 5 Overall KNN-based algorithm

Input: The historical dataset $\mathbb{H} = \{H^1, ..., H^\theta, ..., H^\Theta\}$; the test sample R^δ.
Output: The predicted power consumption P^k_{total}

Initialize the number of k.
Initialize a cluster C_d to store the distances
Initialize a cluster C_k to store the k-nearest neightbors
for $\theta = 1$ to Θ **do**
    $D_{\theta,\delta} = \max_m \left| h^\theta_m - r^\delta_m \right|$
    $C_d \leftarrow D_{\theta,\delta}$
end for
Sort the cluster C_d
Obtain the k nearest neighbors, and store the labels in C_k.
$Pred^\delta = \text{mode}(C_k)$
if the sleeping strategy $Pred^\delta$ can satisfy users' traffic requirements **then**
    Solve the corresponding CBA sub-problem in (4.7), and obtain $bw^k_{i,j}$
    Calculate the total power consumption P^k_{total} for the sleeping strategy $Pred^\delta$ based on (4.4).
    Output P^k_{total}.
else
    break
end if

Table 4.1 Parameters for KNN-based algorithm

Parameter	Symbol	Value
Region of Area	B	$100 \times 100m^2$
No. of BSs	N	3, 5, 8
No. of grids	$M \times M$	25×25
Bandwidth	BW	5MHz
Transmit power of SBSs	P_{tx}	-30dBm/Hz
Static power consumption	P_0	38dBm
Sleep power consumption	P_s	27dBm
Path loss exponent	α	-4
Noise	σ^2	-174dBm/Hz
No. of samples for each pair of μ and σ	TW	1000
Proportion of training set	η	0.7
Spatial inhomogeneity factor	σ	$0.1-1$
Mean traffic load factor	μ	$3.5-5.4$

4.3.2 Testing and Results

In this section, the performance of the proposed scheme is evaluated under different scenarios. Consider a $100 \times 100m^2$ region where five SBSs are randomly but fixedly located. The region is evenly divided into 25×25 grids. The transmission rate requirements in 25×25 grids are simulated by lognormal distribution as shown in (4.5). For each pair of μ and σ, TW samples are generated, and randomly divided into two parts. Samples in the first part ($\eta \times TW$) are put into the historical dataset, $\mathbb{H}$, the other samples are put into the test dataset, $\mathbb{W}$. Parameters used in this work are summarized in Table.4.1. In this work, a most commonly used ratio (70/30) for the training set and testing set is employed [199].

Assume there will always be a sleeping strategy that can satisfy the traffic requirements in the whole dataset, which means the traffic requirements can always be satisfied if all SBSs are switched on. By exhaustively searching all the possible sleeping strategies, the optimal sleeping strategy with minimum power consumption while satisfying the traffic requirements can be obtained. The whole samples in both historical dataset and test dataset are thus labelled by their optimal sleeping strategy.

Four benchmarks, non-sleep (ALLON), probability-based strategic sleeping control (SSC) [200], greedy sleeping control (GSC) [201], and optimal sleeping control (OSC) are presented. In specific, in ALLON scheme, all SBSs remain active all the time. For SSC, each SBS determines its own switch on/off status in a distributed way according to the traffic load in the SBS's neighbor grids, and the transmission rate requirement in each grid is served by the active SBS which provides the maximum SINR. For GSC, since the

system model in [201] is not the same as the model in this work, the author only adopts the centralized SBS sleeping control scheme in [201] and the bandwidth allocation for active SBSs is handled by the solution of CBA sub-problem proposed in this work for comparison reason. As the solution of CBA sub-problem is proved to achieve the optimal bandwidth allocation for active SBSs, the performance of GSC in this experiment will be equal to or greater than the original performance in [201]. For OSC, the sleeping strategy is obtained during the labelling process. After the prediction results (sleeping strategies) are obtained by these algorithms, the bandwidth allocation for the active SBSs will then be obtained by solving the corresponding CBA sub-problem, except SSC algorithm. Thus, the overall power consumption minimization of the system can be obtained.

Notably, it is possible that the CBA sub-problem has no feasible solution for the sleeping strategy given by a specific algorithm. In the situation where constraint C2 cannot be satisfied, (4.7) is modified to a best-effort solution to maximize the served traffic, given by (4.21).

$$\begin{aligned} &\arg\max_{bw_{n,m}} \sum_{m=1}^{M^2} \sum_{n=1}^{N} t_{n,m} \\ &\text{s.t.} \qquad \text{C1, C3} \end{aligned} \tag{4.21}$$

For a specific transmission rate requirement, and a specific sleeping strategy, the total power consumption can be calculated as:

$$PC = \begin{cases} \min\limits_{bw_{n,m}} P_{total}, & \text{if C2 is satisfied} \\ \sum\limits_{n=1}^{N} \{a_n \cdot (P_0 + P_{tx} \cdot BW) + (1 - a_n) \cdot P_s\}, & \text{if C2 is not satisfied} \end{cases} \tag{4.22}$$

And the percentages of served traffic over the total traffic (referred to as the served rate, SR) can be calculated as:

$$SR(\%) = \begin{cases} 100\%, & \text{if C2 is satisfied} \\ \dfrac{\max\limits_{bw_{n,m}} \sum\limits_{m=1}^{M^2} \sum\limits_{n=1}^{N} t_{n,m}}{\sum\limits_{m=1}^{M^2} r_m} \times 100\%, & \text{if C2 is not satisfied} \end{cases} \tag{4.23}$$

Fig.4.1 presents the average total power consumption (APC) for different algorithms under different values of μ when $\sigma = 0.2$. The PC for each sample is calculated by (4.22). It can be seen that as μ increases, the average total power consumptions of all algorithms increase, which is because greater power consumption is needed to serve the traffic requirements as the mean traffic load in the region increases. APC for the ALLON algorithm is always the greatest, while APC for GSC is greater than other algorithms when $\mu > 3.9$. APC for the proposed algorithm under different k are the same as that in GSC and OSC when $\mu \leq 3.9$. The proposed algorithm under different k have similar performance compared with OSC considering APC. And when k increases, the performance of proposed algorithm will be better with smaller power consumption. Specifically, there are some values of μ under which SSC have smaller APC than that of OSC. These phenomena are at the expense of low served rate, which is not recommended in this work.

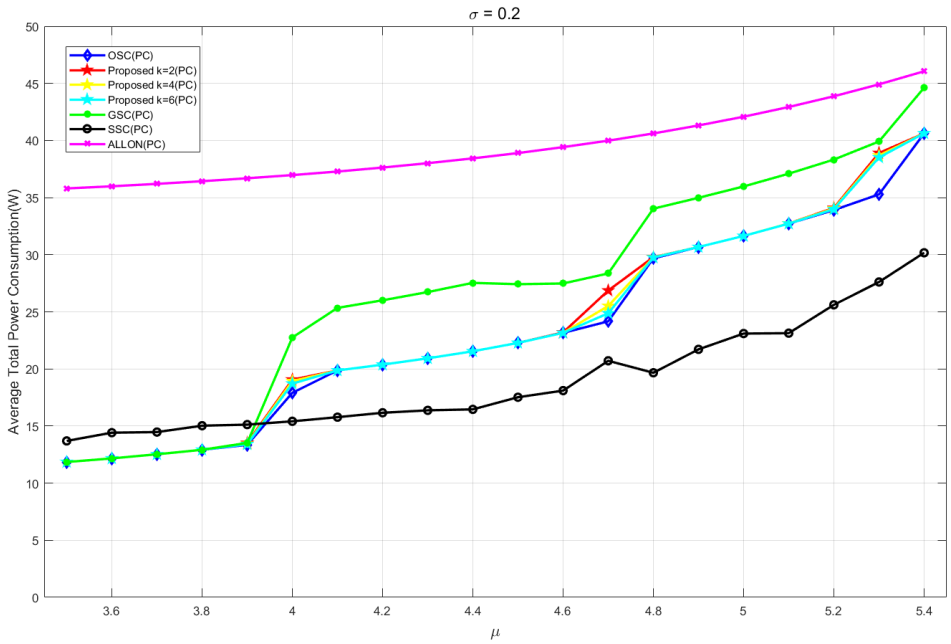

Fig. 4.1 Comparison of average total power consumption for different algorithms under μ with fixed $\sigma = 0.2$.

The served rate (SR) for different algorithms under different values of μ when $\sigma = 0.2$ is shown in Fig.4.2. Based on the assumption that there will always be a sleeping strategy to satisfy the traffic requirements, it is explicit that the SR for ALLON and OSC will always be 100%. Therefore, they will not be shown for this metrics. From Fig.4.2, it can be seen that the SR of SSC rapidly decreases as μ increases. As to proposed algorithm with different k

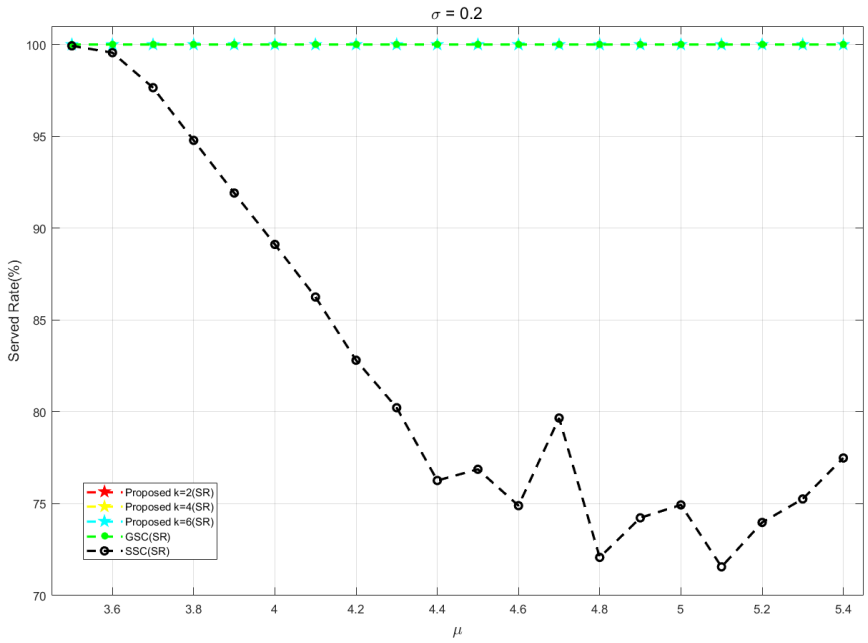

Fig. 4.2 Comparison of served rate for different algorithms under μ with fixed $\sigma = 0.2$.

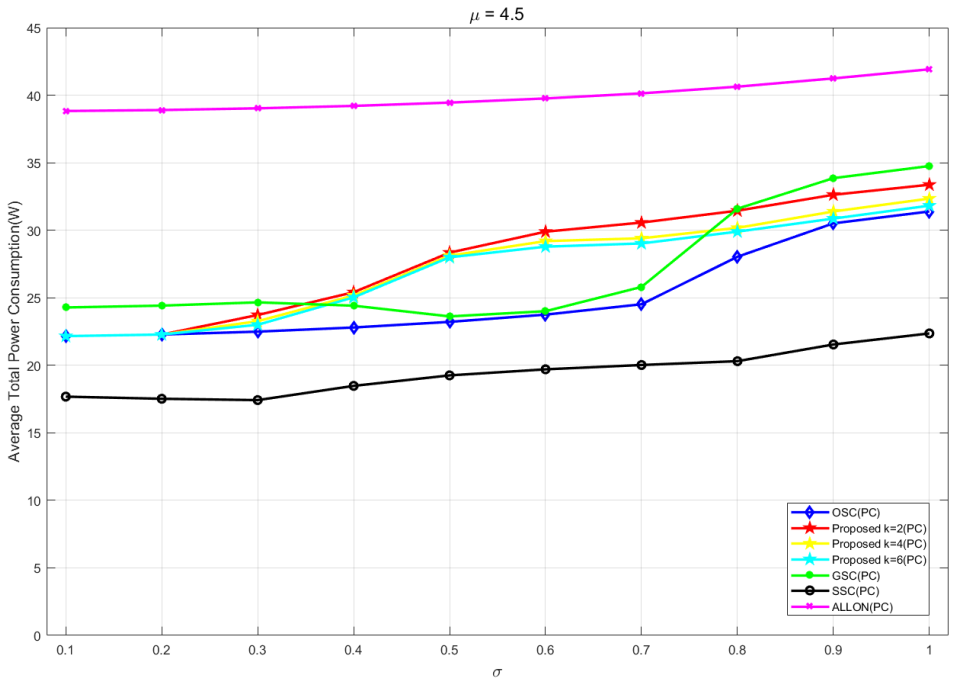

Fig. 4.3 Comparison of average total power consumption for different algorithms under σ with fixed $\mu = 4.5$.

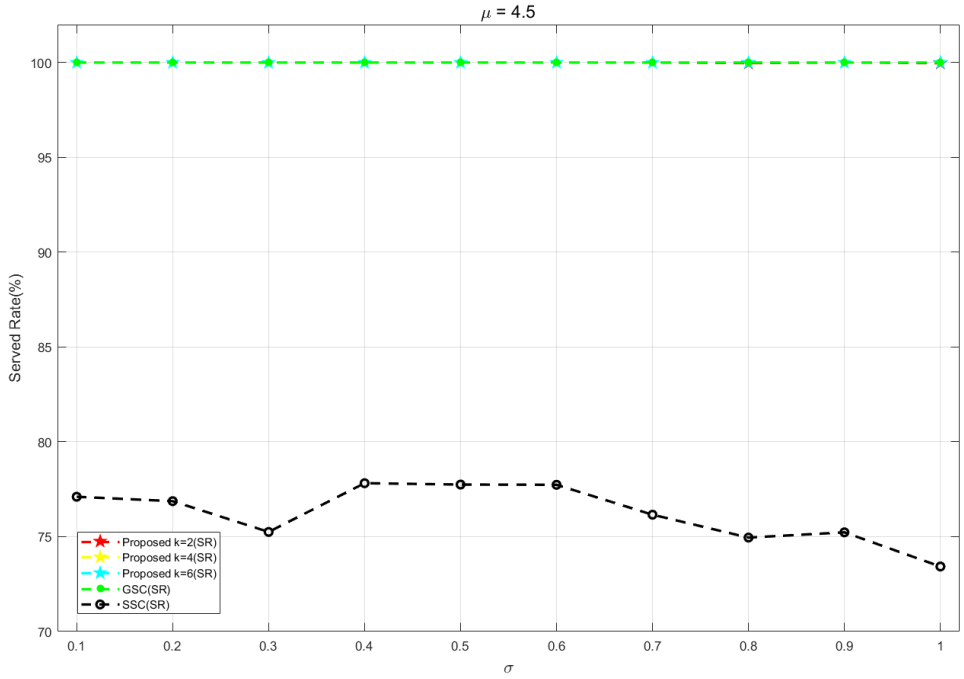

Fig. 4.4 Comparison of served rate for different algorithms under σ with fixed $\mu = 4.5$.

and GSC, the SR remains 100% under different values of μ. Combining the results in Fig.4.1 and Fig.4.2, it can be concluded the proposed algorithm will have a better performance than existing algorithms, the APC can be significantly reduced, and the traffic requirements can be guaranteed.

Fig.4.3 shows the APC for different algorithms under different values of σ when $\mu = 4.5$. From Fig.4.3, it can be found that as σ increases, the APC of all algorithms increase. Specifically, the APC for the proposed algorithm with different k are smaller than that of GSC when $\sigma < 0.4$ and $\sigma \geq 0.8$, while they are greater than that of GSC when $0.4 \leq \sigma < 0.8$. These phenomena are caused by the neighbor-identifying mechanism in the proposed algorithm. If $\sigma < 0.4$ or $\sigma \geq 0.8$, the spatial characteristics of traffic requirements in the region will be relatively uniform, thus the prediction results of proposed algorithm have more chance to be accurate. When $0.4 \leq \sigma < 0.8$, the spatial characteristics of traffic in the region will be uneven, leading to some inaccurate prediction results. It is consistent to the results in Fig.4.1. Besides, increasing k can reduce the APC and improve the performance of proposed algorithm. Notably, the smaller APC for SSC is at the expense of unserved traffic, which is not recommended in this work.

The SR for different algorithms under different values of σ when $\mu = 4.5$ is given in Fig.4.4. Similar to that of Fig.4.2, it can be seen that the SR of GSC and proposed algorithm

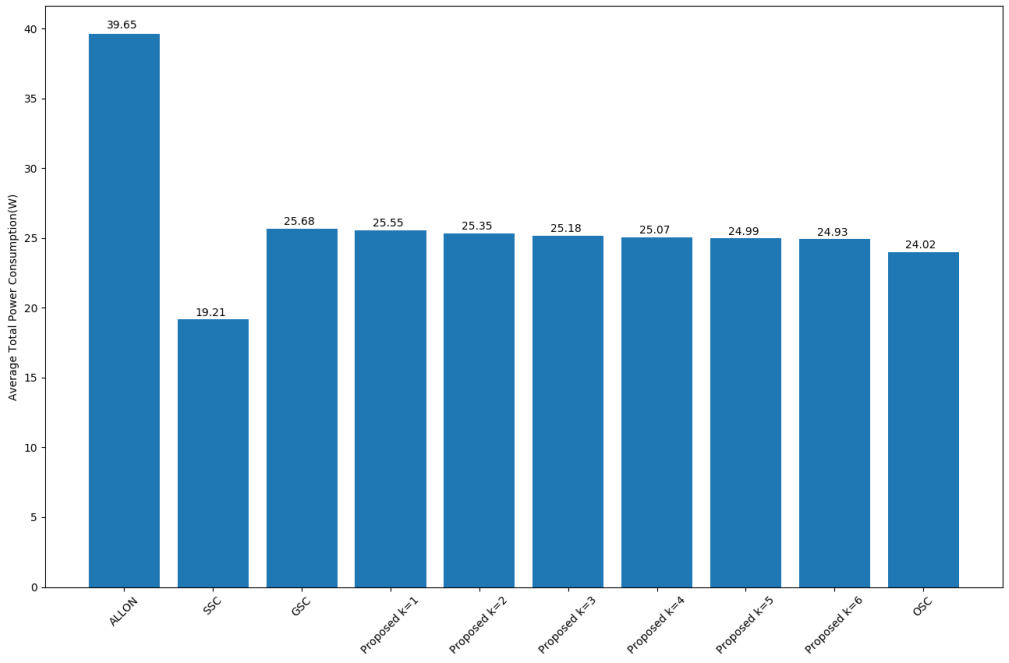

Fig. 4.5 Overall performance for different algorithms about average total power consumption.

remains 100% under different values of σ. As to SSC, the SR remains low (about 75%), which is consistent to previous analysis about Fig.4.3.

An overall evaluation of different algorithms about APC and SR are given in Fig.4.5 and Fig.4.6, respectively. According to the results, it can be found that increasing k can significantly improve the performance of proposed algorithm, with decreasing APC and increasing SR. Specifically, when $k \geq 5$, the SR of proposed algorithm will be 100%. The APC of it is significantly improved compared with GSC. Besides, the small SR of SSC (77.61%) is intolerable in this work.

Table.4.2 demonstrates the complexity and prediction accuracy of different algorithms for different number of BSs. Results are achieved on an Intel i5 2.90GHz 16GB computer. It can be observed that the prediction accuracy of the proposed algorithm is significantly improved compared to other algorithms for any number of SBSs. And the complexity of the proposed algorithm has a better performance when the number of SBSs is equal to or greater than 5. Besides, increasing k for the proposed algorithm can further improve the prediction accuracy with almost the same complexity. Moreover, as the number of BSs increases, the complexity for proposed algorithm is more and more superior compared with existing approaches. Notably, the lowest complexity for SSC is at the cost of low prediction accuracy, which is not recommended in this work.

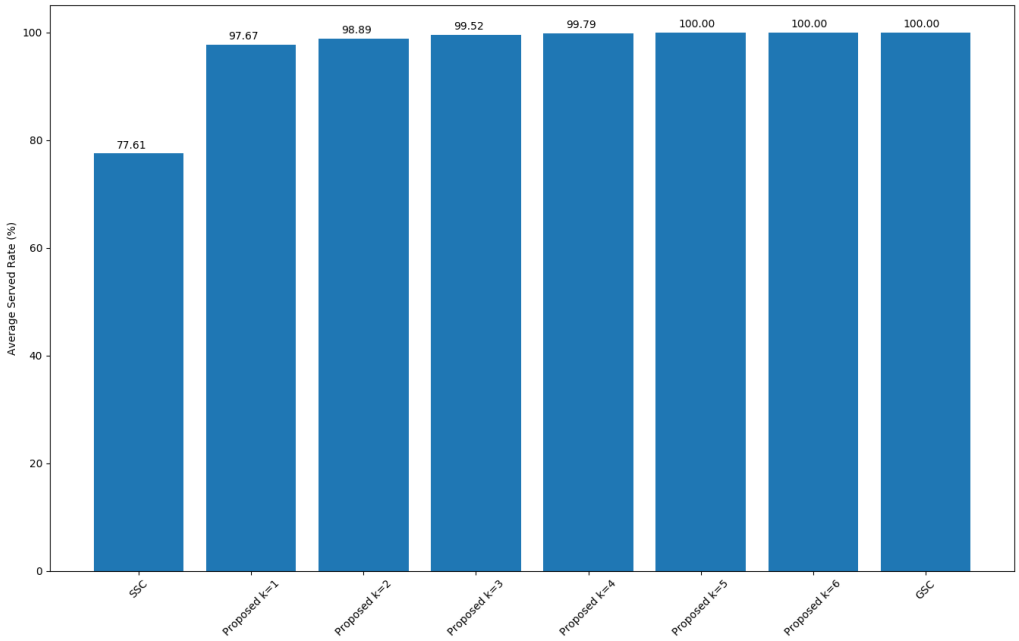

Fig. 4.6 Overall performance for different algorithms about served rate.

Table 4.2 Comparison for KNN-based algorithm under different No. of BSs

No. BSs	Algorithms	Complexity(s)	Prediction accuracy(%)
N =3	Proposed $k=2$	1.3	85.8%
	Proposed $k=4$	1.4	89.3%
	Proposed $k=6$	1.4	92.6%
	GSC	13.3×10^{-3}	56.3%
	SSC	0.6×10^{-3}	15.8%
	OSC	33.6×10^{-3}	100%
N =5	Proposed $k=2$	1.4	78.6%
	Proposed $k=4$	1.3	83.7%
	Proposed $k=6$	1.4	85.5%
	GSC	3.1	33.4%
	SSC	2.6×10^{-3}	6.5%
	OSC	17.6	100%
N =8	Proposed $k=2$	1.4	70.2%
	Proposed $k=4$	1.4	73.5%
	Proposed $k=6$	1.5	76.3%
	GSC	59.1	21.8%
	SSC	12.8×10^{-3}	4.8%
	OSC	386.5	100%

4.3.3 Conclusion

In this section, the author proposes a KNN-based centralized sleeping control and bandwidth allocation scheme to minimize the power consumption while satisfying the transmission rate requirements. A central controller, which can be standalone or integrated with an SBS, determines the sleeping strategy of the considered SBSs via a KNN-based algorithm. Simulation results show that the proposed algorithm has a better performance compared with existing approaches in terms of average total power consumption, served rate, prediction accuracy and complexity.

4.4 CNN-based Centralized Sleeping Control and Bandwidth Allocation Scheme

4.4.1 CNN-Based Solution of the CSC Sub-problem

For any given transmission rate requirements in $M \times M$ grids, it is a straightforward thinking to solve the CBA sub-problems successively corresponding to all the possible sleeping strategies and then find the best one that makes the optimal problem in (4.7) have feasible solutions and the optimal solution in (4.7) achieve the lowest value among all the possible sleeping strategies. However, the computational complexity of exhaustively searching the strategy space increases exponentially as the number of considered SBSs gets larger. In order to reduce the computational complexity, the author utilizes the generalization ability of the state-of-art deep learning technology to generate approximately optimal sleeping strategy for any new given transmission rate requirements based on the knowledge about well-solved CSC sub-problems.

Regarding the transmission rate requirements in $M \times M$ grids as input features, regarding the theoretically optimal sleeping strategy for the N SBSs as the class related to input features, the CSC sub-problem is transformed into a classification problem and can be handled by CNN. Obviously, the class number in this scenario is 2^N.

CNN is a class of deep neural network which is particularly suitable for learning tasks with large dimensions of input features. Due to the deep neural network structure and the sharing of neuronal connection weights, CNN can capture the complex dependencies at different levels from input features and significantly reduce the complexity in training process. CNN has already been widely used in many fields like pattern recognition and image classification. The architecture of CNN used in this section is illustrated in Fig.4.7. The inputs of the CNN is a tensor with shape $M \times M$ representing the normalized transmission rate

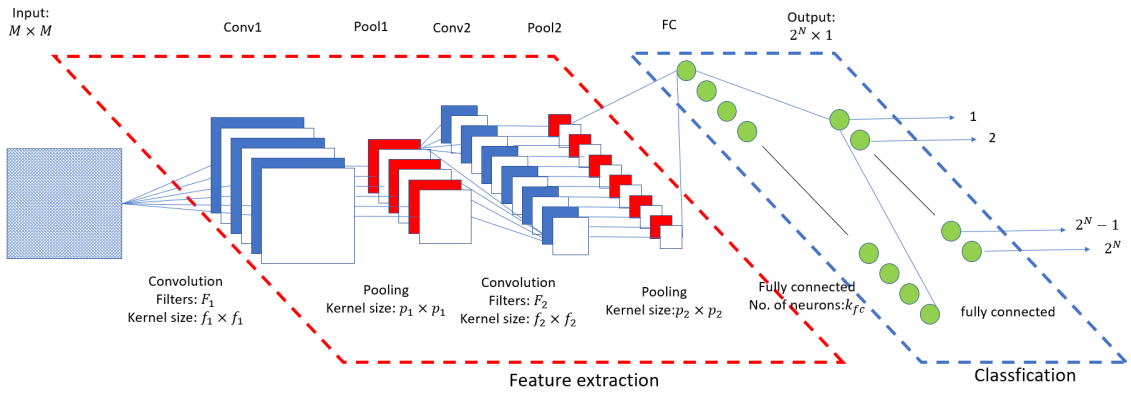

Fig. 4.7 CNN structure used in this paper.

requirements in the $M \times M$ grids (each element is calculated as the ratio of actual transmission rate requirement in a grid to the possibly maximum transmission rate in a grid). The output of the CNN is a 2^N-dimension vector representing the 2^N possible sleeping strategies for the N SBSs. If the i-th element has the largest value among CNN's output vector, the i-th sleeping strategy will be selected as the solution of the CSC sub-problem related to the specific transmission rate requirements in the $M \times M$ grids. The matching of strategy i with the statuses of the N SBSs is a inverse transformation of (4.11), which will not be given here.

As shown in Fig.4.7, the CNN consists of L convolutional layers, L pooling layers, and a fully connected hidden layer. In each convolutional layer l, F_l convolution filters are used to produce F_l feature maps for each input map of this layer. The convolution filters in the convolutional layer l have the same size of $f_l \times f_l$. Convolutional layer l is followed by a pooling layer, which reduces the dimensions of feature maps by sub-sampling them with the same pooling kernel ($p_l \times p_l$), in order to combat overfitting as well as shorten the training complexity. Finally, a fully connected hidden layer with k_{fc} neurons is used to transform the final feature maps into the output vector.

The proposed CNN is trained via examples in a training set $\mathbb{H}$. Each training example H in $\mathbb{H}$ is constructed by labelling the specific normalized transmission rate requirements in the $M \times M$ grids, $T^{(H)}$, with a 2^N-dimension vector, $v^{(H)}$. Besides the $i_{best}^{(H)}$-th element, which equals 1 and represents the theoretically optimal SBS sleeping strategy corresponding to $T^{(H)}$, other elements in $v^{(H)}$ have the same value of 0. Particularly, for any $T^{(H)}$, the theoretically optimal sleeping strategy can be found through exhaustively searching method, which solves the CBA sub-problems related to all the 2^N possible sleeping strategies, then finds the strategy making (4.7) have a feasible solution and the minimal value.

4.4.2 Testing and Results

In this section, the performance of proposed CNN-based scheme is evaluated under different scenarios. The region, and the dataset generation considered in this work are the same as that in **Sect 4.3.2**, which will not be described here. The CNN structure in this work consists of two convolutional layers and two pooling layers. The activation functions for convolutional-layer neurons are ReLU, while each neuron in the output layer is activated by a softmax function. As a standard procedure, back-propagation of an adaptive moment estimation (Adam) optimizer is used for training, and the categorical cross-entropy is taken as the cost function. Notably, other CNN structures can also be adopted in the proposed scheme. However, the optimization of CNN structure is out of scope for this work. Parameters used in this work are summarized in Table 4.3.

For this work, five benchmarks, non-sleep(ALLON), probability-based strategic sleeping control (SSC) [200], greedy sleeping control (GSC) [201], optimal sleeping control (OSC), and the KNN-based algorithm proposed in the previous section are employed for comparison. After the prediction results (sleeping strategies) are obtained by these algorithms, the bandwidth allocation for the active SBSs will then be obtained by solving the corresponding CBA sub-problem, except SSC algorithm, for which the transmission rate requirement in each grid is served by the active SBS which provides the maximum SINR. Thus, the overall power consumption minimization of the system can be obtained.

If the CBA sub-problem has no feasible solution for the sleeping strategy given by a specific algorithm, a best-effort solution will be employed to maximize the served traffic, given in (4.21).

Fig.4.8 presents the average total power consumption (APC) for different algorithms under different values of σ when $\mu = 4.5$. It can be seen that as σ increases, the average total power consumptions of all algorithms increase, which is because greater power consumption is needed to serve the traffic requirements as the spatial inhomogeneity of traffic increases. The APC for the ALLON algorithm is always the greatest. Compared to KNN-based algorithm, the APC for the proposed scheme is always smaller, and is almost the same as that of OSC, achieving near-optimal performance because of the generalization ability of CNN and acquired knowledge. Specifically, the APC of SSC are equal to or smaller than that of OSC, because the traffic requirements are not guaranteed by SSC. Therefore, the smaller APC in SSC is achieved at the expenses of small served rates, which is not recommended in this work.

The served rate (SR) for different algorithms under different values of σ when $\mu = 4.5$ is shown in Fig.4.9. Since there will always be a sleeping strategy to satisfy the traffic requirements, it is explicit that the SR for ALLON and OSC will always be 100%. Therefore,

Table 4.3 Parameters for CNN-based algorithm

Parameter	Symbol	Value
Region of Area	B	$100 \times 100m^2$
No. of BSs	N	3, 5, 8
No. of grids	$M \times M$	25×25
Bandwidth	BW	5MHz
Transmit power of SBSs	P_{tx}	-30dBm/Hz
Static power consumption	P_0	38dBm
Sleep power consumption	P_s	27dBm
Path loss exponent	α	-4
Noise	σ^2	-174dBm/Hz
No. of filters for convolution layers	F_1/F_2	$32/64$
Kernel size for convolution layers	f_1/f_2	$3/3$
Kernel size for pooling layers	p_1/p_2	$2/2$
No. of units in fully connected layer	k_{fc}	512
No. of samples for each pair of μ and σ	TW	1000
Proportion of training set	η	0.7
Spatial inhomogeneity factor	σ	$0.1-1$
Mean traffic load factor	μ	$3.5-5.4$

it will not be shown for this metrics. From Fig.4.9, it can be seen that the SR of SSC remains small as σ increases, which is consistent to previous analysis. Meanwhile, the SR of the proposed algorithm, GSC, and KNN-based algorithm remain 100% under different values of σ. Combining the results in Fig.4.8 and Fig.4.9, it can be concluded the proposed scheme always achieves near-optimal performance with near-optimal APC and 100% SR under different values of σ, while KNN-based algorithm and GSC have an abundant waste of power consumption and SSC experiences low SR.

Fig.4.10 shows the APC for different algorithms under different values of μ when $\sigma = 0.2$. From Fig.4.10, it can be found that as the mean traffic load increases, the APC of all algorithms increase rapidly to serve greater traffic requirements. As μ increases, the APC for the ALLON algorithm is always the greatest. When the traffic load in the region is low ($\mu < 4.0$), it can be seen that the APC of GSC, KNN-based algorithm, proposed algorithm, and OSC are almost the same. Notably, APC for proposed algorithm is slightly smaller than that of OSC when $\mu = 4.0$ at the expense of unserved traffic. When the traffic load gets high ($\mu > 4.0$), GSC and KNN-based algorithm will have an abundant waste of power. As to SSC, it can be seen that it has an abundant waste of power when the traffic load is low ($\mu < 4.0$) and has smaller APC at the expense of unserved traffic when the traffic load is high ($\mu \geq 4.0$).

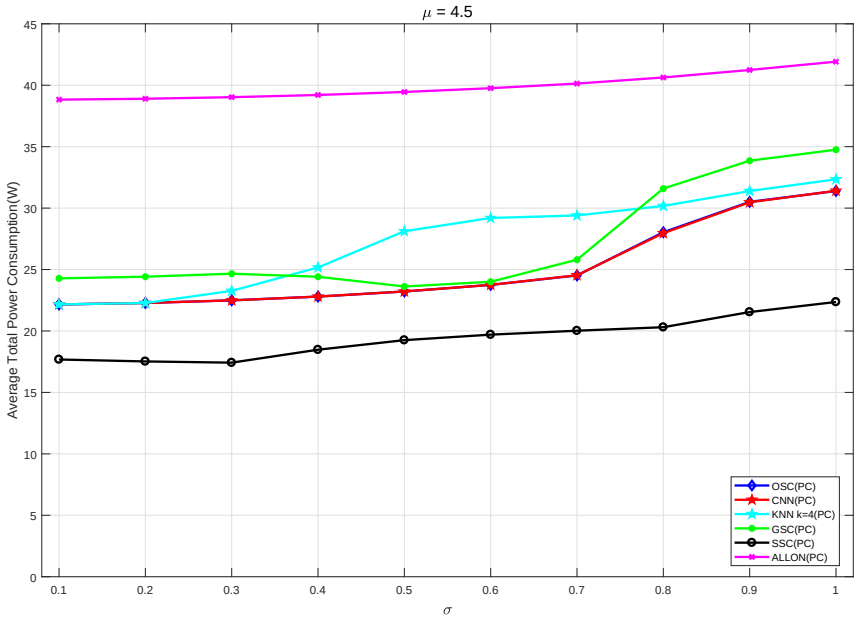

Fig. 4.8 Comparison of average total power consumption for different algorithms under σ with fixed $\mu = 4.5$.

The SR for different algorithms under different values of μ when $\sigma = 0.2$ is given in Fig.4.11. Similar to that of Fig.4.9, it can be seen that the SR of GSC, KNN-based algorithm, and proposed algorithm remains almost 100% under different values of μ. Specifically, the SR of proposed algorithm for $\mu = 4.0$ is 99.98%, which is consistent to the phenomenon in Fig.4.10.

Table.4.4 demonstrates the complexity, prediction accuracy and training time of different algorithms for different number of SBSs. Results are achieved on an Intel i5 2.90GHz 16GB computer. It can be observed that the complexity and the prediction accuracy of the proposed algorithm are significantly improved compared to other algorithms for any number of SBSs, while the offline training time is also acceptable. Moreover, as the number of SBSs increases, the complexity and prediction accuracy for proposed algorithm is more and more superior compared with existing approaches. Notably, the lowest complexity for SSC when $N = 3$ is at the cost of low prediction accuracy, which is not recommended in this work.

4.4.3 Conclusion

In this section, a CNN-based centralized sleeping control and bandwidth allocation scheme is proposed to minimize the power consumption while satisfying the transmission rate requirements in a given region. A central controller determines the sleeping strategy of the

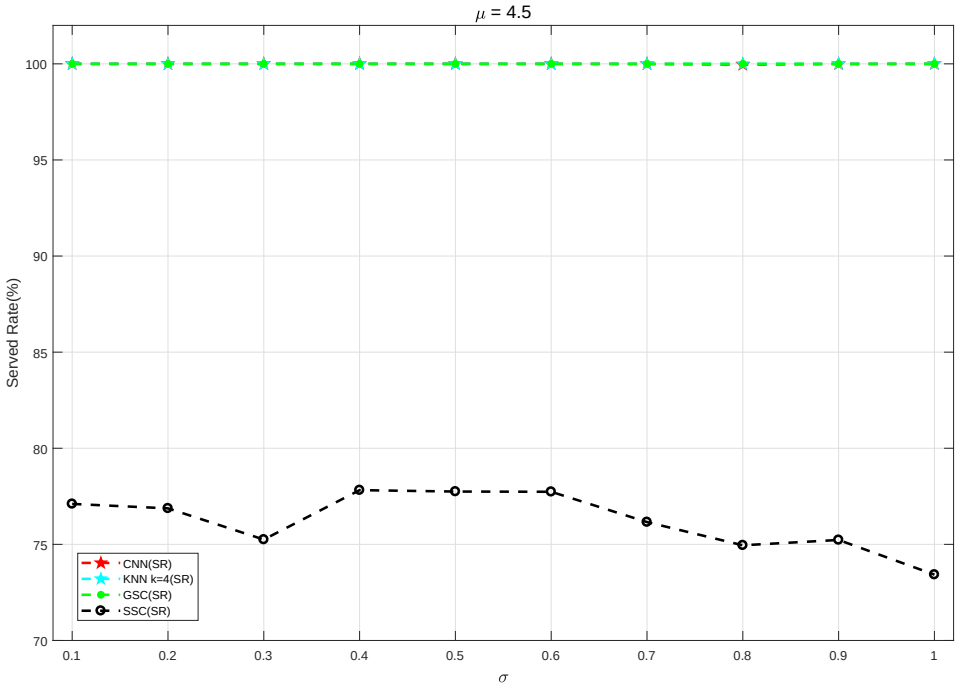

Fig. 4.9 Comparison of served rate for different algorithms under σ with fixed $\mu = 4.5$.

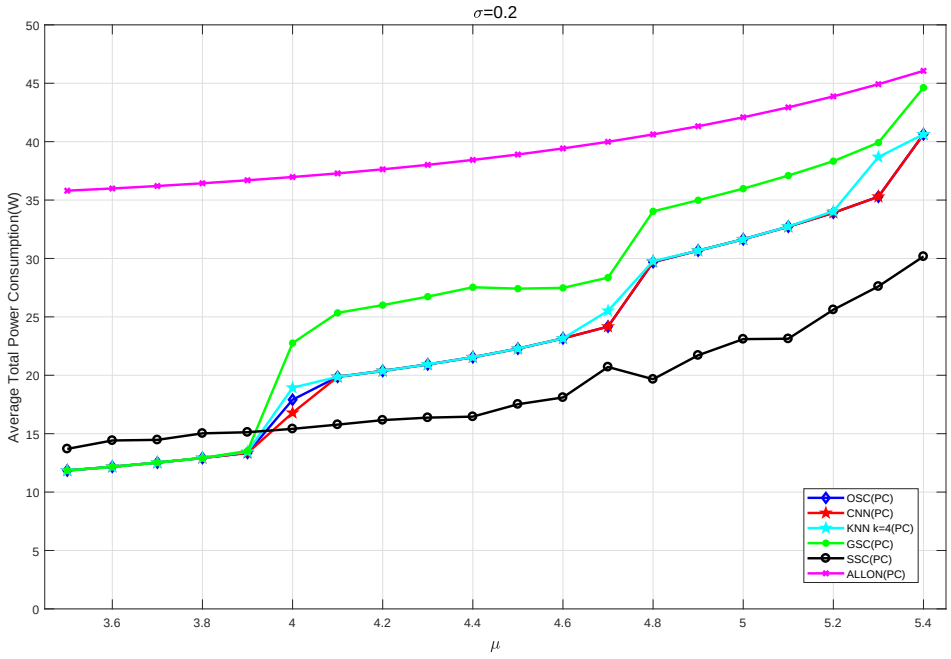

Fig. 4.10 Comparison of average total power consumption for different algorithms under μ with fixed $\sigma = 0.2$.

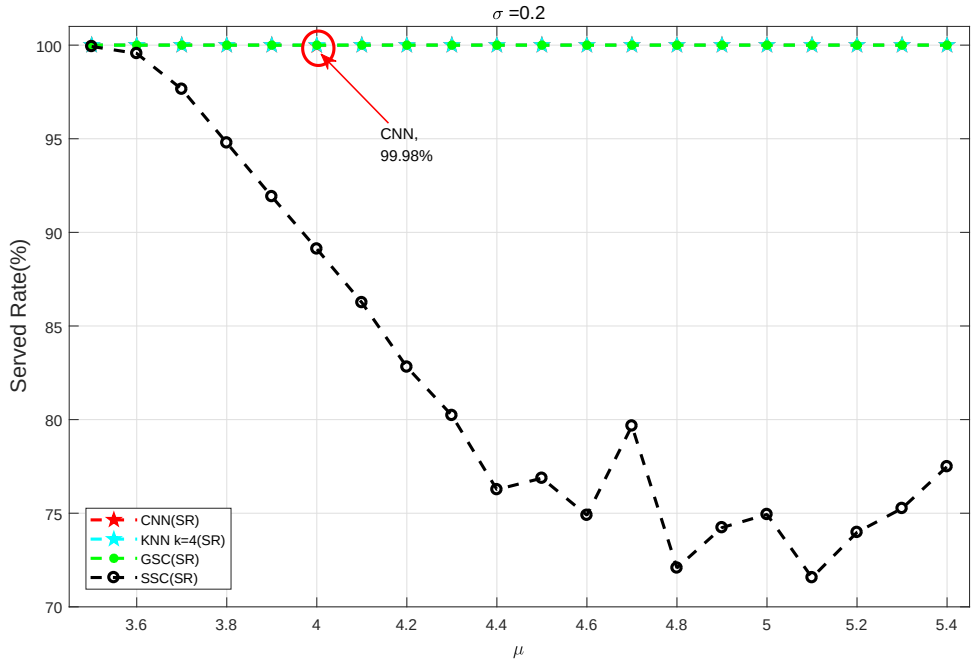

Fig. 4.11 Comparison of served rate for different algorithms under μ with fixed $\sigma = 0.2$.

Table 4.4 Comparison for CNN-based algorithm under different No. of BSs.

No. BSs	Algorithms	Complexity(ms)	Prediction accuracy(%)	Training Time (s)
N =3	Proposed	1.5	99.8%	562
	KNN-based $k = 4$	1.4×10^3	89.3%	
	GSC	13.3	56.3%	/
	SSC	0.6	15.8%	/
	OSC	33.6	100%	/
N =5	Proposed	2.1	97.3%	645
	KNN-based $k = 4$	1.3×10^3	83.7%	
	GSC	3.1×10^3	33.4%	/
	SSC	2.6	6.5%	/
	OSC	17.6×10^3	100%	/
N =8	Proposed	4.4	89.6%	1288
	KNN-based $k = 4$	1.4×10^3	73.5%	
	GSC	5.9×10^4	21.8%	/
	SSC	12.8	4.8%	/
	OSC	3.9×10^5	100%	/

considered SBSs via a well-trained CNN model. Simulation results show that the proposed

scheme has significant performance improvements compared to existing approaches in terms of average total power consumption, served rate, complexity, and prediction accuracy.

4.5 Summary

In this chapter, a joint sleeping control and bandwidth allocation (SCBA) problem is introduced and formulated. The author decouples the joint SCBA problem into centralized bandwidth allocation (CBA) sub-problem which minimizes the power consumption by optimizing the bandwidth allocation of the active SBSs, and centralized sleeping control (CSC) sub-problem which minimizes the power consumption by optimizing the sleeping strategy of all SBSs. The theoretically optimal bandwidth allocation method for active SBSs to serve the traffic requirements and minimize the power consumption is given. Two centralized sleeping control algorithms are proposed based on KNN and CNN, respectively. For the KNN-based algorithm, it is quite simple for implementation since there is no need for training. Simulation results show the superiority of the KNN-based algorithm compared with existing algorithms. However, since it is a lazy learning method, the complexity of this algorithm is relatively high. Besides, the size of historical dataset and the definition of distance in (4.12) will affect the performance of the proposed algorithm (not discussed in this work). To fill the gap, a CNN-based algorithm is proposed with training procedure. Simulation results show that the complexity of this algorithm is low, and the network performance, including average total power consumption, served rate, complexity, and prediction accuracy etc., are significantly improved compared to existing approaches. Since these two algorithms are both based on historical datasets, which sometimes are not available, an alternative algorithm without need of historical datasets will be investigated in next chapter.

Chapter 5

Energy Efficient Centralized Sleeping Control and Bandwidth Allocation for Small Base Stations based on Reinforcement Learning

Overview

To fill the gap mentioned in previous chapter that tremendous datasets is needed, a Q-learning based mechanism is introduced to address the joint sleeping control and bandwidth allocation (SCBA) problem in this chapter. Subject to the transmission rate requirements, the joint SCBA problem is formulated into a mixed integer non-linear programming (MINLP) problem, and decoupled into a centralized bandwidth allocation (CBA) sub-problem and a centralized sleeping control (CSC) sub-problem. By regarding the sleeping strategies as arms, mapping the transmission rate requirements to states, and defining the optimal CBA solution corresponding to a sleeping strategy as the arm's reward function, the CSC sub-problem is transformed into a multi-state multi-arm bandit (MSMAB) problem, and solved by a modified Q-learning algorithm. The convergence of the modified Q-learning algorithm, and the computational complexity of the proposed mechanism are theoretically analyzed. Numerical results show the proposed mechanism has a low computational complexity and can significantly reduce the total energy consumption of all SBSs, subject to the transmission rate requirements compared with existing methods.

5.1 System Model and Problem Formulation

5.1.1 System Model

The system model is illustrated in Fig.5.1. A typical RAN scenario where N SBSs cover a region $\boldsymbol{B}$ is considered. The focus in this chapter is on the downlink. The N SBSs are distributed following a homogeneous Poisson point process. Region $\boldsymbol{B}$ is further divided into $M \times M$ grids, which are small enough so that different mobile users in the same grid are assumed to have equal distances from an arbitrary SBS. Transmission rate requirements generated in $M \times M$ grids are entirely served by the N SBSs. Specifically, each SBS may serve the transmission rate requirements in different grids while the transmission rate requirement generated in a single grid may also be simultaneously served by multiple SBSs. A central controller, which can be standalone, or integrated with a SBS, controls the N SBSs to switch on/off and allocates bandwidth to SBSs periodically based on the system's global information. For analytical tractability, it is assumed that users in each grid see the same external-interference environment and have a constant spectral noise power density. Note that traffic prediction for mobile networks [202–204] is out of scope of this work.

Assume that the N SBSs use orthogonal spectrum resources and occupy equal downlink transmission bandwidth of $\boldsymbol{BW}$ [198]. Each SBS can set multiple downlink connections concurrently in an orthogonal frequency division multiple access (OFDMA) way. A constant P_{tx} is used to denote the spectral transmit power density of the SBSs. The sleeping state of SBS n is denoted by $a_n \in \{0,1\}$. a_n =1 represents that SBS n is active. Otherwise, the SBS n is in the sleep state. Thus, the $SINR_{n,m}$ between SBS n and grid m can be formulated as:

$$SINR_{n,m} = \frac{a_n \cdot P_{tx} \cdot g_{n,m}}{\sigma^2} \tag{5.1}$$

where $g_{n,m}$ denote the channel power gains from SBS n to grid m. For any $n \in \{1,...,N\}$, $g_{n,m} = d_{n,m}^{-\alpha} \cdot |h_{n,m}|^2$, where $d_{n,m}$ is the distance between SBS n and grid m, α ($\alpha > 2$) is the path loss exponent, $h_{n,m}$ denotes the complex Gaussian channel coefficients following $h \sim CN(0,1)$, and σ^2 denotes the constant spectral noise power density.

5.1.2 Problem Formulation

Assume the bandwidth allocated by SBS n to grid m is denoted by $bw_{n,m}$. According to Shannon's theory, the expected transmission rate provided by SBS n to grid m can be

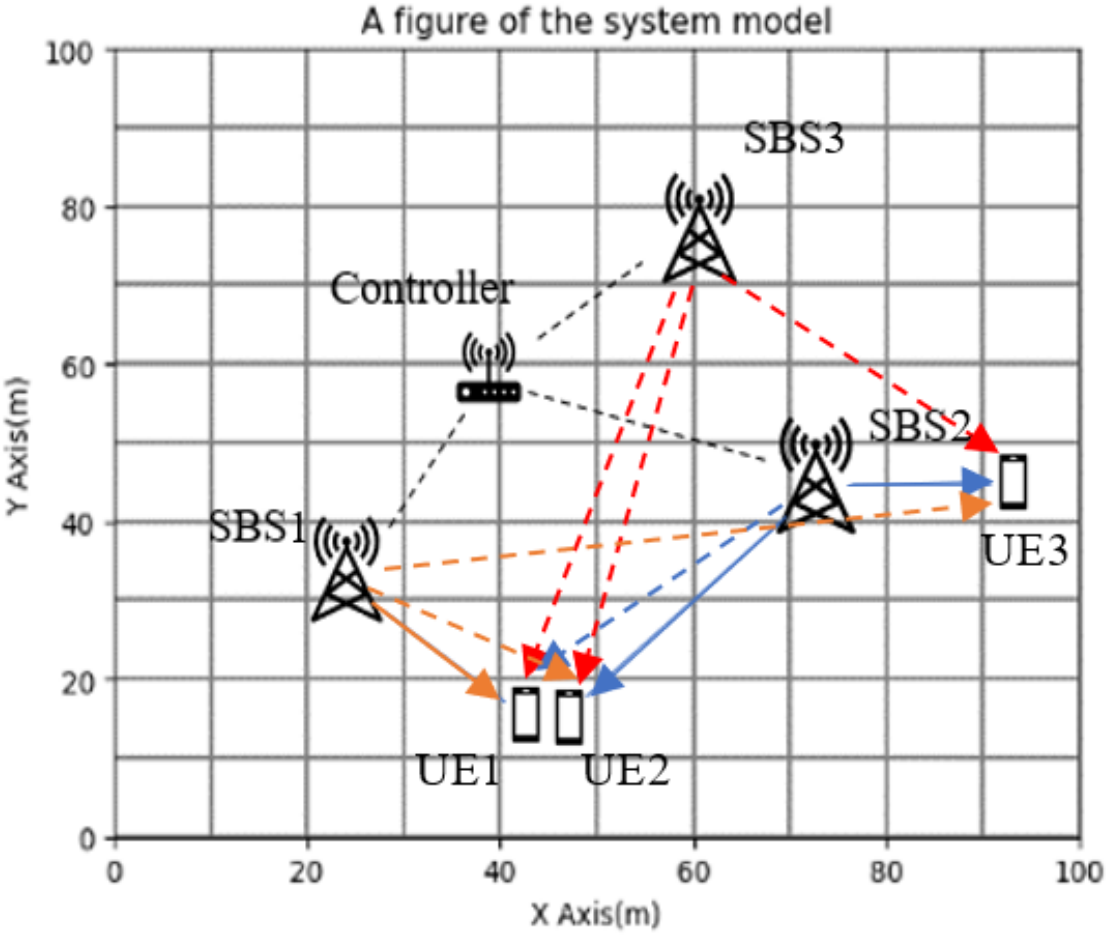

Fig. 5.1 A figure of the system model includes several SBSs and a standalone controller. The solid lines with arrows denote the transmission signals between SBSs and UEs in different grids. The coloured dotted lines with arrow represent the interference signals caused by different SBSs, while the black dotted lines between controller and SBSs denote the control signals.

formulated as:

$$t_{n,m} = bw_{n,m} \cdot \mathbb{E}_{h_{n,m}}[\log_2(1 + SINR_{n,m})] \tag{5.2}$$

Suppose that each time interval has the fixed duration of D, based on the SBS power consumption model proposed in [4], the energy consumption (Wh) of SBS n in the considered time interval can be expressed as:

$$E_n = a_n \cdot (P_0 + P_{tx} \sum_{m=1}^{M^2} bw_{n,m}) \cdot D + (1 - a_n) \cdot P_s \cdot D \tag{5.3}$$

where P_0 is the static power consumption of an active SBS, including the power consumption of radio frequency (RF) circuit, processing, cooling etc., $P_{tx} \sum_{m=1}^{M^2} bw_{n,m}$ denotes the load-dependent dynamic power consumption of SBS n, P_s denotes the power consumption of an SBS when it is in sleep state.

Subject to given transmission rate requirements in the $M \times M$ grids, the author aims to jointly solve the SCBA problem for the N SBSs to minimize the total power consumption of the SBSs. For a considered time interval, t_m is used to denote the transmission rate requirement in grid m during this time interval. The joint optimization problem can be formulated as:

$$\arg\min_{a_n, bw_{n,m}} \sum_{n=1}^{N} E_n \tag{5.4}$$

$$\text{s.t.} \quad \sum_{m=1}^{M^2} bw_{n,m} \leq a_n \cdot BW, \quad \forall n \in \{1, ..., N\} \tag{5.5}$$

$$\sum_{n=1}^{N} t_{n,m} \geq t_m, \quad \forall m \in \{1, ..., M^2\} \tag{5.6}$$

$$a_n \in [0, 1], \quad \forall n \in \{1, ..., N\} \tag{5.7}$$

$$bw_{n,m} \geq 0, \quad \forall n, m \tag{5.8}$$

Eq. (5.4) is the objective of the optimization problem, which aims to minimize the total energy consumption of the SBSs during a considered time interval. Constraint (5.5) denotes that the overall occupied bandwidth of each SBS should be smaller than the total available bandwidth. Constraint (5.6) denotes that the total provided transmission rate from all SBSs to each grid should be equal or greater than its transmission rate requirement. Constraint (5.7) denotes that each SBS can either be active or sleeping, while constraint (5.8) denotes that the allocated bandwidth from any SBS to any grid is non-negative.

5.2 Proposed Mechanism

The optimization problem (5.4) is an MINLP problem, which is hard to solve. Since the sleeping strategy and loads of SBSs both affect the energy consumption, and the bandwidth allocation is performed for active SBSs only, a straightforward idea to address the optimization problem is exhaustive searching, which compares the energy consumptions of optimal bandwidth allocation corresponding to all the possible sleeping strategies of the N SBSs and finds the minimum. However, exhaustive searching techniques are not practical when the network size becomes large. In this chapter, the author proposes to use Q-learning since it is suitable for solving problems with environments that continually change, such as the transmission rate requirements changing along with time, and can learn without need of pre-training procedure. Furthermore, the computational complexity of a Q-learning algorithm is low compared to other exhaustive searching algorithms. The original optimization problem is decoupled into a centralized bandwidth allocation (CBA) sub-problem and a centralized sleeping control (CSC) sub-problem. Since the optimal solution of CBA sub-problem has been proved in **Chapter 4**, it will not be described here.

5.2.1 Transforming the CSC Sub-problem into a MSMAB Problem

A basic diagram of Q learning is illustrated in Fig.5.2. In iteration t, the agent observes the state S_t from the environment, and takes an action A_t based on the accumulated knowledge from historical iterations and a specific action selecting policy. After the action A_t is carried out, the environment will be transformed into a new state S_{t+1}, and give the agent a reward R_{t+1}, which may be affected by the state transformation and action adopted by the agent. After enough iterations, the agent can learn which action is the best for a specific state to achieve a goal, such as maximizing the instantaneous reward in this iteration or the accumulative rewards in some future successive iterations.

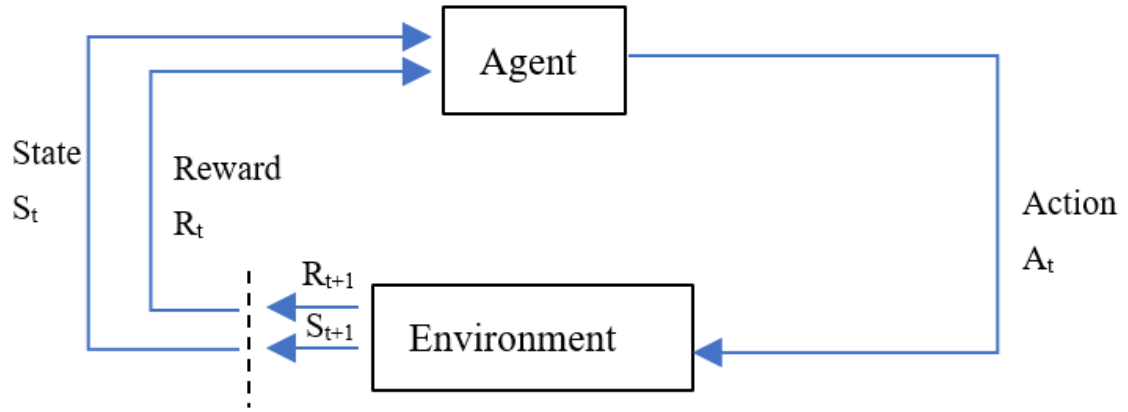

Fig. 5.2 A basic diagram of Q learning[7]

Consider the controller as the agent while considering the $M \times M$ grids in the region as the environment. The state space in proposed algorithm is based on the transmission rate requirements in the $M \times M$ grids, rather than the load of SBSs used in some other researches[187, 189, 175]. A specific state in this work not only contains the information of traffic load in each grid, but also captures the traffic's spatial characteristics, which will help the agent make global optimal decisions. Inspired by the common sense that similar spatio-temporal distributions of traffic will lead to approximate system performances in terms of traffic unserved rate and total power consumption if they are served by the same group of active SBSs, a discrete state space where multiple similar transmission rate requirements are mapped to the same state is considered. The 2^N possible sleeping strategies of the N SBSs are considered as different actions.

Specifically, the agent, the environment, the state, the action and the reward in this work are defined as follows:

- Agent: The controller of the system.
- Environment: The $M \times M$ grids
- State: Based on the expected transmission rate requirements in the $M \times M$ grids, the transmission rate requirement in grid m is quantized by a grid depth, β, which represents the number of quantization levels, based on the following equation:

$$Stepsize = \frac{t_{max}}{\beta} \tag{5.9}$$

$$s_m = \left\lfloor \frac{t_m}{Stepsize} \right\rfloor \tag{5.10}$$

where t_{max} is defined as the upper bound of the transmission rate requirement in each grid. $Stepsize$ refers to the quantization step size. s_m denotes the quantization level in grid m. $\left\lfloor \frac{t_m}{Stepsize} \right\rfloor$ represents the largest integer equal or smaller than $\frac{t_m}{Stepsize}$. The state of the environment is then given by

$$S = [s_1, ..., s_m, ..., s_{M^2}] \tag{5.11}$$

For the convenience of representation, the author uses an index i to represent a specific state in state space, the mapping equation is given by:

$$i = \sum_{m=1}^{M^2} s_m \cdot \beta^{m-1} + 1 \tag{5.12}$$

- Action: An actions A is defined as one possible sleeping strategy, which contains the sleeping choices of all the N SBSs, given by

$$A = [a_1, ..., a_n, ..., a_N] \tag{5.13}$$

where $a_n = \{0,1\}$. For example, if $A = [1,0,0,...,0]$, it means the agent takes an action to switch on the first SBS and switch off the other SBSs. For N SBSs, it is obvious that there are 2^N actions. For the convenience of representation, the author uses an index j to represent a specific action as follows:

$$j = \sum_{n=1}^{N} a_n \cdot 2^{n-1} + 1 \tag{5.14}$$

- Reward: The reward function is designed to reflect the system performance achieved by a selected action. For given transmission rate requirements in the $M \times M$ grids $T = [t_1, ..., t_m, ..., t_{M^2}]$, and a given action j, if the CBA sub-problem has no feasible solution, thereby meaning some grids' transmission rate requirements cannot be satisfied by

the active SBSs, the reward value is defined as a large negative constant to represent the penalty factor for this action. Conversely, if the CBA sub-problem has feasible solutions, the reward value is defined as the opposite number of the optimal value in the CBA sub-problem. An action may achieve a larger reward value if the active SBSs can satisfy the transmission rate requirements and lead to a lower total energy consumption of the SBSs. The mathematical expression of reward value is given as follows:

$$r = \begin{cases} \lambda, \\ \quad \textit{CBA sub-problem has no feasible solution} \\ -1 \cdot \min\limits_{bw_{n,m}} \sum\limits_{n=1}^{N} E_n, \\ \quad \textit{CBA sub-problem has feasible solution} \end{cases} \tag{5.15}$$

where λ is a negative constant, the absolute value of which should be greater than the maximal total energy consumption in the system.

At the beginning of each time interval, the agent (controller) will transform the expected transmission rate requirements in the $M \times M$ grids into a specific state and choose a proper action (sleeping strategy) according to an action selecting policy. Then, for the given transmission rate requirements and action (sleeping strategy), the agent will calculate and record the reward in this time interval according to (5.15). Notably, since various transmission rate requirements in the $M \times M$ grids are concluded in one state, the agent may obtain different values of reward in different time intervals even though it observes the same state and adopts the same action. Since the states are independent from one another, and the reward value achieved by an arbitrary action is only determined by the current state (transmission rate requirements) and the action (sleeping strategy), the CSC sub-problem is equivalent to a MSMAB problem if the 2^N actions are defined as arms.

5.2.2 Modified Q-learning Algorithm for CSC Sub-problem

To handle the MSMAB problem, a modified Q-learning algorithm is presented to minimize the energy consumption for the current state while neglecting the influence of the next state. The objective of the proposed algorithm is to train an intelligent agent that will automatically

	1	2	.....	j	.....
1	$Q_{1,1}$	$Q_{1,2}$	.....	$Q_{1,j}$	.....
2	$Q_{2,1}$	$Q_{2,2}$	.....	$Q_{2,j}$	.....
⋮	.....	.....	.....	.....	.....
i	$Q_{i,1}$	$Q_{i,2}$	.....	$Q_{i,j}$	.....
⋮	.....	.....	.....	.....	.....

Fig. 5.3 A basic diagram of Q table

select the action (sleeping strategy) with the largest expected Q value for any given state through historical experience. A Q table is constructed and maintained to record the average reward value for every state-action pair. As shown in Fig.5.3, the columns of the Q table represent the possible states, while the rows denote the possible actions. An arbitrary element $Q_{i,j}$ in the Q table is calculated as:

$$Q_{i,j} = \frac{1}{C_{i,j}}[r_{i,j}(T^{(1)}) + r_{i,j}(T^{(2)}) + ... + r_{i,j}(T^{(C_{i,j})})] \tag{5.16}$$

where $T^{(1)}, T^{(2)}, ..., T^{(C_{i,j})}$ are the samples of transmission rate requirements in the $M \times M$ grids mapped to state i, $C_{i,j}$ is the times that action j was chosen for state i in the past, and $r_{i,j}(T^{(c)})$ is the corresponding reward when the action j is c-th chosen for state i.

The agent confronts an explore-exploit dilemma at every iteration. On one hand, for the given transmission rate requirements in the $M \times M$ grids and the corresponding state, choosing the action with the largest Q value in the Q table is more likely to acquire a good reward in this iteration. On the other hand, some actions may be performed unsatisfactorily

by accident. If the actions with the best performance in the past are always adopted, the better actions with larger reward values might be neglected due to inadequate exploration.

In this work, the author seeks to utilize the decreasing ε-greedy policy to address the explore-exploit dilemma mentioned above. At each iteration, the agent will observe the current state i^* and select either a random action among the 2^N actions with the probability of ε or the action that has a maximum Q value in the Q table for state i^* with the probability of $1-\varepsilon$. Then the agent will solve the CBA sub-problem corresponding to the selected action j^* (sleeping strategy) and obtain the reward value in this iteration. Then, the agent will update Q_{i^*,j^*} in the Q table using the following equation:

$$Q_{i^*,j^*} \Leftarrow \frac{Q_{i^*,j^*} \times C_{i^*,j^*} + r^*_{i^*,j^*}}{C_{i^*,j^*}+1} \tag{5.17}$$

where C_{i^*,j^*} denotes the times that action j^* was chosen for state i^* in the past, $r^*_{i^*,j^*}$ is the corresponding reward in current iteration.

The pseudo code of the training module for Q-learning-based algorithm is given in **Algorithm 6**. To give the agent more chances to test the performances of different actions for each state at the early stage of the reinforcement learning procedure, ε is initilized by a relatively large value in the proposed algorithm. Then ε decreases gradually as the iteration number becomes larger, thus the agent will be more likely to exploit the historical knowledge and choose the action with the maximum expected reward value.

Given a Q table with M^β rows and 2^N columns, the maximum iteration number K_{max}, the decaying period K_{dec}, and the decay rate η, the first two steps for this algorithm are to initialize the Q table and count table with the a specific value and zero, respectively. Then ε and iteration counting number k are initialized in step 3 and step 4. While the iteration counting number k is smaller than the maximum iteration number K_{max}, the algorithm will go to the training procedure. Step 6 firstly check if the iteration counting number k is divisible by the decaying period K_{dec}, if divisible, ε will be updated by $\eta \times \varepsilon$. By feeding a transmission rate requirement sample in step 9, the index of the corresponding system state i^k can be obtained based on (5.9), (5.10) and (5.12) in step 10. In step 11, the agent randomly selects an action j^* among the 2^N possible actions with probability ε, and selects the action j^* which has the largest Q value in the i^k-th row of the Q table with probability $1-\varepsilon$. Based on the chosen action and the system state, the reward value can be calculated based on (5.15) in step 12. Then the corresponding Q value and the count number will be updated in step 13

Algorithm 6 Proposed training module for Q-learning-based algorithm

Input: The Q table with M^{β} rows and 2^N columns, the maximum iteration number K_{max}, the decaying period K_{dec}, and the decay rate η.

Output: The well-trained Q table

Initialize the elements $Q_{i,j}$ ($i = 1,...,M^{\beta}, j = 1,...,2^N$) with the same value.
Initialize the counting number $C_{i,j}$ ($i = 1,...,M^{\beta}, j = 1,...,2^N$) with zero.
Initialize ε , ε belongs to (0,1].
Initialize the iteration counting number k with 1.
while $k \leq K_{max}$ **do**
  if $k \mod K_{dec} = 0$ **then**
    $\varepsilon = \eta \times \varepsilon$
  end if
  Acquire the transmission rate requirements of the M grids in this iteration $T^k = [t_1^k,...,t_m^k,...,t_{M^2}^k]$.
  Transform T^k into a specific state using (5.9) and (5.10), and then calculate the state index, i^k, using (5.12);
  With probability ε randomly select an action j^* among the 2^N possible actions, otherwise, select j^* that has the largest Q value in the i^k-th row of the Q table:

$$j^* = \arg\max_j Q_{i,j}$$

  Set $j^k = j^*$, and calculate the reward value of j^k , $r_{i^k,j^k}(T^k)$, using (5.15).
  Update the value of Q_{i^*,j^*} in the Q table based on (5.17).
  Update the counting number $C_{i^*,j^*} = C_{i^*,j^*} + 1$
  $k = k + 1$
end while

and 14. Finally, iteration counting number k is updated by $k+1$, and the algorithm goes to step 5 for next iteration.

For **Algorithm 6**, the following two **Lemmas** and **Corollary 1** are proven, respectively.

Lemma 1. The Q table will converge after enough iterations.

Proof:

For any given state i, and any given action j, the Q value in the Q table is calculated based on (5.17).

When $C_{i,j}$ is large enough, $Q_{i,j}$ will be the mean value of the reward. Assuming the number of all the possible samples of transmission rate requirements in state i is finite, denoted by Ω, and each of them has the same possibility p, then

$$Q_{i,j} = \sum_{\alpha=1}^{\Omega} p \times r_{i,j}(T^{\alpha}) \tag{5.18}$$

where $r_{i,j}(T^{\alpha})$ denotes the corresponding reward of transmission rate requirements sample T^{α} in state i when the action j is chosen.

Without loss of generality, it is assumed that part of possible traffic samples in each state have a reward of λ according to (5.15). The number of those traffic samples is denoted by Δ.

Then, (5.16) can be re-written as:

$$\begin{aligned}
Q_{i,j} &= \sum_{\alpha=1}^{\Delta} p \times r_{i,j}(T^{\alpha}) + \sum_{\beta=\Delta+1}^{\Omega} p \times r_{i,j}(T^{\beta}) \\
&= \lambda \cdot p \cdot \Delta - \sum_{\beta=\Delta+1}^{\Omega} p \cdot D \cdot \{ \sum_{n=1}^{N} [a_n \cdot (P_0 + P_{tx} \cdot \sum_{m=1}^{M^2} bw_{n,m}^{\beta}) + (1-a_n) \cdot P_s] \} \\
&= \lambda \cdot p \cdot \Delta - \sum_{\beta=\Delta+1}^{\Omega} p \cdot D \cdot \sum_{n=1}^{N} [a_n \cdot P_0 + (1-a_n) \cdot P_s] \\
&\qquad - \sum_{\beta=\Delta+1}^{\Omega} p \cdot D \cdot \sum_{n=1}^{N} a_n \cdot P_{tx} \cdot \sum_{m=1}^{M^2} bw_{n,m}^{\beta}
\end{aligned} \tag{5.19}$$

The first two parts of (5.19) are constants for a given action j and probability p. For a finite discrete random variable of the possible samples of transmission rate requirements, the

third part of (5.19) is also a constant. Therefore, $Q_{i,j}$ will converge after enough iterations for any given state and action.

More generally, considering a continuous distribution of the possible transmission rate requirements with any given probability distribution P, it can be similarly proven $Q_{i,j}$ will converge after enough iterations.

Lemma 2. $T^k = [t_1^k, ..., t_m^k, ..., t_{M^2}^k]$ and $T^l = [t_1^l, ..., t_m^l, ..., t_{M^2}^l]$ are two samples of transmission rate requirements in the $M \times M$ grids. If T^k and T^l simultaneously have feasible solutions or not for the CBA sub-problem of a given action j^* and $\left|t_m^k - t_m^l\right| \leq \mu$ for any $m \in \{1, ..., M^2\}$, a linear function of μ , $f_{j^*}(\mu)$ can be found, which satisfies $\left|r_{i,j^*}(T^k) - r_{i,j^*}(T^l)\right| \leq f_{j^*}(\mu)$ for any $\mu \geq 0$.

Proof:

For any sample of transmission rate requirements, the optimal solution of the CBA sub-problem can be obtained if it exists. If the samples of transmission rate requirements T^k and T^l do not have a feasible solution for the CBA sub-problem, the $r_{i,j^*}(T^k)$ and $r_{i,j^*}(T^l)$ equal λ according to (5.15). Then $\left|r_{i,j^*}(T^k) - r_{i,j^*}(T^l)\right|$ will be zero.

If both of them have feasible solutions for the CBA sub-problem, the optimal solution can and only can be obtained when the equality is established according to the characteristics of linear programming. Therefore, the optimal solutions for $T^k = [t_1^k, ..., t_m^k, ..., t_{M^2}^k]$ and $T^l = [t_1^l, ..., t_m^l, ..., t_{M^2}^l]$ will satisfy:

$$\begin{aligned} \sum_{n=1}^{N} bw_{n,m}^k \cdot \gamma_{n,m} &= t_m^k, \quad \forall m \in \{1, ..., M^2\} \\ \sum_{n=1}^{N} bw_{n,m}^l \cdot \gamma_{n,m} &= t_m^l, \quad \forall m \in \{1, ..., M^2\} \end{aligned} \tag{5.20}$$

where $\gamma_{n,m} = \mathbb{E}_{h_{n,m}}[\log_2(1 + SINR_{n,m})]$.

For the given condition, the following equation can be obtained,

$$\begin{aligned}\left|t_m^k - t_m^l\right| &= \left|\sum_{n=1}^{N} bw_{n,m}^k \cdot \gamma_{n,m} - \sum_{n=1}^{N} bw_{n,m}^l \cdot \gamma_{n,m}\right| \\ &= \left|\sum_{n=1}^{N} (bw_{n,m}^k - bw_{n,m}^l) \cdot \gamma_{n,m}\right| \\ &= \left|\sum_{n=1}^{N} bw_{n,m}^{\Delta} \cdot \gamma_{n,m}\right| \leq \mu, \quad \forall m \in \{1,...,M^2\}\end{aligned} \tag{5.21}$$

Thus,

$$\left|\sum_{n=1}^{N} bw_{n,m}^{\Delta}\right| \leq \frac{\mu}{\min\limits_{n} \gamma_{n,m}}, \quad \forall m \in \{1,...,M^2\} \tag{5.22}$$

where $bw_{n,m}^{\Delta} = bw_{n,m}^k - bw_{n,m}^l, \quad \forall n,m.$

Consider that both samples of transmission rate requirements have an optimal solution, then substitute (5.15) to the problem,

$$\begin{aligned}&\left|r_{i,j^*}(T^k) - r_{i,j^*}(T^l)\right| \\ &= \left|-D \cdot \left\{\sum_{n=1}^{N} [a_n \cdot (P_0 + P_{tx} \cdot \sum_{m=1}^{M^2} bw_{n,m}^k) + (1-a_n) \cdot P_s]\right\}\right. \\ &\qquad \left. + D \cdot \left\{\sum_{n=1}^{N} [a_n \cdot (P_0 + P_{tx} \cdot \sum_{m=1}^{M^2} bw_{n,m}^l) + (1-a_n) \cdot P_s]\right\}\right| \\ &= P_{tx} \cdot D \cdot \left|\sum_{n=1}^{N} a_n \cdot (\sum_{m=1}^{M^2} bw_{n,m}^l - \sum_{m=1}^{M^2} bw_{n,m}^k)\right| \\ &= P_{tx} \cdot D \cdot \left|\sum_{m=1}^{M^2} \sum_{n=1}^{N} a_n \cdot bw_{n,m}^{\Delta}\right|\end{aligned} \tag{5.23}$$

Then the boundary of $\left|r_{i,j^*}(T^k) - r_{i,j^*}(T^l)\right|$ can be found as

$$\begin{aligned}\left|r_{i,j^*}(T^k) - r_{i,j^*}(T^l)\right| &= P_{tx} \cdot D \cdot \left|\sum_{m=1}^{M^2}\sum_{n=1}^{N} a_n \cdot bw_{n,m}^{\Delta}\right| \\ \leq P_{tx} \cdot D \cdot \left|\sum_{m=1}^{M^2}\sum_{n=1}^{N} bw_{n,m}^{\Delta}\right| &\leq P_{tx} \cdot D \cdot \sum_{m=1}^{M^2} \frac{\mu}{\min\limits_{n} \gamma_{n,m}} = f_{j^*}(\mu)\end{aligned} \tag{5.24}$$

Thus, $f_{j^*}(\mu)$ is a linear function of μ and the coefficient is dependent on the parameters $\gamma_{n,m}$. When μ approaches zero, $f_{j^*}(\mu)$ will be approaching zero.

Corollary 1. Consider an arbitrary state i in the state space when the Q table has converged. If action j^* has the largest Q value in the i-th row of the Q table and all the possible samples of transmission rate requirements in the $M \times M$ grids mapped to state i simultaneously have feasible solutions or not for the CBA sub-problem corresponding to each action among the 2^N actions, then for any transmission rate requirements $T = [t_1, ..., t_m, ..., t_{M^2}]$ belonging to state i, j^* is the theoretical optimal action with maximum reward value as long as the grid depth β is large enough.

Proof:

Suppose the action j^* has the largest Q value in the i-th row of the Q table, $j^{'}$ has the second largest Q value in the i-th row, and $Q_{i,j^*} - Q_{i,j^{'}} = \omega, (\omega > 0)$. According to (5.16), the Q value can be re-written as $Q_{i,j^*} = \frac{1}{C_{i,j^*}}[r_{i,j^*}(T^{(1)}) + r_{i,j^*}(T^{(2)}) + ... + r_{i,j^*}(T^{(C_{i,j^*})})]$. For any two samples of transmission rate requirements $T^k = [t_1^k, ..., t_m^k, ..., t_{M^2}^k]$ and $T^l = [t_1^l, ..., t_m^l, ..., t_{M^2}^l]$ in the same state i, it can be obtained that $\left|t_m^k - t_m^l\right| \leq Stepsize = \frac{t_{max}}{\beta}$ according to (5.9).

Since $T^{(c)}$ $(c \in \{1, ..., C_{i,j^*}\})$ is a transmission rate requirements sample in the state i, and $\left|r_{i,j^*}(T^k) - r_{i,j^*}(T^{(c)})\right| \leq f_{j^*}(\mu), \forall c \in \{1, ..., C_{i,j^*}\}$ according to **Lemma 2**, it can be obtained

$$\begin{aligned}\left|r_{i,j^*}(T^k) - Q_{i,j^*}\right| &= \left|r_{i,j^*}(T^k) - \frac{1}{C_{i,j^*}}[r_{i,j^*}(T^{(1)}) + ... + r_{i,j^*}(T^{(C_{i,j^*})})]\right| \\ &= \frac{1}{C_{i,j^*}}\left|\sum_{c=1}^{C_{i,j^*}}\left(r_{i,j^*}(T^k) - r_{i,j^*}(T^{(c)})\right)\right| \leq \frac{1}{C_{i,j^*}}\sum_{c=1}^{C_{i,j^*}} f_{j^*}(\mu) \\ &\Rightarrow Q_{i,j^*} - f_{j^*}(\mu) \leq r_{i,j^*}(T^k) \leq Q_{i,j^*} + f_{j^*}(\mu)\end{aligned} \tag{5.25}$$

Similarly,

$$Q_{i,j'} - f_{j'}(\mu) \leq r_{i,j'}(T^k) \leq Q_{i,j'} + f_{j'}(\mu) \tag{5.26}$$

Then, for a specific transmission rate requirements sample $T^k = [t_1^k, ..., t_m^k, ..., t_{M^2}^k]$, the difference between the rewards of action j^* and $j^{'}$ is

$$\begin{aligned} r_{i,j^*}(T^k) - r_{i,j'}(T^k) &\geq Q_{i,j^*} - Q_{i,j'} - f_{j^*}(\mu) - f_{j'}(\mu) \\ &= \omega - f_{j^*}(\mu) - f_{j'}(\mu) \end{aligned} \tag{5.27}$$

Therefore, as long as the grid depth β is large enough satisfying that $f_{j^*}(\mu) + f_{j'}(\mu) \leq \omega$, where $\mu = Stepsize = \frac{t_{max}}{\beta}$ and $f_{j^*}(\mu), f_{j'}(\mu)$ are linear functions of μ, the action j^* will always be the theoretical optimal action for any transmission rate requirements $T = [t_1, ..., t_m, ..., t_{M^2}]$ belonging to state i.

When the grid depth β becomes large, the transmission rate requirements in the $M \times M$ grids mapped to the same state will be more approximate to each other, according to the definition of state in (5.9) and (5.10); thus these transmission rate requirements will have more opportunities to be simultaneously located inside or outside the feasible domain of the CBA sub-problem corresponding to each action. From **Lemmas 1, 2,** and **Corollary 1**, it can be concluded that, as long as the grid depth β is large enough, the Q table will converge at last and theoretically help the agent find the optimal action (sleeping strategy) exploiting the accumulated knowledge for any given transmission rate requirements.

The overall Q-learning-based algorithm is given in **Algorithm 7**. Given the well-trained Q table with M^β rows and 2^N columns, the corresponding count table, the test sample T^k, and the time duration D, the first step for **Algorithm 7** is to initialize the ε. By feeding the test sample in step 2, the index of the corresponding system state i^k can be obtained based on (5.9), (5.10) and (5.12). In step 3, the agent randomly selects an action j^* among the 2^N possible actions with probability ε, and selects the action j^* which has the largest Q value in the i^k-th row of the Q table with probability $1 - \varepsilon$. Based on the chosen action and the system state, the reward value can be calculated based on (5.15) in step 4. Then the corresponding Q value and the count number will be updated in step 5 and 6. After the

predicted sleeping strategy for the test sample j^* is obtained in Step 3, it will be estimated that if the sleeping strategy j^* can satisfy the testing traffic requirements or not in step 7. If possible, the corresponding CBA sub-problem for sleeping strategy j^* will be solved based on (4.7), and $bw_{i,j}^k$ will be obtained. Then the total energy consumption E_{total}^k for the sleeping strategy j^* will be calculated based on (5.3) in step 9, and be outputted in step 10. If the predicted sleeping strategy j^* cannot satisfy the testing traffic requirements, the algorithm will break in step 12. It should be noted that **Algorithm 7** can be modified to an online algorithm as long as the well-trained Q table and the corresponding count table are replaced by untrained Q table and count table.

Algorithm 7 Proposed overall algorithm for Q-learning-based algorithm

Input: The well-trained Q table with M^β rows and 2^N columns, the corresponding count table, the test sample T^k, and the time duration D.
Output: The predicted energy consumption E_{total}^k
1: Initialize ε , ε belongs to (0,1].
2: Transform T^k into a specific state using (5.9) and (5.10), and then calculate the state index, i^k, using (5.12);
3: With probability ε, randomly select an action j^* among the 2^N possible actions, otherwise, select j^* that has the largest Q value in the i^k-th row of the Q table:
$$j^* = \arg\max_j Q_{i,j}$$
4: Set $j^k = j^*$, and calculate the reward value of j^k , $r_{i^k,j^k}(T^k)$, using (5.15).
5: Update the value of Q_{i^*,j^*} in the Q table based on (5.17).
6: Update the counting number $C_{i^*,j^*} = C_{i^*,j^*} + 1$
7: **if** the sleeping strategy j^* can satisfy the traffic requirements T^k. **then**
8: Solve the corresponding CBA sub-problem in (4.7), and obtain $bw_{i,j}^k$
9: Calculate the total energy consumption E_{total}^k for the sleeping strategy j^* based on (5.3).
10: Output E_{total}^k.
11: **else**
12: break
13: **end if**

5.2.3 Computational Complexity Analysis

In this chapter, the joint SCBA problem with NP-hard complexity is decoupled into two sub-problems. For the CSC sub-problem, the agent first needs to map the observed transmission rate requirements T into a certain state using (5.9)-(5.12), whose computational complexity are bounded by $O(\beta \cdot M^2)$. Then, the agent will either randomly select an action among the 2^N possible actions or select the action with the largest Q value corresponding to the current

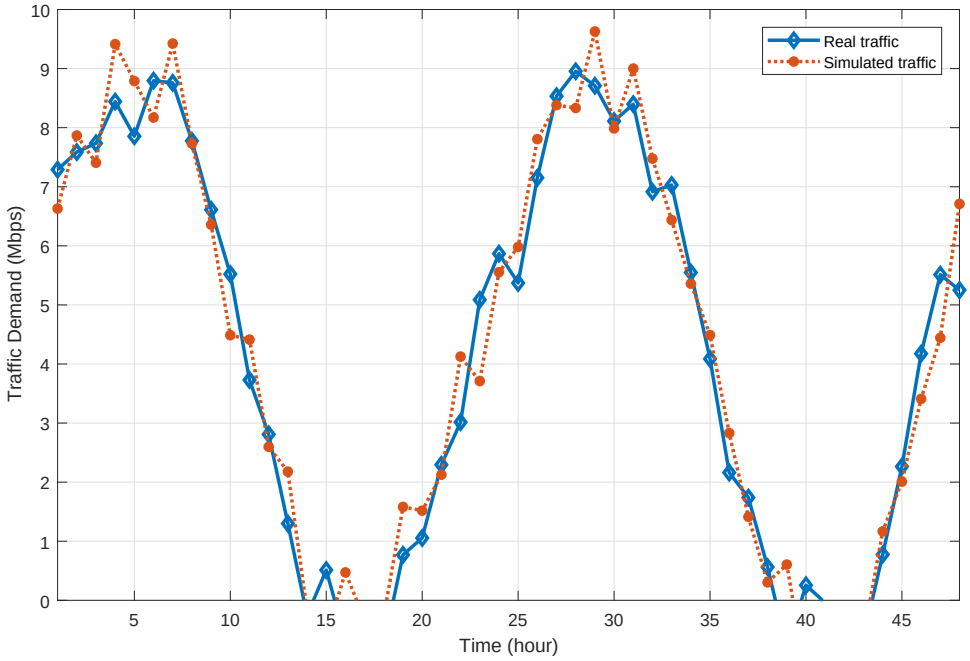

Fig. 5.4 The comparison of the traffic distribution.

state. Since a vector is used to record the column number for the maximum Q value of each row in the Q table, the computational complexities of both ways of action selecting will be bounded by $O(1)$.

When the action (sleeping strategy) of the N SBSs is determined, it is proven that the CBA sub-problem can be transformed into a LP problem about variables $bw_{n,m}$, $(n = 1,...N, m = 1,...,M^2)$. The parameters $\gamma_{n,m}$, $(n = 1,...N, m = 1,...,M^2)$ in the LP problem's constraints are constants, which can be calculated off-line. Thus, for a certain transmission rate requirements T and a certain SBS sleeping strategy, solving the CBA sub-problem has the maximum computational complexity of $O(N^4 \cdot M^8)$. The overall computational complexity of the proposed mechanism is bounded by $O(N^4 \cdot M^8 + \beta \cdot M^2 + 1)$.

5.3 Testing and Results

In this section, the performance of the proposed mechanism is evaluated through a series of semi-authentic transmission rate requirements. Consider a $100 \times 100m^2$ region that is evenly divided into 3×3 grids. Three SBSs are supposed to be fixedly allocated in the region with the same height, H.

Table 5.1 Parameters for Q-learning based algorithm

Parameter	Symbol	Value
Region of Area	B	$100 \times 100m^2$
No. of BSs	N	3,5,8
Path loss exponent	α	-4
No. of grids	$M \times M$	$3 \times 3, 4 \times 4, 5 \times 5$
Bandwidth	BW	5MHz
Transmit power of SBSs	P_{tx}	-30dBm/Hz
Static power consumption	P_0	38dBm
Sleep power consumption	P_s	27dBm
Noise	σ^2	-174dBm/Hz
Height of SBSs	H	5m
The duration of each Time interval	D	1 hour
Grid depth	β	2-6
No. of test samples	N_T	672(4 weeks)
Large negative constant	λ	-100

The duration of each time interval, D, is set as an hour. Based on the temporal model of mobile traffic variation proposed in [95] and the observations of mobile traffic records collected in London, the downlink mobile traffic volume of grid m in each time interval is set by the following equation:

$$v_m(TI_{num}) = A_m sin(\frac{2\pi}{24} \times TI_{num} + \varphi_m) + k_m + \sigma_m(TI_{num}) \tag{5.28}$$

where TI_{num} is the order number of time interval, A_m, φ_m and k_m are fixed factors used to fit the traffic load variation in each grid m according to realistic mobile traffic records generated in a $100 \times 100m^2$ belonging to the center area of Greater London from 2012-06-10 to 2012-06-24, $\sigma_m(TI_{num})$ is a random variable uniformly distributed in $[\sigma_{min}, \sigma_{max}]$. The realistic mobile traffic pattern and the imitated mobile traffic pattern of a randomly selected grid are illustrated in Fig.5.4.

For a certain time interval (TI), the transmission rate requirement in grid m is calculated as follows:

$$t_m(TI_{num}) = \frac{v_m(TI_{num})}{D} \tag{5.29}$$

When the Q table has converged after sufficient time intervals, the author compares the performance of proposed mechanism over N_T test samples (a number of N_T samples of transmission rate requirements in the $100 \times 100m^2$ region) with other existing sleeping control algorithms proposed in previous research studies. Same as that in **Chapter 4**, four benchmarks, non-sleep(ALLON), probability-based strategic sleeping control (SSC) [200], greedy sleeping control (GSC) [201], and optimal sleeping control (OSC) are employed for comparison. After the prediction results (sleeping strategies) are obtained by these algorithms, the bandwidth allocation for the active SBSs will then be obtained by solving the corresponding CBA sub-problem, except SSC algorithm, for which the transmission rate requirement in each grid is served by the active SBS which provides the maximum SINR. Thus, the overall power consumption minimization of the system can be obtained.

If the CBA sub-problem has no feasible solution for the sleeping strategy given by a specific algorithm, a best-effort solution will be employed to maximize the served traffic. The parameters used in this work are summarized in Table 5.1.

5.3.1 Convergence

The convergence speed of proposed mechanism under different values of grid depth, β, for N = 3 and M = 9 is illustrated in Fig.5.5. From Fig.5.5, it can be observed that the proposed mechanism will always converge after enough iterations. Additionally, as the grid depth β, increases from 2 to 6, the mechanism's convergence speed slows down (from about 200000 TIs with $\beta = 2$ to about 600000 TIs with $\beta = 6$) and the average reward value achieved when the approach has had steady increases (from -13.23 to -12.81). These phenomena are consistent with the theoretical analyses and common sense that dividing finer state space will raise the mechanism's complexity and extend training time, while on the other hand, elevating the mechanism's performance according to **Corollary 1**.

5.3.2 Accuracy

The accuracies of sleeping strategy selection for proposed mechanism and other existing algorithms are illustrated in Fig.5.6. For any test sample of transmission rate requirements, if the action decided by the evaluated algorithm is the same as the action decided by OSC, it will be called an accurate one. The accuracy is thus calculated according to the following

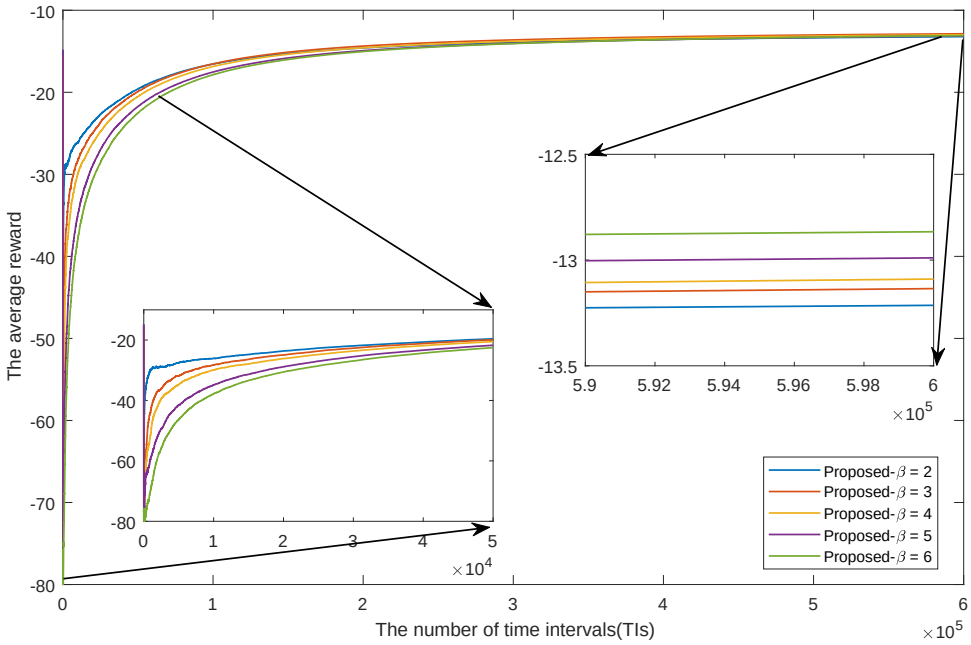

Fig. 5.5 Convergence of proposed mechanism under different values of grid depth for N = 3 and M = 9.

equation,

$$Accuracy(\%) = \frac{The\ No.\ \ of\ \ accurate\ samples}{The\ total\ No.\ of\ test\ samples} \times 100\% \tag{5.30}$$

From Fig.5.6, it can be observed that the accuracies of the proposed mechanism under different values of grid depth are greater than those of GSC and SSC (49.71% and 34.08%, respectively). Furthermore, the accuracy of proposed mechanism increases along with the increase of the grid depth β (from 86.91% with $\beta = 2$ to 91.22% with $\beta = 6$). Notably, for any grid depth β, the accuracy of proposed mechanism will always be greater than 85%.

5.3.3 Average Total Energy Consumption

Fig.5.7 depicts the comparison of average total energy consumption for the proposed mechanism and other existing algorithms. From Fig.5.7, it can be observed that the average total energy consumptions of the proposed mechanism decrease with the increase of grid depth approaching the theoretical minimum of 11.52Wh. When the grid depth equals 6, the difference between the average total energy consumption of the proposed mechanism and the

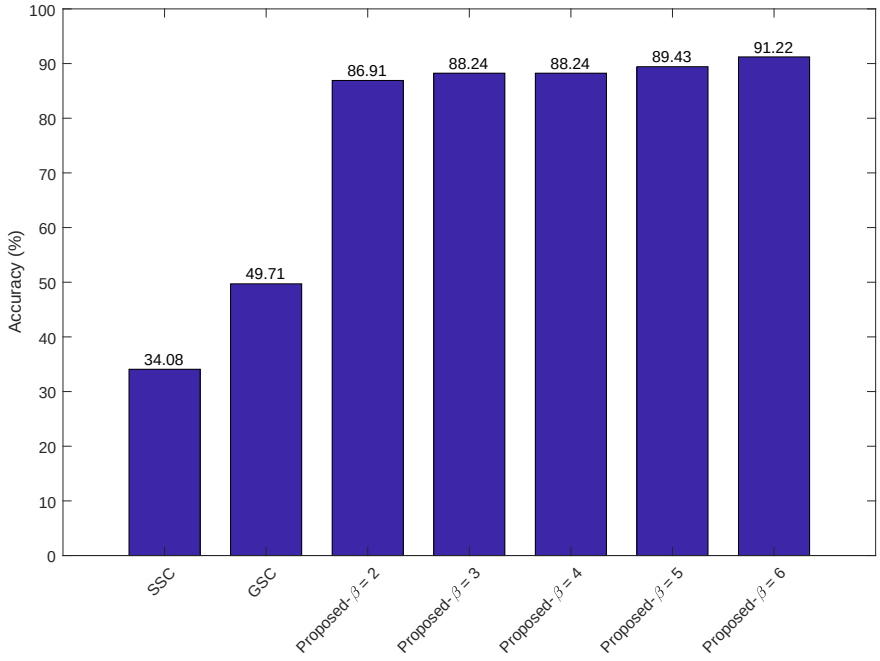

Fig. 5.6 Comparison of the accuracy of sleeping strategy selection for proposed mechanism and other existing algorithms for N = 3 and M = 9.

theoretical minimum is 2.95%. The performance of the proposed mechanism is comparable to that of GSC, and will have a better performance when $\beta \geq 5$.

5.3.4 Served Rate

Another concern about the proposed mechanism is the percentage of served traffic over the total traffic (referred to as the served rate, SR), which is defined as:

$$SR(\%) = \frac{The\ served\ \ traffic}{The\ total\ traffic} \times 100\% \tag{5.31}$$

Fig.5.8 compares the served rates of different algorithms. The results show that the served rates of the proposed mechanism under different values of grid depth are all equal to 100%, while the served rates of GSC and SSC are 100% and 89.46%, respectively. The good performance of the proposed mechanism about the served rate results from the large negative constant in (5.15), which is consistent with previous analysis.

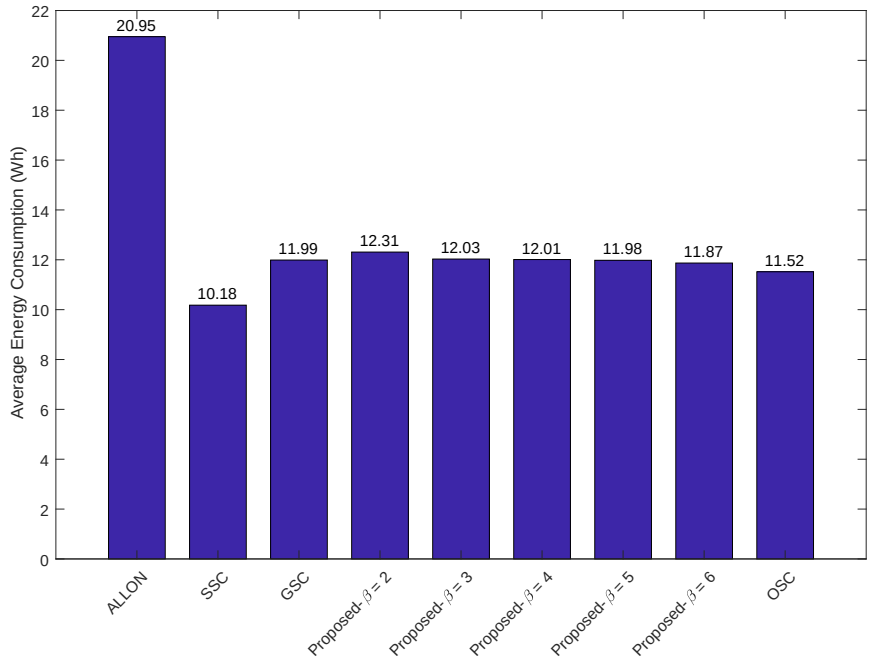

Fig. 5.7 Comparison of the average total energy consumption for proposed mechanism and other existing algorithms for N = 3 and M = 9.

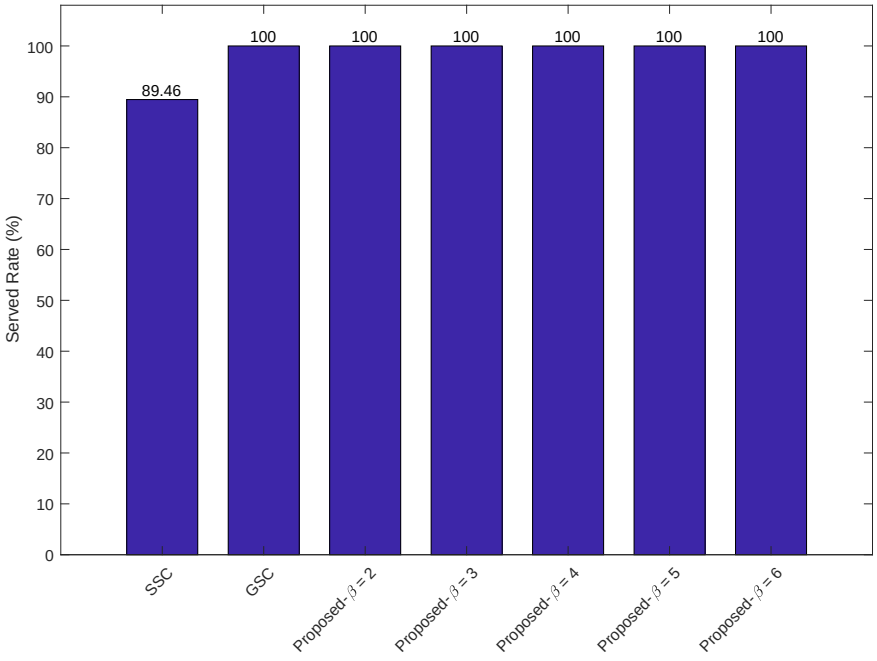

Fig. 5.8 Comparison of the served rate for proposed mechanism and other existing algorithms for N = 3 and M = 9.

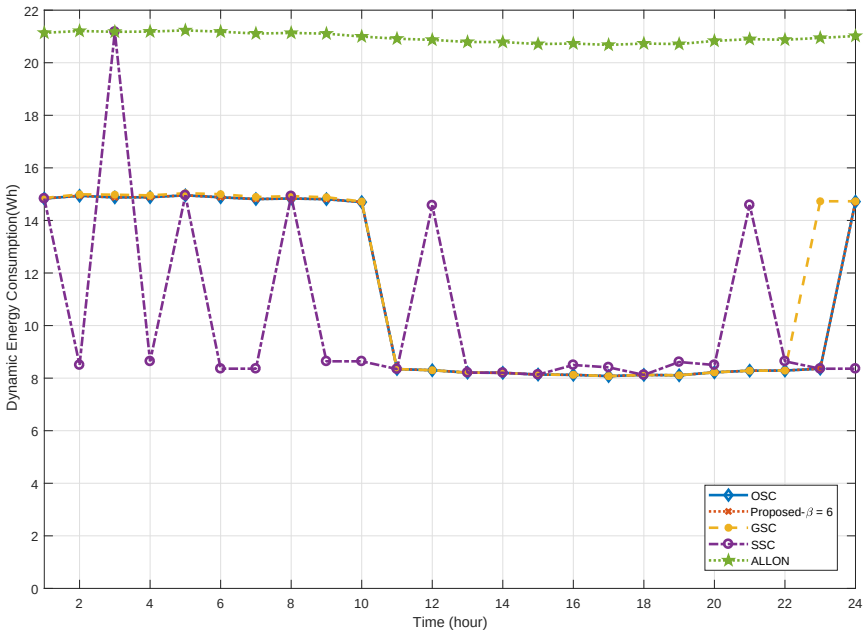

Fig. 5.9 Comparison of the dynamic total energy consumption of different algorithms over hours of a day.

5.3.5 Dynamic Total Energy Consumption

The dynamic total energy consumption of different algorithms is evaluated in Fig.5.9 and Fig.5.10. Fig.5.9 denotes the dynamic total energy consumption over hours of a day, while Fig.5.10 denotes the dynamic total energy consumption in different days. It can be observed that the dynamic total energy consumption of the proposed mechanism with $\beta = 6$ is approximately the same as that of OSC, no matter in Fig.5.9 or Fig.5.10, while the dynamic total energy consumption of ALLON is almost unchanged along with time. The fluctuation of the dynamic total energy consumption for SSC is violent and irregular in a day since the switching ON/OFF of SBS for SSC is probability-based. Moreover, the dynamic performance of GSC is also good since it is a centralized sleeping algorithm and tries to find a global optimal solution.

5.3.6 Complexity

The complexity of the proposed algorithm is also investigated for different number of BSs and different number of grids. Table 5.2 depicts the complexity for the decision-making of different algorithms. Experimental results are achieved on an Intel i7 2.60GHz 12GB

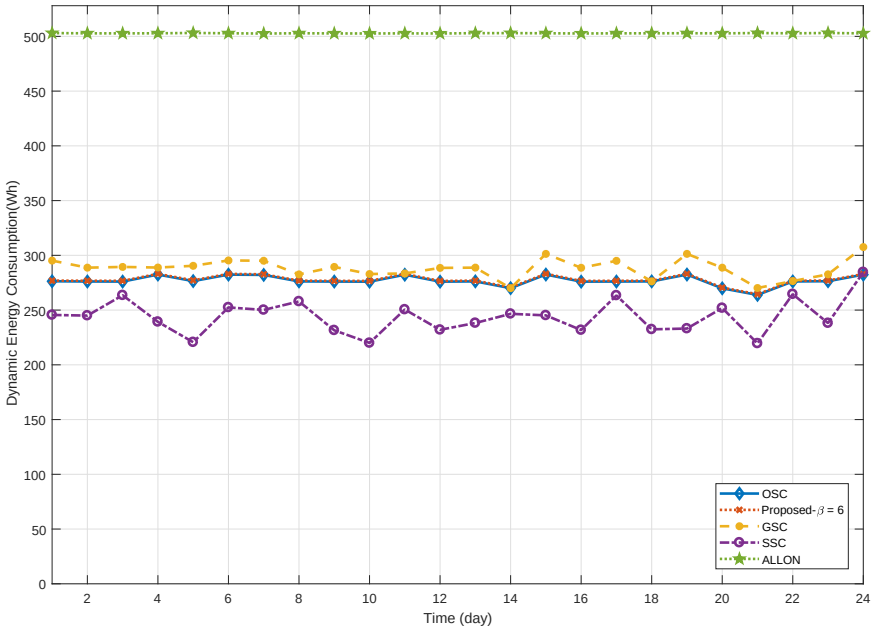

Fig. 5.10 Comparison of the dynamic total energy consumption of different algorithms over different days.

computer. From Table 5.2, it can be found that proposed algorithm always makes the fastest decision compared with other algorithms. As to a specific pair N and M, the complexity for proposed algorithm is almost the same under different value of β. As the number of BSs increases, the complexity for all algorithms increase, while the increase for proposed algorithm is modest. Similar conclusions can be obtained for increasing number of grids. Therefore, the complexity for proposed algorithm is more and more superior compared with existing algorithms with the increasing number of BSs or grids.

5.4 Conclusions

In this chapter, a centralized, low-complexity mechanism is proposed to minimize the total energy consumption of the SBSs by properly switching SBSs into sleep mode and allocating the bandwidth of the active SBSs to satisfy the transmission rate requirements. The author decouples the joint SCBA problem into CBA sub-problem and CSC sub-problem, and solve them by linear programming and a modified Q-learning algorithm, respectively.

Numerical results confirm the effectiveness of the proposed mechanism. An additional 42.8%-45.5% and 60.8%-62.6% accuracy can be achieved for proposed mechanism compared

Table 5.2 Comparison of the complexity for different algorithms

Algorithms	N = 3 (ms)			N = 5 (ms)			N = 8 (ms)		
	M=3	M=4	M=5	M=3	M=4	M=5	M=3	M=4	M=5
Proposed-β = 2	5.1	6.2	9.3	5.3	8.2	10.5	6.1	10.9	16.0
Proposed-β = 3	5.0	5.7	9.1	5.3	8.6	10.1	6.1	11.1	14.6
Proposed-β = 4	5.1	5.9	8.8	5.3	8.5	10.2	5.9	10.5	15.2
Proposed-β = 5	5.1	5.8	9.4	5.3	8.4	10.2	6.3	10.5	13.7
Proposed-β = 6	5.3	6.4	8.9	5.3	8.2	10.1	7.1	10.4	15.1
SSC	7.4	9.5	11.4	9.0	12.4	14.4	8.2	13.8	15.2
GSC	19.5	27.7	33.8	22.8	29.0	32.2	22.0	31.1	35.6
OSC	45.7	53.2	72.0	248.0	333.7	415.8	2405.1	3405.2	4420.9

with GSC and SSC from $\beta = 2$ to $\beta = 6$. Moreover, the proposed algorithm has a good performance for energy saving and the served rate. The served rates of proposed mechanism under different grid depth remains 100%, while the difference between the average total energy consumption of the proposed mechanism and the theoretical minimum is 3% when the grid depth equals 6. Furthermore, the complexity of different algorithms for different number of BSs and grids are also analyzed. The numerical results show that compared with existing sleeping control schemes, the complexity of proposed algorithm is significantly reduced for different number of BSs and grids.

For future work, the restrictions of the training time in this work need to be investigated.

Chapter 6

Conclusions and Future Works

How to achieve green communication and minimize the energy consumption remain open issues. This thesis studied two promising categories for green communication: energy efficient BS deployment and energy efficient BS sleeping. According to the literature review of the state-of-art techniques, it can be found that there has been works in these fields. Although effective, existing works have limitations such as high-complexity, low accuracy, or not good enough performance, etc. In this thesis, the author investigated the potential of these two methods based on online social network data and machine learning techniques.

In Chapter 3, it is shown that existing deployment methods, such as SPPP model, hexogonal model, are no longer suitable for current networks, especially for SBS networks. To fill the gap, the author developed a joint optimization scheme to minimize the power consumption and satisfy the constraints of coverage or capacity. Further, to reduce the computational complexity of the joint optimization scheme and achieve a good performance, two different k-means based deployment methods subject to different constraints were proposed based on Twitter data.

Energy efficient BS strategies were discussed are proposed in Chapter 4 and Chapter 5. In Chapter 4, a joint optimization scheme combining sleeping control and bandwidth allocation (SCBA) is introduced and formulated as a mixed integer non-linear programming problem subject to transmission rate requirements. To reduce the computational complexity of the joint SCBA optimization scheme, KNN-based algorithm and CNN based algorithm were proposed. In Chapter 5, the author considers the SCBA optimization scheme for the scenarios where few realistic traffic datasets are available. In this situation, a Q-learning based algorithm was proposed to enable continuously learning and improvement.

In this chapter, the contributions and limitations of current work are firstly discussed. Then the future directions for energy consumption minimization are proposed within the scope of this thesis.

6.1 Conclusions

- **BS deployment and BS sleeping are promising for green communication.** In Chapter 1 and Chapter 2, different energy efficient technologies are discussed. According to the discussions, existing works for BS deployment and BS sleeping have the limitations of high complexity, low accuracy, or not good enough performance, while effective. More efficient methods are required.

- **Online social network data and clustering algorithms can significantly improve the performance for BS deployment.** In Chapter 3, the author proposed two novel k-means based SBS deployment methods subject to different constraints based on Twitter data. For a HetNet scenario where existing networks provide poor coverage, a data-driven SBS deployment method is proposed to minimize the power consumption while guaranteeing the coverage. For a dense urban scenario, a data-driven SBS deployment method is proposed to minimize the power consumption while satisfying the traffic requirements. The performances of proposed methods are evaluated in various regions. Simulation results show the performance can be significantly improved by proposed methods, with smaller power consumptions and better QoS under the same number of BSs. Although significant results have been obtained, there are some unsolved problems. Firstly, as to the first scenario, only coverage is considered as the constraint in current work. In the future, other tradeoffs or other KPIs need to be investigated. Secondly, as to the second scenario, SBS network is considered in current work. In the future, HetNet will be considered. Thirdly, the traffic requirements from all users are assumed to be the same in the second scenario. In the future, more practical traffic patterns need to be considered. Lastly, k-means used in this work is based on spatial extent, thus it cannot accurately capture the difference of traffic requirements for different users. In the future, other methods will be investigated such as DBSCAN, weighted-k-means, etc.

- **Deep learning techniques can significantly improve the performance for BS sleeping when historical datasets are available.** In Chapter 4, a joint sleeping control and bandwidth allocation (SCBA) optimization problem is introduced and formulated as a mixed integer non-linear programming problem subject to the transmission rate requirements. The joint optimization problem is then decoupled into two sub-problems: a centralized bandwidth allocation (CBA) sub-problem that minimizes the power consumption of the system by optimizing the allocated bandwidth of the active SBSs; and a centralized sleeping control (CSC) sub-problem that finds the optimal SBS sleeping strategy among all the possible ones. Given the historical datasets, KNN-

based algorithm and CNN-based algorithm are proposed to reduce the computational complexity and achieve good performances. Numerical results show the proposed algorithms both have better performances compared with existing approaches, while the CNN-based method has a superiority over KNN-based method at the expenses of pre-training. Despite the significant improvements, proposed algorithms have some limitations which need to be solved in the future. Firstly, the influence of the size of historical datasets and the ratio of train/test set need to be investigated. Secondly, since the definition of distance between two samples may affect the performance of KNN-based algorithm, different distance calculation methods should be discussed in the future. Thirdly, the training time of the CNN-based algorithm for different number of BSs also need to be investigated in the future.

- **Reinforcement learning techniques can significantly improve the performance for BS sleeping when few or no historical datasets are available.** In Chapter 5, a similar optimization problem to Chapter 4 is considered, while a Q learning based algorithm is proposed based on few realistic datasets. Theoretically, the convergence of the proposed Q-learning algorithm is analyzed. Simulation results confirm the effectiveness of the proposed algorithm with convergence, greater accuracy, smaller energy consumption, greater served rate, and lower computational complexity. This work also faces challenges. Firstly, the system model in current work is based on ideal assumptions that there is no inter-cell interference. In the future, more practical models need to be considered. Secondly, the training time for different number of BSs should be investigated in the future. Thirdly, for an online training algorithm, the performance at the early stage will be poor, how to improve it will be investigated for future work.

6.2 Future Works

In this thesis, the author studied two proposing energy efficient technologies for green communications: energy efficient BS deployment and energy efficient BS sleeping. The contributions of current works have been summarized in previous section. Although significant results have been obtained, there are some remaining problems and potentials of improvement which are worth further investigation. The future research directions related to the topics of this thesis are summarized below.

As it can be seen from Chapter 3, there remain many limitations in current research for BS deployment. As the first stage of deploying networks, the potential of energy efficient BS deployment is worth further research in the following directions:

- **Introduce other tradeoffs or other KPIs.** In the work that SBSs are deployed to uncover blackspots, only coverage is taken into consideration. However, more concern about blackspots are focused on capacity and latency in current networks, especially in 5G networks [13]. Therefore, the blackspots detection based on capacity and latency should be introduced in the future, resulting in more practical energy efficient BS deployment method.

- **Introduce complex network models and propagation models.** In the work that S-BSs are deployed to provide traffic, only small cell networks are considered. In the future, K-tier HetNet need to be introduced, since it is much closer to realistic networks. Besides, more accurate propagation models which contains fading and channel variations need to be considered in the future, since the link budgeting considered in current works is based on ideal assumption that fading effect is ignored.

- **Introduce more practical traffic patterns.** The traffic requirements for different users are assumed to be the same in current works, which is not practical. In realistic, the spatial-temporal characteristics of traffic distribution is extremely uneven. Based on existing works, more practical traffic patterns which contain variations in spatial and temporal domain will be considered, such as lognormal distribution with mobility [205, 206].

- **Introduce other cluster algorithms.** k-means used in current works is based on spatial extent, thus it cannot accurately capture the difference of traffic requirements for different users. In the future, k-means will be no longer suitable if more practical traffic patterns are considered. Alternatively, weighted-k-means [207] or DBSCAN [208] algorithms can be introduced since both of them can capture the weight information for different points.

Chapter 4 and 5 focus on the joint optimization of sleeping strategy and bandwidth allocation. The future works are listed as follows.

- **Consider more practical interference model.** In current works, the system models are based on ideal assumptions that there is no inter-cell interference. In realistic, the inter-cell interference may be non-neglectful. Therefore, more accurate channel models which contains inter-cell interference need to be considered in the future.

- **Evaluate the influence of the size of dataset and the ratio of train/test set.** In current works, the size of dataset and the ratio of train/test set remain the same for simulations. However, the size of dataset and the ratio of train/test set can significantly

affect the complexity and the performance of proposed algorithms. Recent years, how to achieve good training results with few samples, which is called few-shot learning[209], has drawn more and more attention. For current works, few-shot learning is also meaningful, since the available traffic datasets is usually sparse.

- **Introduce other definitions of distance for KNN-based algorithm.** For KNN-based algorithm, the definition of distance between two samples has a great influence on the performance. In current works, the Chebyshev distance [210] is utilized to evaluate the similarities between two samples. Two samples are regarded as more and more similar while the Chebyshev distance between them decreases. However, this method may not be best method for similarity evaluation. In the future work, other similarity evaluation methods, such as cosine similarity [211], Pearson correlation coefficient [212], etc, will be investigated.

- **Evaluate the training time for CNN-based algorithm.** Since there is an offline training procedure, the training time has a significant impact on the evaluation of CNN-based algorithm. Although the performance for CNN-based algorithm is outstanding, it may be unacceptable for real-time scenarios if the training time is considerable. Therefore, the training time for CNN-based algorithm need to be further investigated considering different sizes of datasets and different number of BSs.

- **Evaluate the training time and improve the performance at the early stage for Q-learning based algorithm.** Since Q-learning based algorithm can be regarded as an online training algorithm, the performance for it at the early stage may be poor due to the explore/exploit process. Hence, the training time for convergence can significantly affect the performance. In the future, how to shorten the training time and improve the performance at the early stage will be investigated.

Appendix A

Analysis of BSs Spatial Characteristics in London

Based on a London dataset from an operator in 2012, the spatial characteristics of BS (2289) in London are investigated according to the testing method of SPPP distribution proposed in [66]. The regions in Greater London is categorized into: dense urban, urban, suburban. For each type of region, tremendous examples are tested. An example for each region type is randomly chosen and shown in the following figures. According to the results, similar conclusion can be obtained, that is, SPPP model is not suitable for dense urban region anymore because of the considerable number of SBSs in those regions. Since the locations of SBSs are highly related to the users traffic demand rather than randomness, the SPPP model is becoming more and more unsuitable for current networks.

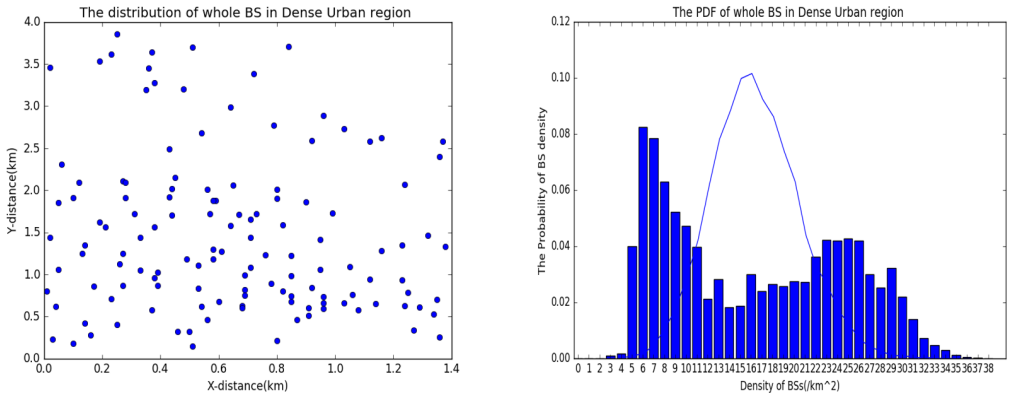

Fig. A.1 (Left) BSs in dense urban region. (Right) Comparison between distribution of BSs and SPPP model

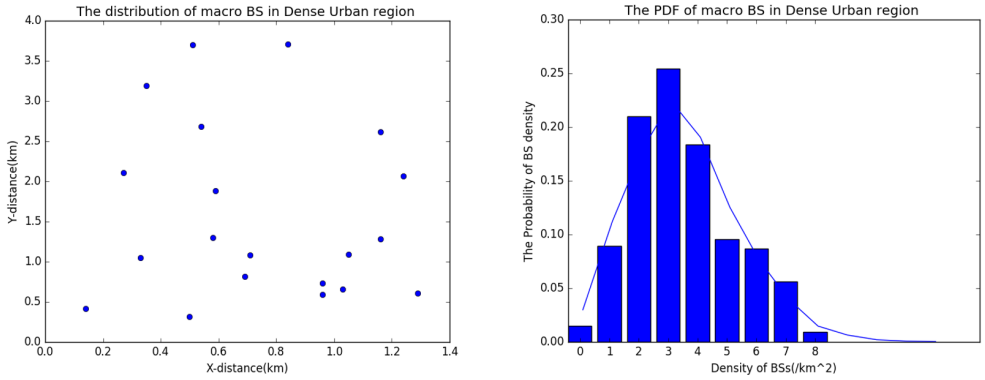

Fig. A.2 (Left) MBSs in dense urban region. (Right) Comparison between distribution of MBSs and SPPP model

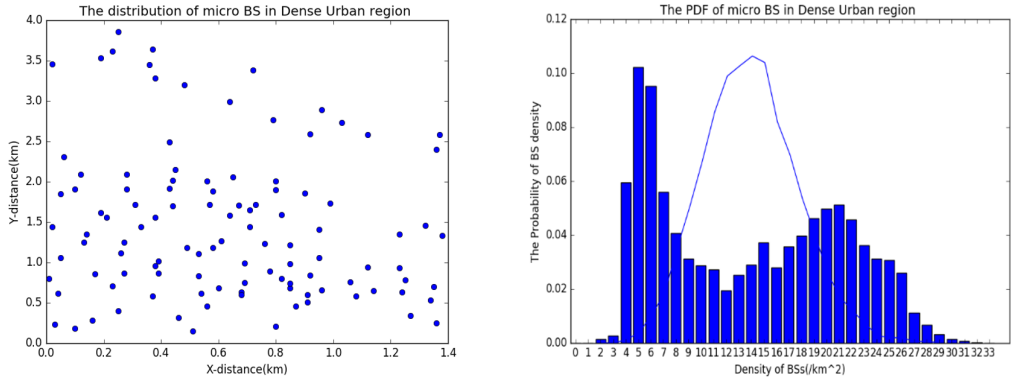

Fig. A.3 (Left) SBSs in dense urban region. (Right) Comparison between distribution of SBSs and SPPP model

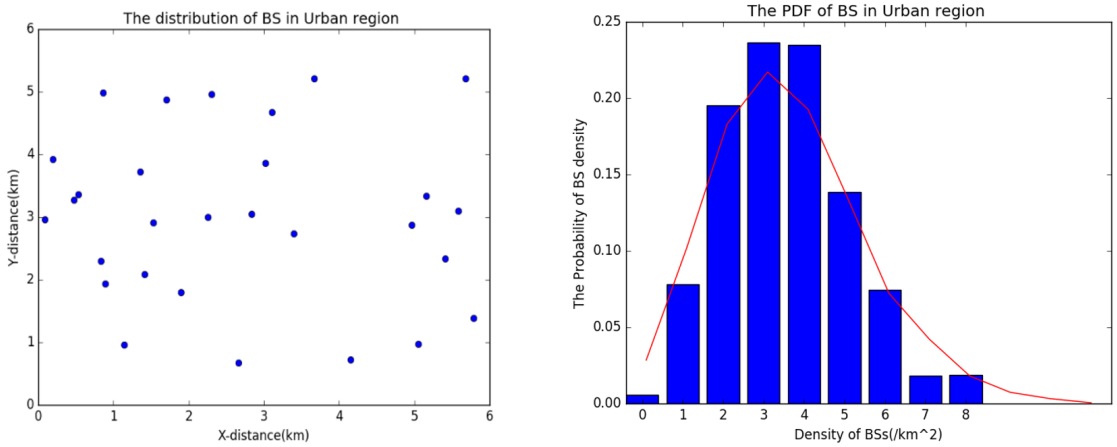

Fig. A.4 (Left) BSs in urban region. (Right) Comparison between distribution of BSs and SPPP model

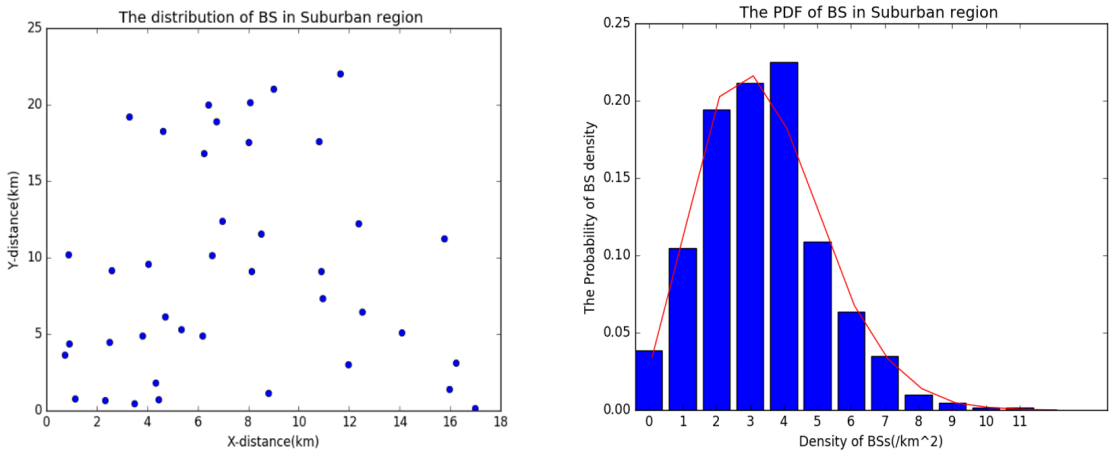

Fig. A.5 (Left) BSs in suburban region. (Right) Comparison between distribution of BSs and SPPP model

Appendix B

COST-231-Walfisch-Ikegami Model

COST-231-Walfisch-Ikegami Model utilizes the theoretical Walfisch-Bertoni model [213, 214], and takes the reflection and scattering above and between buildings into consideration. According to the distance between BS and UE, two situations are proposed in this model: line of sight (LOS) and non-line of sight (NLOS). According to researches, it is suitable for network performance prediction in metropolitan areas [215, 216].

If the distance between the UE and BS is equal to or smaller than 20 m, this situation can be regarded as LOS, and the model is approximated to the free-space propagation model, given as :

$$L_{LOS} = 42.6 + 26 \times log(d) + 20 \times log(f), \quad d \leq 20m \tag{B.1}$$

where $d(km)$ is the distance between UE and BS. $f(MHz)$ refers to the radio frequency.

If $d > 20m$, the model will take reflection, scattering and diffraction of the buildings into account, the model thus is given by :

$$L_{NLOS} = L_0 + max\{0, L_{rts} + L_{msd}\}, \quad d > 20m \tag{B.2}$$

where L_0 denotes the free space path loss, L_{rts} is the loss resulted from the diffraction and scattering between rooftop and street, and L_{msd} refers to the diffraction from the buildings. The detailed information of these terms is shown in Table.B.1.

Table B.1 Parameters for COST-231-Walfisch-lkegami model

Symbol	Meaning and Equation
f (MHz)	Radio frequency
d (km)	Distance of radio path
w (m)	Average street width
h_m (m)	Height of mobile
h_{roof} (m)	Height of building
h_B (m)	Height of base station
φ ($^\circ$)	Road orientation with respect to direct radio path
b (m)	Average building separation
Δh_M (m)	$h_{roof} - h_M$
Δh_B (m)	$h_B - h_{roof}$
L_0	$32.4 + 20 \cdot log(d) + 20 \cdot log(f)$
L_{rts}	$-16.9 - 10 \cdot log(w) + 10 \cdot log(f) + 20 \cdot log(\Delta h_M) + L_{ori}$
L_{ori}	$\begin{cases} -10 + 0.354\varphi, & 0^\circ \le \varphi < 35^\circ \\ 2.5 + 0.075(\varphi - 35), & 35^\circ \le \varphi < 55^\circ \\ 4.0 - 0.114(\varphi - 55), & 55^\circ \le \varphi < 90^\circ \end{cases}$
L_{msd}	$L_{bsh} + k_a + k_d log(d) + k_f log(f) - 9log(b)$
L_{bsh}	$\begin{cases} -18log(1 + \Delta h_B), & h_B > h_{roof} \\ 0, & h_B \le h_{roof} \end{cases}$
k_a	$\begin{cases} 54, & h_B > h_{roof} \\ 54 - 0.8\Delta h_B, & h_B \le h_{roof} \text{ and } d \ge 0.5km \\ 54 - 1.6\Delta h_B d, & h_B \le h_{roof} \text{ and } d < 0.5km \end{cases}$
k_d	$\begin{cases} 18, & h_B > h_{roof} \\ 18 - 15\frac{\Delta h_B}{h_{roof}}, & h_B \le h_{roof} \end{cases}$
k_f	$\begin{cases} -4 + 0.7(\frac{f}{925} - 1), & \textit{for medium cities, suburbs with medium tree density} \\ -4 + 1.5(\frac{f}{925} - 1), & \textit{for metropolitan centers} \end{cases}$

Appendix C

Additional Simulations for Suburban Region and Dense Urban Region for Chapter 3.2

A suburban region ($28km \times 23km$) with 37 MBSs, and 11058 users, and a dense urban region ($2.5km \times 4.5km$) with 20 MBSs, 108 MiBSs and 32246 users are chosen as the scenario, shown in Fig.C.1 and Fig.C.6, respectively. The parameters used for these regions are the same as those in Table 3.1. The results for the suburban region are shown in Fig.C.2 - Fig.C.5, while the results for the dense urban region are shown in Fig.C.7 - Fig.C.10. According to the simulation results, similar conclusion can be obtained that compared with existing SPPP model, the coverage probability can be significantly improved under the same number of SBSs, and the power consumption can be significantly reduced under the same coverage probability threshold for the proposed model in various regions.

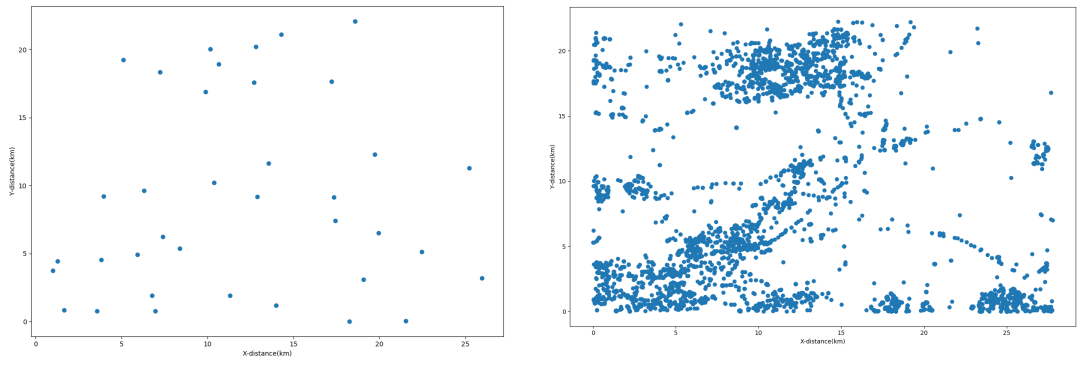

(a) (b)

Fig. C.1 (a) MBSs in the subruban region. (b) Users in the subruban region.

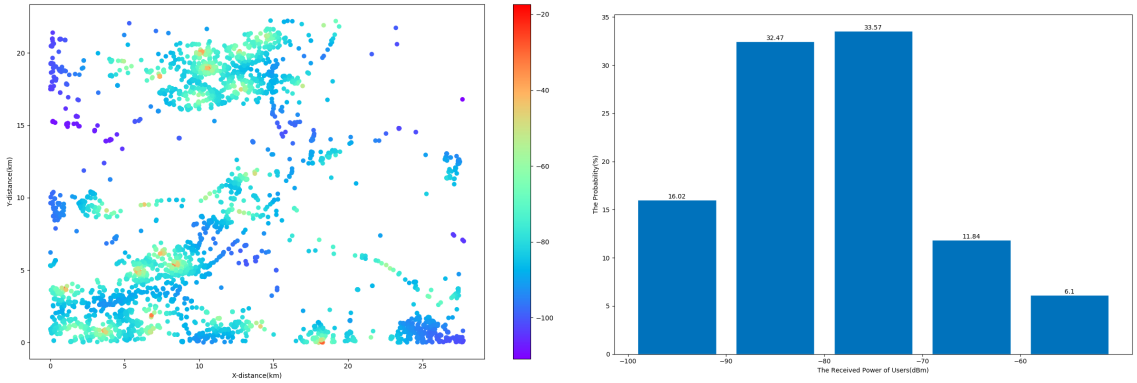

(a) (b)

Fig. C.2 (a)The heatmap of the received power (dBm) of users in the suburban region. (b) The PDF of the received power in the suburban region.

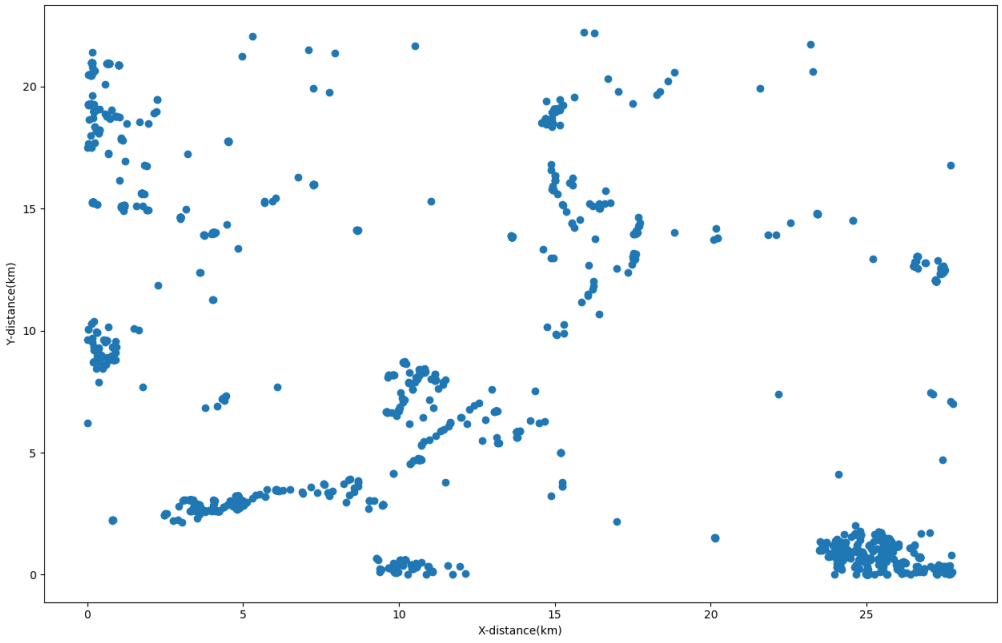

Fig. C.3 Users suffering from poor coverage in the suburban region.

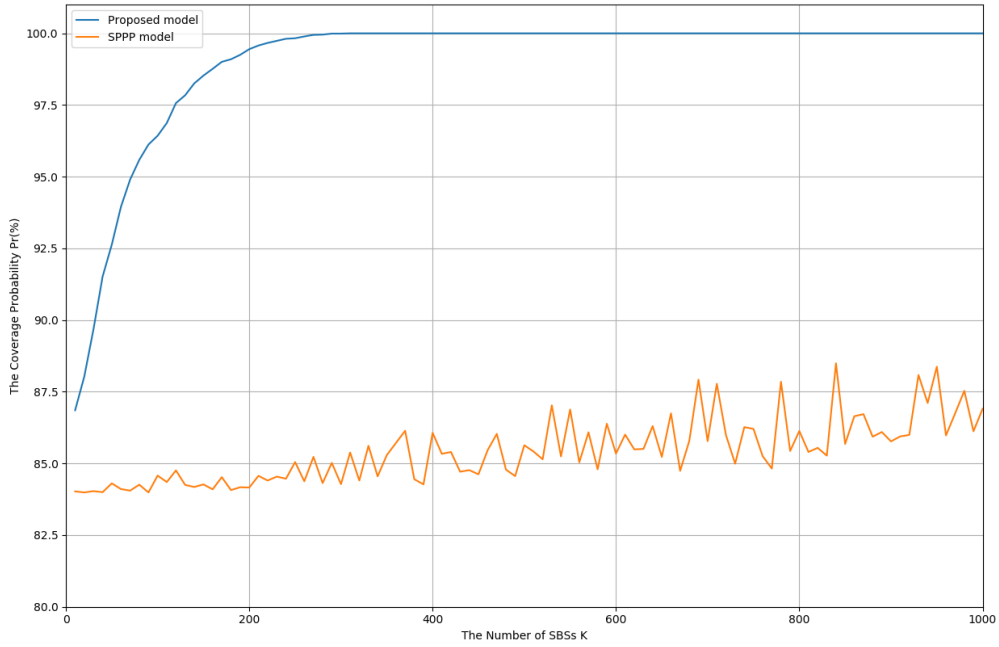

Fig. C.4 Comparison of coverage probability for two models under different number of SBSs in the suburban region.

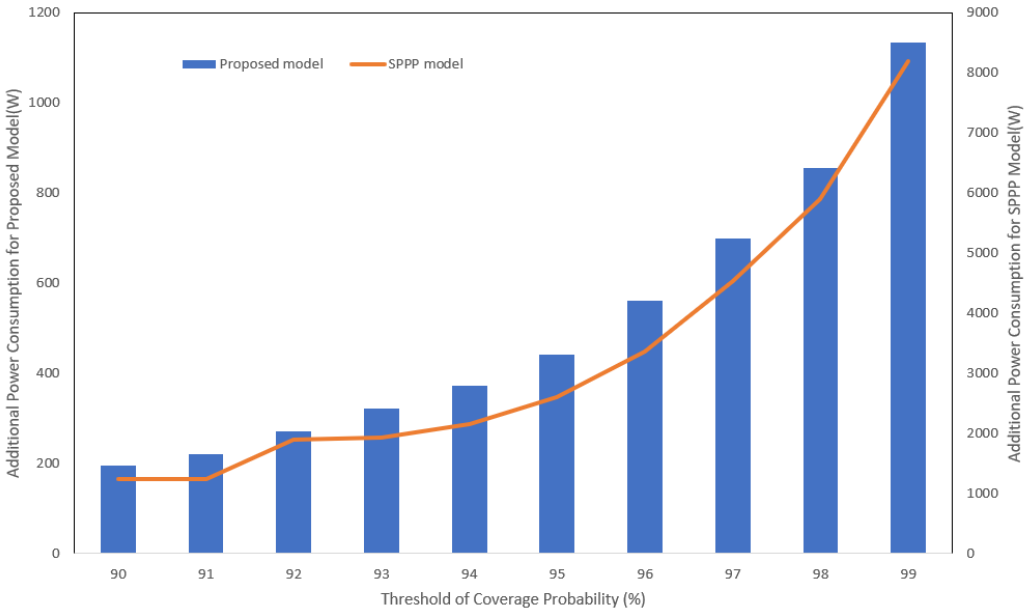

Fig. C.5 Comparison of the additional power consumption for two models under different coverage probability threshold in the suburban region.

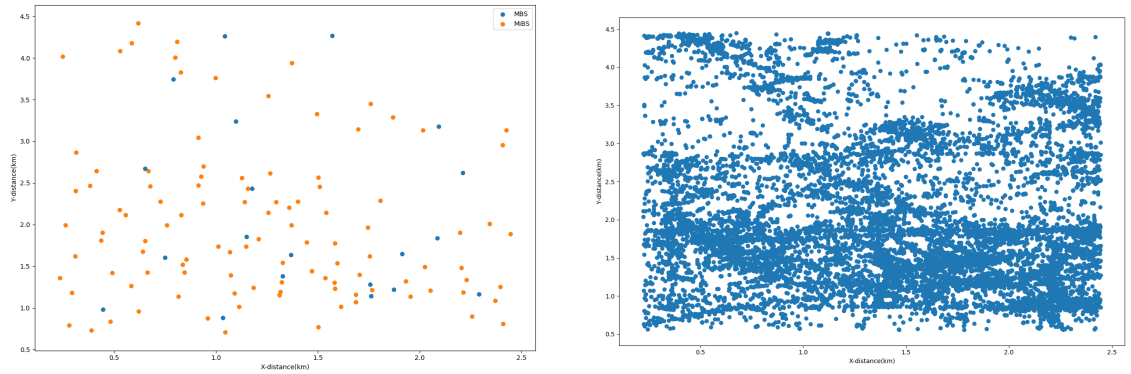

(a) (b)

Fig. C.6 (a) MBSs in the dense urban region. (b) Users in the dense urban region.

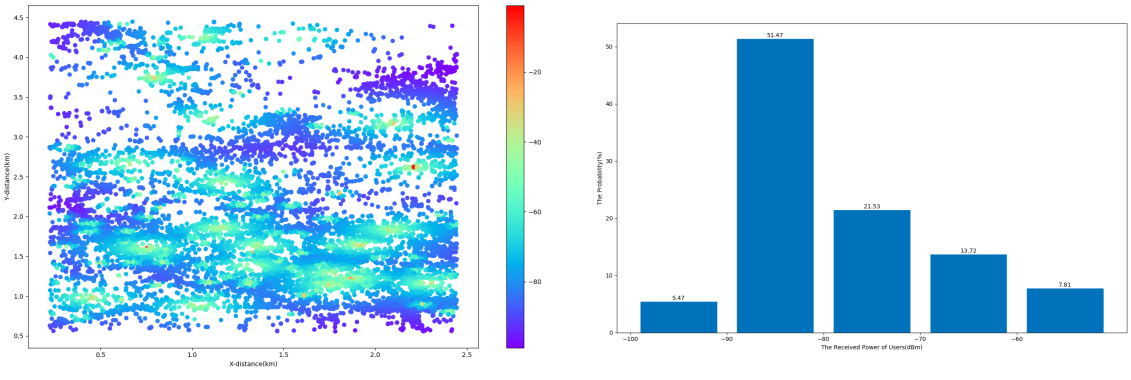

(a) (b)

Fig. C.7 (a)The heatmap of the received power (dBm) of users in the dense urban region. (b) The PDF of the received power in the dense urban region.

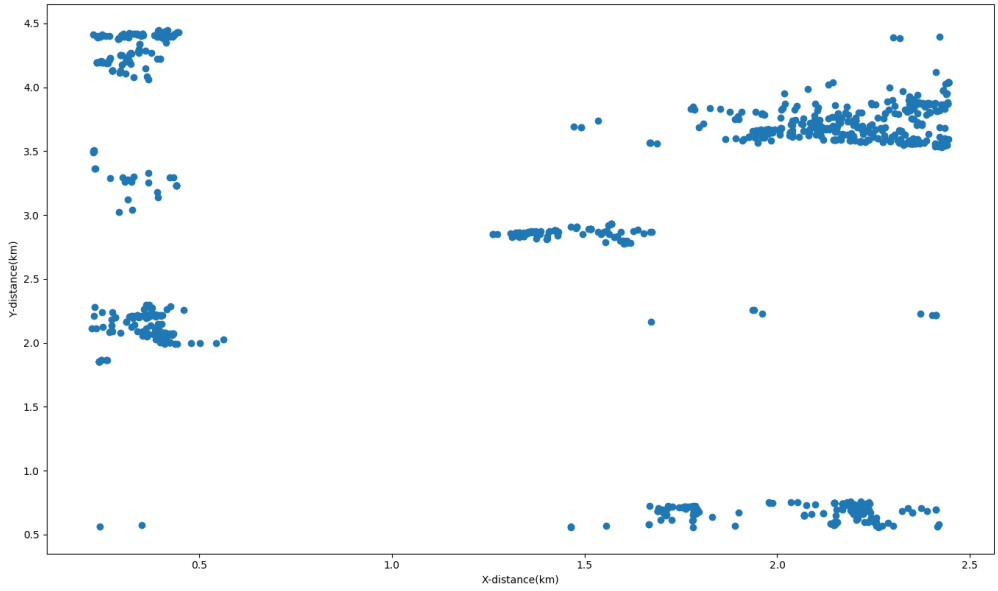

Fig. C.8 Users suffering from poor coverage in the dense urban region.

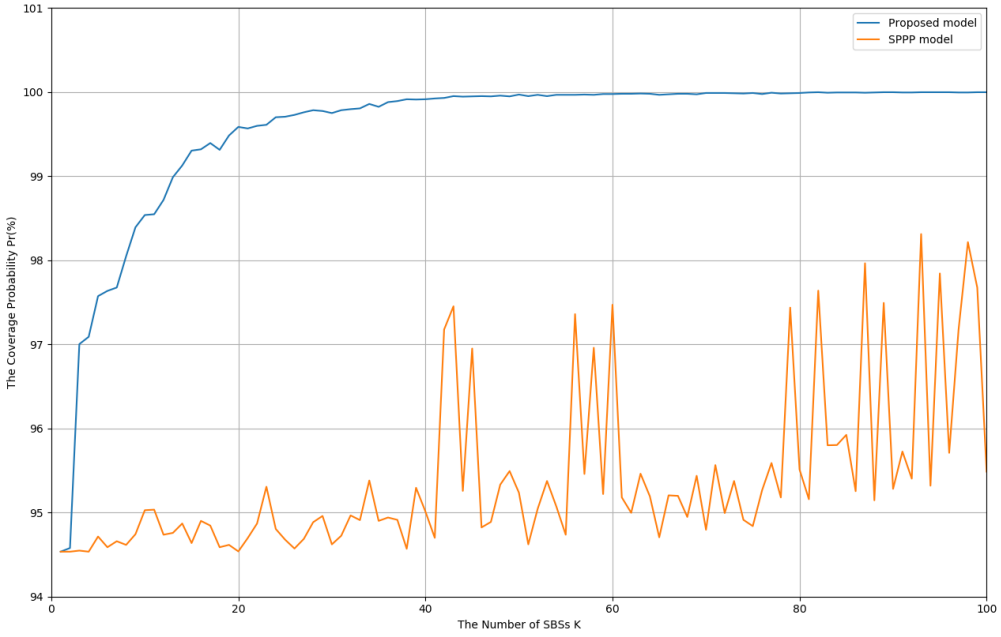

Fig. C.9 Comparison of coverage probability for two models under different number of SBSs in the dense urban region.

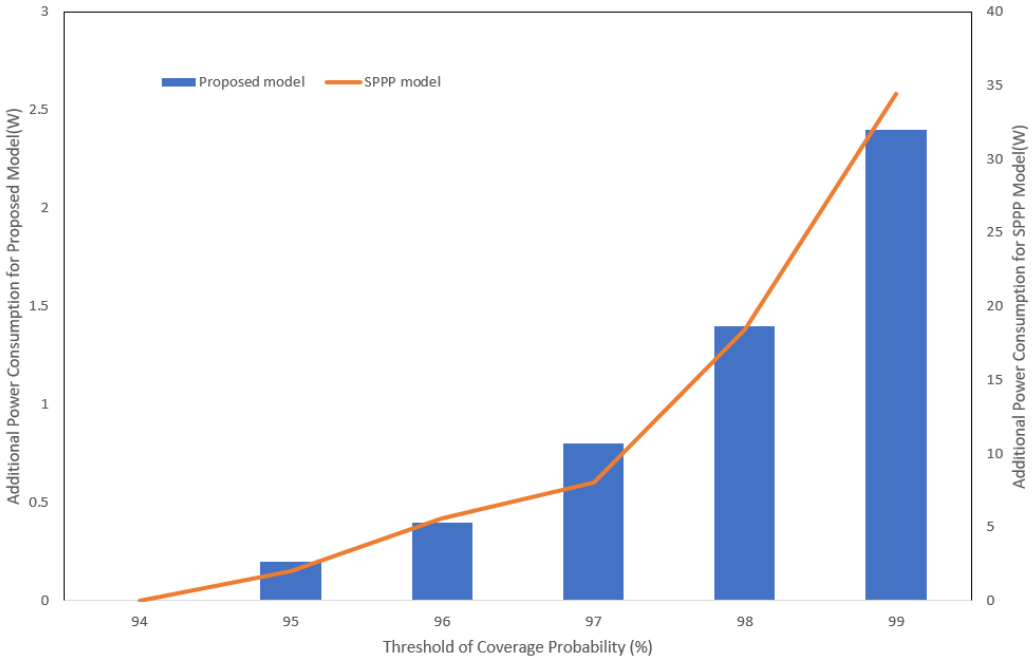

Fig. C.10 Comparison of the additional power consumption for two models under different coverage probability threshold in the dense urban region.

References

[1] Refik Caglar Kizilirmak and Hossein Khaleghi Bizaki. Non-orthogonal multiple access (noma) for 5g networks. *Towards 5G Wireless Networks-A Physical Layer Perspective*, 83, 2016.

[2] Ericsson. Ericsson mobility report. 2020.

[3] Congzheng Han, Tim Harrold, Simon Armour, Ioannis Krikidis, Stefan Videv, Peter M Grant, Harald Haas, John S Thompson, Ivan Ku, Cheng-Xiang Wang, et al. Green radio: radio techniques to enable energy-efficient wireless networks. *IEEE communications magazine*, 49(6):46–54, 2011.

[4] Gunther Auer, Vito Giannini, Claude Desset, Istvan Godor, Per Skillermark, Magnus Olsson, Muhammad Ali Imran, Dario Sabella, Manuel J Gonzalez, Oliver Blume, et al. How much energy is needed to run a wireless network? *IEEE wireless communications*, 18(5):40–49, 2011.

[5] Eunsung Oh, Kyuho Son, and Bhaskar Krishnamachari. Dynamic base station switching-on/off strategies for green cellular networks. *IEEE transactions on wireless communications*, 12(5):2126–2136, 2013.

[6] Yaohua Sun, Mugen Peng, Yangcheng Zhou, Yuzhe Huang, and Shiwen Mao. Application of machine learning in wireless networks: Key techniques and open issues. *IEEE Communications Surveys & Tutorials*, 21(4):3072–3108, 2019.

[7] Richard S Sutton and Andrew G Barto. *Reinforcement learning: An introduction*. MIT press, 2018.

[8] Cisco. Cisco annual internet report (2018–2023) white paper. 2020.

[9] Michel Mouly, Marie-Bernadette Pautet, and Thomas Foreword By-Haug. *The GSM system for mobile communications*. Telecom publishing, 1992.

[10] Ajay R Mishra. *Fundamentals of cellular network planning and optimisation: 2G/2.5 G/3G... evolution to 4G*. John Wiley & Sons, 2004.

[11] Erik Dahlman, Stefan Parkvall, Johan Skold, and Per Beming. *3G evolution: HSPA and LTE for mobile broadband*. Academic press, 2010.

[12] Erik Dahlman, Stefan Parkvall, and Johan Skold. *4G: LTE/LTE-advanced for mobile broadband*. Academic press, 2013.

[13] Jeffrey G Andrews, Stefano Buzzi, Wan Choi, Stephen V Hanly, Angel Lozano, Anthony CK Soong, and Jianzhong Charlie Zhang. What will 5g be? *IEEE Journal on selected areas in communications*, 32(6):1065–1082, 2014.

[14] L. Verma, M. Fakharzadeh, and S. Choi. Backhaul need for speed: 60 ghz is the solution. *IEEE Wireless Communications*, 22(6):114–121, 2015.

[15] Y. Yamao, H. Suda, N. Umeda, and N. Nakajima. Radio access network design concept for the fourth generation mobile communication system. In *VTC2000-Spring. 2000 IEEE 51st Vehicular Technology Conference Proceedings (Cat. No.00CH37026)*, volume 3, pages 2285–2289 vol.3, 2000.

[16] Andrea Goldsmith, Syed Ali Jafar, Nihar Jindal, and Sriram Vishwanath. Capacity limits of mimo channels. *IEEE Journal on selected areas in Communications*, 21(5):684–702, 2003.

[17] David Tse and Pramod Viswanath. *Fundamentals of wireless communication*. Cambridge university press, 2005.

[18] Yuya Saito, Yoshihisa Kishiyama, Anass Benjebbour, Takehiro Nakamura, Anxin Li, and Kenichi Higuchi. Non-orthogonal multiple access (noma) for cellular future radio access. In *2013 IEEE 77th vehicular technology conference (VTC Spring)*, pages 1–5. IEEE, 2013.

[19] TL Marzetta. Multi-cellular wireless with base stations employing unlimited numbers of antennas. In *Proc. UCSD Inf. Theory Applicat. Workshop*, 2010.

[20] Thomas L Marzetta. Noncooperative cellular wireless with unlimited numbers of base station antennas. *IEEE transactions on wireless communications*, 9(11):3590–3600, 2010.

[21] Bertrand M Hochwald, Thomas L Marzetta, and Vahid Tarokh. Multiple-antenna channel hardening and its implications for rate feedback and scheduling. *IEEE transactions on Information Theory*, 50(9):1893–1909, 2004.

[22] Aamod Khandekar, Naga Bhushan, Ji Tingfang, and Vieri Vanghi. Lte-advanced: Heterogeneous networks. In *2010 European wireless conference (EW)*, pages 978–982. Citeseer, 2010.

[23] Ronny Yongho Kim, Jin Sam Kwak, and Kamran Etemad. Wimax femtocell: requirements, challenges, and solutions. *IEEE Communications Magazine*, 47(9):84–91, 2009.

[24] Insoo Hwang, Bongyong Song, and Samir S Soliman. A holistic view on hyper-dense heterogeneous and small cell networks. *IEEE Communications Magazine*, 51(6):20–27, 2013.

[25] M. M. A. Hossain, K. Koufos, and R. Jäntti. Energy efficient deployment of hetnets: Impact of power amplifier and delay. In *2013 IEEE Wireless Communications and Networking Conference (WCNC)*, pages 778–782, 2013.

[26] T. E. Bogale and L. B. Le. Massive mimo and mmwave for 5g wireless hetnet: Potential benefits and challenges. *IEEE Vehicular Technology Magazine*, 11(1):64–75, 2016.

[27] K. M. S. Huq, S. Mumtaz, J. Bachmatiuk, J. Rodriguez, X. Wang, and R. L. Aguiar. Green hetnet comp: Energy efficiency analysis and optimization. *IEEE Transactions on Vehicular Technology*, 64(10):4670–4683, 2015.

[28] Aleksandar Damnjanovic, Juan Montojo, Yongbin Wei, Tingfang Ji, Tao Luo, Madhavan Vajapeyam, Taesang Yoo, Osok Song, and Durga Malladi. A survey on 3gpp heterogeneous networks. *IEEE Wireless communications*, 18(3):10–21, 2011.

[29] How many 5g cell towers and base stations worldwide? [html]. https://www.operatorwatch.com/2020/08/how-many-cell-towers-base-stations.html, 2020.

[30] Beyond the energy techlash: The real climate impacts of information technology. https://itif.org/publications/2020/07/06/beyond-energy-techlash-real-climate-impacts-information-technology, 2020.

[31] Exponential data growth – constant ict footprints. https://www.ericsson.com/en/reports-and-papers/research-papers/the-future-carbon-footprint-of-the-ict-and-em-sectors, 2019.

[32] Yan Chen, Shunqing Zhang, Shugong Xu, and Geoffrey Ye Li. Fundamental trade-offs on green wireless networks. *IEEE Communications Magazine*, 49(6):30–37, 2011.

[33] Aruna Prem Bianzino, Claude Chaudet, Dario Rossi, and Jean-Louis Rougier. A survey of green networking research. *IEEE Communications Surveys & Tutorials*, 14(1):3–20, 2010.

[34] Jingjin Wu, Yujing Zhang, Moshe Zukerman, and Edward Kai-Ning Yung. Energy-efficient base-stations sleep-mode techniques in green cellular networks: A survey. *IEEE communications surveys & tutorials*, 17(2):803–826, 2015.

[35] Oliver Arnold, Fred Richter, Gerhard Fettweis, and Oliver Blume. Power consumption modeling of different base station types in heterogeneous cellular networks. In *2010 Future Network & Mobile Summit*, pages 1–8. IEEE, 2010.

[36] Jinseong Jeong, Donald F Kimball, Myoungbo Kwak, Paul Draxler, Chin Hsia, Craig Steinbeiser, Thomas Landon, Oleh Krutko, Lawrence E Larson, and Peter M Asbeck. High-efficiency wcdma envelope tracking base-station amplifier implemented with gaas hvhbts. *IEEE journal of solid-state circuits*, 44(10):2629–2639, 2009.

[37] Kyoung-Joon Cho, Jong-Heon Kim, and Shawn P Stapleton. A highly efficient doherty feedforward linear power amplifier for w-cdma base-station applications. *IEEE Transactions on Microwave Theory and Techniques*, 53(1):292–300, 2005.

[38] Yun Wei, Joseph Staudinger, and Monte Miller. High efficiency linear gaas mmic amplifier for wireless base station and femto cell applications. In *2012 IEEE Topical Conference on Power Amplifiers for Wireless and Radio Applications*, pages 49–52. IEEE, 2012.

[39] Ian H Rowlands, Paul Parker, and Daniel Scott. Consumer perceptions of 'green power'. *Journal of consumer marketing*, 19(2):112–129, 2002.

[40] Yeow-Khiang Chia, Sumei Sun, and Rui Zhang. Energy cooperation in cellular networks with renewable powered base stations. *IEEE Transactions on Wireless Communications*, 13(12):6996–7010, 2014.

[41] Daquan Feng, Chenzi Jiang, Gubong Lim, Leonard J Cimini, Gang Feng, and Geoffrey Ye Li. A survey of energy-efficient wireless communications. *IEEE Communications Surveys & Tutorials*, 15(1):167–178, 2012.

[42] Shuguang Cui, Andrea J Goldsmith, and Ahmad Bahai. Energy-efficiency of mimo and cooperative mimo techniques in sensor networks. *IEEE Journal on selected areas in communications*, 22(6):1089–1098, 2004.

[43] Geoffrey Ye Li, Zhikun Xu, Cong Xiong, Chenyang Yang, Shunqing Zhang, Yan Chen, and Shugong Xu. Energy-efficient wireless communications: tutorial, survey, and open issues. *IEEE Wireless Communications*, 18(6):28–35, 2011.

[44] Jie Tang, Daniel KC So, Emad Alsusa, and Khairi Ashour Hamdi. Resource efficiency: A new paradigm on energy efficiency and spectral efficiency tradeoff. *IEEE Transactions on Wireless Communications*, 13(8):4656–4669, 2014.

[45] Yulong Zou, Jia Zhu, and Rui Zhang. Exploiting network cooperation in green wireless communication. *IEEE Transactions on Communications*, 61(3):999–1010, 2013.

[46] Cong Xiong, Geoffrey Ye Li, Shunqing Zhang, Yan Chen, and Shugong Xu. Energy- and spectral-efficiency tradeoff in downlink ofdma networks. *IEEE transactions on wireless communications*, 10(11):3874–3886, 2011.

[47] Cong Xiong, Geoffrey Ye Li, Shunqing Zhang, Yan Chen, and Shugong Xu. Energy-efficient resource allocation in ofdma networks. *IEEE Transactions on Communications*, 60(12):3767–3778, 2012.

[48] Ming Li, Pan Li, Xiaoxia Huang, Yuguang Fang, and Savo Glisic. Energy consumption optimization for multihop cognitive cellular networks. *IEEE Transactions on Mobile Computing*, 14(2):358–372, 2014.

[49] Vikram Chandrasekhar, Jeffrey Andrews, and Alan Gatherer. Femtocell networks: a survey. *arXiv preprint arXiv:0803.0952*, 2008.

[50] Ali Rıza Ekti, Muhammad Zeeshan Shakir, Erchin Serpedin, and Khalid A Qaraqe. Downlink power consumption of hetnets based on the probabilistic traffic model of mobile users. In *2013 IEEE 24th Annual International Symposium on Personal, Indoor, and Mobile Radio Communications (PIMRC)*, pages 2797–2802. IEEE, 2013.

[51] Sourjya Bhaumik, Girija Narlikar, Subhendu Chattopadhyay, and Satish Kanugovi. Breathe to stay cool: adjusting cell sizes to reduce energy consumption. In *Proceedings of the first ACM SIGCOMM workshop on Green networking*, pages 41–46. ACM, 2010.

[52] Chang Li, Jun Zhang, and Khaled Ben Letaief. Energy efficiency analysis of small cell networks. In *2013 IEEE international conference on communications (ICC)*, pages 4404–4408. IEEE, 2013.

[53] Anwesha Mukherjee, Srimoyee Bhattacherjee, Sucheta Pal, and Debashis De. Femtocell based green power consumption methods for mobile network. *Computer Networks*, 57(1):162–178, 2013.

[54] Dantong Liu, Yue Chen, Kok Keong Chai, and Tiankui Zhang. Distributed delay-energy aware user association in 3-tier hetnets with hybrid energy sources. In *2014 IEEE Globecom Workshops (GC Wkshps)*, pages 1109–1114. IEEE, 2014.

[55] Weisi Guo and Tim O'Farrell. Green cellular network: Deployment solutions, sensitivity and tradeoffs. In *2011 Wireless Advanced*, pages 42–47. IEEE, 2011.

[56] Holger Claussen, Imran Ashraf, and Lester TW Ho. Dynamic idle mode procedures for femtocells. *Bell Labs Technical Journal*, 15(2):95–116, 2010.

[57] Wei Li, Wei Zheng, Yuanbao Xie, and Xiangming Wen. Clustering based power saving algorithm for self-organized sleep mode in femtocell networks. In *The 15th International Symposium on Wireless Personal Multimedia Communications*, pages 379–383. IEEE, 2012.

[58] Jyrki T Louhi. Energy efficiency of modern cellular base stations. In *INTELEC 07-29th International Telecommunications Energy Conference*, pages 475–476. IEEE, 2007.

[59] Jian Wu, Sheng Zhou, and Zhisheng Niu. Traffic-aware base station sleeping control and power matching for energy-delay tradeoffs in green cellular networks. *IEEE Transactions on Wireless Communications*, 12(8):4196–4209, 2013.

[60] Pål Frenger, Peter Moberg, Jens Malmodin, Ylva Jading, and István Gódor. Reducing energy consumption in lte with cell dtx. In *2011 IEEE 73rd vehicular technology conference (VTC Spring)*, pages 1–5. IEEE, 2011.

[61] Imran Ashraf, Federico Boccardi, and Lester Ho. Sleep mode techniques for small cell deployments. *IEEE Communications Magazine*, 49(8):72–79, 2011.

[62] Marco Ajmone Marsan, Luca Chiaraviglio, Delia Ciullo, and Michela Meo. On the effectiveness of single and multiple base station sleep modes in cellular networks. *Computer Networks*, 57(17):3276–3290, 2013.

[63] Alagan Anpalagan, Mehdi Bennis, and Rath Vannithamby. *Design and deployment of small cell networks*. Cambridge University Press, 2015.

[64] Hesham ElSawy, Ekram Hossain, and Martin Haenggi. Stochastic geometry for modeling, analysis, and design of multi-tier and cognitive cellular wireless networks: A survey. *IEEE Communications Surveys & Tutorials*, 15(3):996–1019, 2013.

[65] Anjin Guo and Martin Haenggi. Spatial stochastic models and metrics for the structure of base stations in cellular networks. *IEEE Transactions on Wireless Communications*, 12(11):5800–5812, 2013.

[66] Jiaxin Zhang, Wenbo Wang, Xing Zhang, Yu Huang, Zhuowen Su, and Zongchao Liu. Base stations from current mobile cellular networks: Measurement, spatial modeling and analysis. In *2013 IEEE Wireless Communications and Networking Conference Workshops (WCNCW)*, pages 1–5. IEEE, 2013.

[67] Fengli Xu, Yong Li, Huandong Wang, Pengyu Zhang, and Depeng Jin. Understanding mobile traffic patterns of large scale cellular towers in urban environment. *IEEE/ACM transactions on networking*, 25(2):1147–1161, 2016.

[68] M Ajmone Marsan, Luca Chiaraviglio, Delia Ciullo, and Michela Meo. Optimal energy savings in cellular access networks. In *2009 IEEE International Conference on Communications Workshops*, pages 1–5. IEEE, 2009.

[69] Kyuho Son, Hongseok Kim, Yung Yi, and Bhaskar Krishnamachari. Base station operation and user association mechanisms for energy-delay tradeoffs in green cellular networks. *IEEE journal on selected areas in communications*, 29(8):1525–1536, 2011.

[70] Zhisheng Niu. Tango: Traffic-aware network planning and green operation. *IEEE Wireless Communications*, 18(5):25–29, 2011.

[71] Jianchao Zheng, Yueming Cai, Xianfu Chen, Rongpeng Li, and Honggang Zhang. Optimal base station sleeping in green cellular networks: A distributed cooperative framework based on game theory. *IEEE Transactions on Wireless Communications*, 14(8):4391–4406, 2015.

[72] Qi Wang and Jun Zheng. A distributed base station on/off control mechanism for energy efficiency of small cell networks. In *2015 IEEE International Conference on Communications (ICC)*, pages 3317–3322. IEEE, 2015.

[73] Jihwan Kim, Hyang-Won Lee, and Song Chong. Traffic-aware energy-saving base station sleeping and clustering in cooperative networks. *IEEE Transactions on Wireless Communications*, 17(2):1173–1186, 2017.

[74] Imran Ashraf, Federico Boccardi, and Lester Ho. Power savings in small cell deployments via sleep mode techniques. In *2010 IEEE 21st International Symposium on Personal, Indoor and Mobile Radio Communications Workshops*, pages 307–311. IEEE, 2010.

[75] Zhang Xuan and Chuai Gang. An energy-saving cooperative small-cell switch on/off optimization for hetnets. In *2016 2nd IEEE International Conference on Computer and Communications (ICCC)*, pages 2884–2890. IEEE, 2016.

[76] Prabhu Chandhar and Suvra Sekhar Das. Energy saving in ofdma cellular networks with multi-objective optimization. In *2014 IEEE International Conference on Communications (ICC)*, pages 3951–3956. IEEE, 2014.

[77] Ying Wang, Xiangming Dai, Jason Min Wang, and Brahim Bensaou. A reinforcement learning approach to energy efficiency and qos in 5g wireless networks. *IEEE Journal on Selected Areas in Communications*, 37(6):1413–1423, 2019.

[78] Attai Ibrahim Abubakar, Metin Ozturk, Sajjad Hussain, and Muhammad Ali Imran. Q-learning assisted energy-aware traffic offloading and cell switching in heterogeneous networks. In *2019 IEEE 24th International Workshop on Computer Aided Modeling and Design of Communication Links and Networks (CAMAD)*, pages 1–6. IEEE, 2019.

[79] Muhammad Ismail and Weihua Zhuang. Network cooperation for energy saving in green radio communications. *IEEE Wireless Communications*, 18(5):76–81, 2011.

[80] Yong Sheng Soh, Tony QS Quek, Marios Kountouris, and Hyundong Shin. Energy efficient heterogeneous cellular networks. *IEEE Journal on selected areas in communications*, 31(5):840–850, 2013.

[81] Sibel Tombaz, Anders Vastberg, and Jens Zander. Energy-and cost-efficient ultra-high-capacity wireless access. *IEEE wireless Communications*, 18(5):18–24, 2011.

[82] Shengrong Bu, F Richard Yu, Yegui Cai, and Xiaoping P Liu. When the smart grid meets energy-efficient communications: Green wireless cellular networks powered by the smart grid. *IEEE Transactions on Wireless Communications*, 11(8):3014–3024, 2012.

[83] Margot Deruyck, Dieter De Vulder, Wout Joseph, and Luc Martens. Modelling the power consumption in femtocell networks. In *2012 IEEE Wireless Communications and Networking Conference Workshops (WCNCW)*, pages 30–35. IEEE, 2012.

[84] Roberto Riggio and Douglas J Leith. A measurement-based model of energy consumption in femtocells. In *2012 IFIP Wireless Days*, pages 1–5. IEEE, 2012.

[85] Albrecht J Fehske, Fred Richter, and Gerhard P Fettweis. Energy efficiency improvements through micro sites in cellular mobile radio networks. In *2009 IEEE Globecom Workshops*, pages 1–5. IEEE, 2009.

[86] Fred Richter, Albrecht J Fehske, and Gerhard P Fettweis. Energy efficiency aspects of base station deployment strategies for cellular networks. In *2009 IEEE 70th Vehicular Technology Conference Fall*, pages 1–5. IEEE, 2009.

[87] Eunsung Oh and Bhaskar Krishnamachari. Energy savings through dynamic base station switching in cellular wireless access networks. In *2010 IEEE Global Telecommunications Conference GLOBECOM 2010*, pages 1–5. IEEE, 2010.

[88] Md Farhad Hossain, Kumudu S Munasinghe, and Abbas Jamalipour. A protocooperation-based sleep-wake architecture for next generation green cellular access networks. In *2010 4th International Conference on Signal Processing and Communication Systems*, pages 1–8. IEEE, 2010.

[89] Marco Ajmone Marsan and Michela Meo. Energy efficient management of two cellular access networks. *ACM SIGMETRICS Performance Evaluation Review*, 37(4):69–73, 2010.

[90] Jeffrey G Andrews, François Baccelli, and Radha Krishna Ganti. A tractable approach to coverage and rate in cellular networks. *IEEE Transactions on communications*, 59(11):3122–3134, 2011.

[91] Harpreet S Dhillon, Radha Krishna Ganti, François Baccelli, and Jeffrey G Andrews. Modeling and analysis of k-tier downlink heterogeneous cellular networks. *IEEE Journal on Selected Areas in Communications*, 30(3):550–560, 2012.

[92] Sandra Almeida, José Queijo, and Luis M Correia. Spatial and temporal traffic distribution models for gsm. In *Gateway to 21st Century Communications Village. VTC 1999-Fall. IEEE VTS 50th Vehicular Technology Conference (Cat. No. 99CH36324)*, volume 1, pages 131–135. IEEE, 1999.

[93] Son Nguyen and R Akl. Approximating user distributions in wcdma networks using 2-d gaussian. In *Proceedings of International Conf. on Comput., Commun., and Control Technol*. Citeseer, 2005.

[94] Byungchan Ahn, Hyunsoo Yoon, and Jung Wan Cho. A design of macro-micro cdma cellular overlays in the existing big urban areas. *IEEE journal on selected areas in communications*, 19(10):2094–2104, 2001.

[95] Shuo Wang, Xing Zhang, Jiaxin Zhang, Jian Feng, Wenbo Wang, and Ke Xin. An approach for spatial-temporal traffic modeling in mobile cellular networks. In *2015 27th International Teletraffic Congress*, pages 203–209. IEEE, 2015.

[96] P Kurpas, F Brunner, R Doemer, B Janke, P Heymann, A Maasdorf, W Doser, Ph Auxemery, H Blanck, D Pons, et al. High-voltage gaas power-hbts for base-station amplifiers. In *2001 IEEE MTT-S International Microwave Sympsoium Digest (Cat. No. 01CH37157)*, volume 2, pages 633–636. IEEE, 2001.

[97] Frank Hin-Fai Chau, Barry Jia-Fu Lin, Yan Chen, Mark Kretschmar, Chien-Ping Lee, Nan-lei Larry Wang, Xiaopeng Sun, Wenlong Ma, Sarah Xu, and Peter Hu. Reliability study of ingap/gaas hbt for 28v operation. In *2006 IEEE Compound Semiconductor Integrated Circuit Symposium*, pages 191–194. IEEE, 2006.

[98] J Nicholas Laneman and Gregory W Wornell. Energy-efficient antenna sharing and relaying for wireless networks. In *2000 IEEE Wireless Communications and Networking Conference. Conference Record (Cat. No. 00TH8540)*, volume 1, pages 7–12. IEEE, 2000.

[99] Pramod Viswanath, David N. C. Tse, and Rajiv Laroia. Opportunistic beamforming using dumb antennas. *IEEE transactions on information theory*, 48(6):1277–1294, 2002.

[100] Feng Cao, Li-ping Liu, and Zhi Wang. A new energy-efficient wsn deployment algorithm. *INFORMATION AND CONTROL-SHENYANG-*, 35(2):147, 2006.

[101] Zheng-yi ZHAI and Lun ZHANG. A method of regular hexagonal grid plot in wireless sensor network [j]. *Computer Knowledge and Technology (Academic Exchange)*, 19, 2007.

[102] Sangbum Kim, Daehyoung Hong, and Jaeweon Cho. Hierarchical cell deployment for high speed data cdma systems. In *2002 IEEE Wireless Communications and Networking Conference Record. WCNC 2002 (Cat. No. 02TH8609)*, volume 1, pages 7–10. IEEE, 2002.

[103] Holger Claussen. Co-channel operation of macro-and femtocells in a hierarchical cell structure. *International Journal of Wireless Information Networks*, 15(3-4):137–147, 2008.

[104] Yiqun Wu and Zhisheng Niu. Energy efficient base station deployment in green cellular networks with traffic variations. In *2012 1st IEEE international conference on communications in China (ICCC)*, pages 399–404. IEEE, 2012.

[105] Fengming Cao and Zhong Fan. The tradeoff between energy efficiency and system performance of femtocell deployment. In *2010 7th International Symposium on Wireless Communication Systems*, pages 315–319. IEEE, 2010.

[106] Sung Nok Chiu, Dietrich Stoyan, Wilfrid S Kendall, and Joseph Mecke. *Stochastic geometry and its applications*. John Wiley & Sons, 2013.

[107] Dongxu Cao, Sheng Zhou, and Zhisheng Niu. Optimal combination of base station densities for energy-efficient two-tier heterogeneous cellular networks. *IEEE Transactions on Wireless Communications*, 12(9):4350–4362, 2013.

[108] H. Jo, Y. J. Sang, P. Xia, and J. G. Andrews. Heterogeneous cellular networks with flexible cell association: A comprehensive downlink sinr analysis. *IEEE Transactions on Wireless Communications*, 11(10):3484–3495, 2012.

[109] Tony QS Quek, Wang Chi Cheung, and Marios Kountouris. Energy efficiency analysis of two-tier heterogeneous networks. In *17th European Wireless 2011-Sustainable Wireless Technologies*, pages 1–5. VDE, 2011.

[110] S. Singh, H. S. Dhillon, and J. G. Andrews. Offloading in heterogeneous networks: Modeling, analysis, and design insights. *IEEE Transactions on Wireless Communications*, 12(5):2484–2497, 2013.

[111] L. Xiang, X. Ge, C. Wang, F. Y. Li, and F. Reichert. Energy efficiency evaluation of cellular networks based on spatial distributions of traffic load and power consumption. *IEEE Transactions on Wireless Communications*, 12(3):961–973, 2013.

[112] T. Zhang, J. Zhao, L. An, and D. Liu. Energy efficiency of base station deployment in ultra dense hetnets: A stochastic geometry analysis. *IEEE Wireless Communications Letters*, 5(2):184–187, 2016.

[113] Ying Hou and David I Laurenson. Energy efficiency of high qos heterogeneous wireless communication network. In *2010 IEEE 72nd Vehicular Technology Conference-Fall*, pages 1–5. IEEE, 2010.

[114] Kyuho Son, Eunsung Oh, and Bhaskar Krishnamachari. Energy-aware hierarchical cell configuration: from deployment to operation. In *2011 ieee conference on computer communications workshops (infocom wkshps)*, pages 289–294. IEEE, 2011.

[115] Liang Hu, Istvan Z Kovacs, Preben Mogensen, Ole Klein, and Wolfgang Stormer. Optimal new site deployment algorithm for heterogeneous cellular networks. In *2011 IEEE Vehicular Technology Conference (VTC Fall)*, pages 1–5. IEEE, 2011.

[116] Cemil Can Coskun and Ender Ayanoglu. Energy-efficient base station deployment in heterogeneous networks. *IEEE Wireless Communications Letters*, 3(6):593–596, 2014.

[117] Dongheon Lee, S. Zhou, and Z. Niu. Spatial modeling of scalable spatially-correlated log-normal distributed traffic inhomogeneity and energy-efficient network planning. In *2013 IEEE Wireless Communications and Networking Conference (WCNC)*, pages 1285–1290, 2013.

[118] L. Zhou, X. Hu, C. Zhu, E. C. . Ngai, S. Wang, J. Wei, and V. C. M. Leung. Green small cell planning in smart cities under dynamic traffic demand. In *2015 IEEE Conference on Computer Communications Workshops (INFOCOM WKSHPS)*, pages 618–623, 2015.

[119] Ioannis Kamitsos, Lachlan Andrew, Hongseok Kim, and Mung Chiang. Optimal sleep patterns for serving delay-tolerant jobs. In *Proceedings of the 1st International Conference on Energy-Efficient Computing and Networking*, pages 31–40. ACM, 2010.

[120] Jian Wu, Yanan Bao, Guowang Miao, Sheng Zhou, and Zhisheng Niu. Base-station sleeping control and power matching for energy–delay tradeoffs with bursty traffic. *IEEE Transactions on Vehicular Technology*, 65(5):3657–3675, 2015.

[121] Zhisheng Niu, Xueying Guo, Sheng Zhou, and Panganamala Ramana Kumar. Characterizing energy–delay tradeoff in hyper-cellular networks with base station sleeping control. *IEEE Journal on Selected Areas in Communications*, 33(4):641–650, 2015.

[122] Xueying Guo, Zhisheng Niu, Sheng Zhou, and PR Kumar. Delay-constrained energy-optimal base station sleeping control. *IEEE Journal on Selected Areas in Communications*, 34(5):1073–1085, 2016.

[123] Ziyu Pan and Qi Zhu. Energy efficiency optimization in 3-d small cell networks-based sleep strategy. *IEEE Communications Letters*, 21(5):1131–1134, 2017.

[124] Chang Liu, Balasubramaniam Natarajan, and Hongxing Xia. Small cell base station sleep strategies for energy efficiency. *IEEE Transactions on Vehicular Technology*, 65(3):1652–1661, 2015.

[125] Juwo Yang, Xing Zhang, and Wenbo Wang. Two-stage base station sleeping scheme for green cellular networks. *Journal of Communications and Networks*, 18(4):600–609, 2016.

[126] Ayad Atiyah Abdulkafi, Tiong Sieh Kiong, David Chieng, Alvin Ting, and Johnny Koh. Energy efficiency improvements in heterogeneous network through traffic load balancing and sleep mode mechanisms. *Wireless personal communications*, 75(4):2151–2164, 2014.

[127] Willem Vereecken, Margot Deruyck, Didier Colle, Wout Joseph, Mario Pickavet, Luc Martens, and Piet Demeester. Evaluation of the potential for energy saving in macrocell and femtocell networks using a heuristic introducing sleep modes in base stations. *EURASIP Journal on Wireless Communications and Networking*, 2012(1):170, 2012.

[128] Yiwei Xu and Jin Chen. An optimal load-aware base station sleeping strategy in small cell networks based on marginal utility. In *2017 3rd International Conference on Big Data Computing and Communications (BIGCOM)*, pages 291–296. IEEE, 2017.

[129] Jie Wu, Shi Jin, Lei Jiang, and Gang Wang. Dynamic switching off algorithms for pico base stations in heterogeneous cellular networks. *EURASIP Journal on Wireless Communications and Networking*, 2015(1):117, 2015.

[130] Zhehan Li, David Grace, and Paul Mitchell. Traffic-aware cell management for green ultradense small-cell networks. *IEEE Transactions on Vehicular Technology*, 66(3):2600–2614, 2016.

[131] Alexandra Bousia, Angelos Antonopoulos, Luis Alonso, and Christos Verikoukis. " green" distance-aware base station sleeping algorithm in lte-advanced. In *2012 IEEE International Conference on Communications (ICC)*, pages 1347–1351. IEEE, 2012.

[132] Shijie Cai, Yueling Che, Lingjie Duan, Jing Wang, Shidong Zhou, and Rui Zhang. Green 5g heterogeneous networks through dynamic small-cell operation. *IEEE Journal on Selected Areas in Communications*, 34(5):1103–1115, 2016.

[133] Bei Liu, Ming Zhao, Wuyang Zhou, Jinkang Zhu, and Peng Dong. Flow-level-delay constraint small cell sleeping with macro base station cooperation for energy saving in hetnet. In *2015 IEEE 82nd Vehicular Technology Conference (VTC2015-Fall)*, pages 1–5. IEEE, 2015.

[134] Shan Zhang, Jie Gong, Sheng Zhou, and Zhisheng Niu. How many small cells can be turned off via vertical offloading under a separation architecture? *IEEE Transactions on Wireless Communications*, 14(10):5440–5453, 2015.

[135] Simone Morosi, Pierpaolo Piunti, and Enrico Del Re. Improving cellular network energy efficiency by joint management of sleep mode and transmission power. In *2013 24th Tyrrhenian International Workshop on Digital Communications-Green ICT (TIWDC)*, pages 1–6. IEEE, 2013.

[136] Simone Morosi, Pierpaolo Piunti, and Enrico Del Re. Sleep mode management in cellular networks: a traffic based technique enabling energy saving. *Transactions on Emerging Telecommunications Technologies*, 24(3):331–341, 2013.

[137] Guoxiang Wang, Caili Guo, Shengsen Wang, and Chunyan Feng. A traffic prediction based sleeping mechanism with low complexity in femtocell networks. In *2013 IEEE International Conference on Communications Workshops (ICC)*, pages 560–565. IEEE, 2013.

[138] Louai Saker, Salah-Eddine Elayoubi, Richard Combes, and Tijani Chahed. Optimal control of wake up mechanisms of femtocells in heterogeneous networks. *IEEE Journal on Selected Areas in Communications*, 30(3):664–672, 2012.

[139] Shan Zhang, Jian Wu, Jie Gong, Sheng Zhou, and Zhisheng Niu. Energy-optimal probabilistic base station sleeping under a separation network architecture. In *2014 IEEE Global Communications Conference*, pages 4239–4244. IEEE, 2014.

[140] Zhaoxu Wang and Wenyi Zhang. A separation architecture for achieving energy-efficient cellular networking. *IEEE Transactions on Wireless Communications*, 13(6):3113–3123, 2014.

[141] Sheng Zhou, Jie Gong, Zexi Yang, Zhisheng Niu, and Peng Yang. Green mobile access network with dynamic base station energy saving. In *ACM MobiCom*, pages 10–12, 2009.

[142] Atm Shafiul Alam, Laurence S Dooley, and Adrian S Poulton. Traffic-and-interference aware base station switching for green cellular networks. In *2013 IEEE 18th International Workshop on Computer Aided Modeling and Design of Communication Links and Networks (CAMAD)*, pages 63–67. IEEE, 2013.

[143] Jie Gong, Sheng Zhou, Zhisheng Niu, and Peng Yang. Traffic-aware base station sleeping in dense cellular networks. In *2010 IEEE 18th International Workshop on Quality of Service (IWQoS)*, pages 1–2. IEEE, 2010.

[144] Luca Chiaraviglio, Delia Ciullo, Michela Meo, M Ajmone Marsan, and I Torino. Energy-aware umts access networks, 2008.

[145] Konstantinos Samdanis, Dirk Kutscher, and Marcus Brunner. Self-organized energy efficient cellular networks. In *21st Annual IEEE International Symposium on Personal, Indoor and Mobile Radio Communications*, pages 1665–1670. IEEE, 2010.

[146] Juhee Kim, Wha Sook Jeon, and Dong Geun Jeong. Base-station sleep management in open-access femtocell networks. *IEEE Transactions on Vehicular Technology*, 65(5):3786–3791, 2015.

[147] Chang Liu, Yi Wan, Lin Tian, Yiqing Zhou, and Jinglin Shi. Base station sleeping control with energy-stability tradeoff in centralized radio access networks. In *2015 IEEE Global Communications Conference (GLOBECOM)*, pages 1–6. IEEE, 2015.

[148] Lin Tian, Chang Liu, Yi Wan, Yiqing Zhou, and Jinglin Shi. Energy efficiency analysis of base stations in centralized radio access networks. In *2015 IEEE Global Conference on Signal and Information Processing (GlobalSIP)*, pages 133–136. IEEE, 2015.

[149] Shinobu Namba, Takayuki Warabino, and Shoji Kaneko. Bbu-rrh switching schemes for centralized ran. In *7th International Conference on Communications and Networking in China*, pages 762–766. IEEE, 2012.

[150] Weisi Guo and Timothy O'Farrell. Dynamic cell expansion with self-organizing cooperation. *IEEE Journal on Selected Areas in Communications*, 31(5):851–860, 2013.

[151] Yutao Zhu, Tian Kang, Tiankui Zhang, and Zhimin Zeng. Qos-aware user association based on cell zooming for energy efficiency in cellular networks. In *2013 IEEE 24th International Symposium on Personal, Indoor and Mobile Radio Communications (PIMRC Workshops)*, pages 6–10. IEEE, 2013.

[152] Salah-Eddine Elayoubi, Louai Saker, and Tijani Chahed. Optimal control for base station sleep mode in energy efficient radio access networks. In *2011 Proceedings IEEE INFOCOM*, pages 106–110. IEEE, 2011.

[153] Haluk Celebi, Yavuz Yapıcı, Ismail Güvenç, and Henning Schulzrinne. Load-based on/off scheduling for energy-efficient delay-tolerant 5g networks. *IEEE Transactions on Green Communications and Networking*, 3(4):955–970, 2019.

[154] Efe F Orumwense, Thomas J Afullo, and Viranjay M Srivastava. On increasing the energy efficiency of cognitive radio network base stations. In *2017 IEEE 7th Annual Computing and Communication Workshop and Conference (CCWC)*, pages 1–6. IEEE, 2017.

[155] SH Manjula, E Bindu Reddy, K Shaila, L Nalini, KR Venugopal, and LM Patnaik. Base-station controlled clustering scheme in wireless sensor networks. In *2008 1st IFIP Wireless Days*, pages 1–5. IEEE, 2008.

[156] Donald Michie, David J Spiegelhalter, CC Taylor, et al. Machine learning. *Neural and Statistical Classification*, 13, 1994.

[157] Thomas M Mitchell et al. Machine learning, 1997.

[158] Frank Rosenblatt. The perceptron: a probabilistic model for information storage and organization in the brain. *Psychological review*, 65(6):386, 1958.

[159] Hans P Moravec. *Robot: mere machine to transcendent mind*. Oxford University Press on Demand, 2000.

[160] Daniel Crevier. *AI: the tumultuous history of the search for artificial intelligence*. Basic Books, 1993.

[161] Stuart J Russell and Peter Norvig. *Artificial intelligence: a modern approach*. Malaysia; Pearson Education Limited,, 2016.

[162] John J Hopfield. Neural networks and physical systems with emergent collective computational abilities. *Proceedings of the national academy of sciences*, 79(8):2554–2558, 1982.

[163] David E Rumelhart, Geoffrey E Hinton, and Ronald J Williams. Learning representations by back-propagating errors. *nature*, 323(6088):533–536, 1986.

[164] Rich Caruana and Alexandru Niculescu-Mizil. An empirical comparison of supervised learning algorithms. In *Proceedings of the 23rd international conference on Machine learning*, pages 161–168. ACM, 2006.

[165] David A Freedman. *Statistical models: theory and practice*. cambridge university press, 2009.

[166] Xin Yan and Xiaogang Su. *Linear regression analysis: theory and computing*. World Scientific, 2009.

[167] Strother H Walker and David B Duncan. Estimation of the probability of an event as a function of several independent variables. *Biometrika*, 54(1-2):167–179, 1967.

[168] Brian S Everitt, Sabine Landau, Morven Leese, and Daniel Stahl. Miscellaneous clustering methods. *Cluster analysis*, pages 215–255, 2011.

[169] Vladimir N Vapnik. An overview of statistical learning theory. *IEEE transactions on neural networks*, 10(5):988–999, 1999.

[170] Horace B Barlow. Unsupervised learning. *Neural computation*, 1(3):295–311, 1989.

[171] James MacQueen et al. Some methods for classification and analysis of multivariate observations. In *Proceedings of the fifth Berkeley symposium on mathematical statistics and probability*, volume 1, pages 281–297. Oakland, CA, USA, 1967.

[172] Martin Ester, Hans-Peter Kriegel, Jörg Sander, Xiaowei Xu, et al. A density-based algorithm for discovering clusters in large spatial databases with noise. In *Kdd*, volume 96, pages 226–231, 1996.

[173] P Yves Glorennec. Fuzzy q-learning and dynamical fuzzy q-learning. In *Proceedings of 1994 IEEE 3rd International Fuzzy Systems Conference*, pages 474–479. IEEE, 1994.

[174] Nguyen Cong Luong, Dinh Thai Hoang, Shimin Gong, Dusit Niyato, Ping Wang, Ying-Chang Liang, and Dong In Kim. Applications of deep reinforcement learning in communications and networking: A survey. *IEEE Communications Surveys & Tutorials*, 2019.

[175] Jingchu Liu, Bhaskar Krishnamachari, Sheng Zhou, and Zhisheng Niu. Deepnap: Data-driven base station sleeping operations through deep reinforcement learning. *IEEE Internet of Things Journal*, 5(6):4273–4282, 2018.

[176] YE Junhong and Ying Jun Zhang. Drag: Deep reinforcement learning based base station activation in heterogeneous networks. *IEEE Transactions on Mobile Computing*, 2019.

[177] Sebastian Ruder. An overview of gradient descent optimization algorithms. *arXiv preprint arXiv:1609.04747*, 2016.

[178] Bowei Yang, Weisi Guo, Bozhong Chen, Guangpu Yang, and Jie Zhang. Estimating mobile traffic demand using twitter. *IEEE Wireless Communications Letters*, 5(4):380–383, 2016.

[179] Bozhong Chen, Zitian Zhang, Xiaoli Chu, and Jie Zhang. Data driven optimisation of small cell depolyment. *Electronics Letters*, 56(1):48–50, 2019.

[180] Lingcheng Dai and Hongtao Zhang. Propagation-model-free base station deployment for mobile networks: Integrating machine learning and heuristic methods. *IEEE Access*, 8:83375–83386, 2020.

[181] Xiao Liu, Yuanwei Liu, Yue Chen, and Lajos Hanzo. Trajectory design and power control for multi-uav assisted wireless networks: A machine learning approach. *IEEE Transactions on Vehicular Technology*, 68(8):7957–7969, 2019.

[182] Jin Qiu, Jiangbin Lyu, and Liqun Fu. Placement optimization of aerial base stations with deep reinforcement learning. In *ICC 2020-2020 IEEE International Conference on Communications (ICC)*, pages 1–6. IEEE, 2020.

[183] Rozhina Ghanavi, Elham Kalantari, Maryam Sabbaghian, Halim Yanikomeroglu, and Abbas Yongacoglu. Efficient 3d aerial base station placement considering users mobility by reinforcement learning. In *2018 IEEE Wireless Communications and Networking Conference (WCNC)*, pages 1–6. IEEE, 2018.

[184] Sumudu Samarakoon, Mehdi Bennis, Walid Saad, and Matti Latva-aho. Dynamic clustering and on/off strategies for wireless small cell networks. *IEEE Transactions on Wireless Communications*, 15(3):2164–2178, 2015.

[185] Qiyang Zhao, David Grace, Andrej Vilhar, and Tomaž Javornik. Using k-means clustering with transfer and q learning for spectrum, load and energy optimization in opportunistic mobile broadband networks. In *2015 International Symposium on Wireless Communication Systems (ISWCS)*, pages 116–120. IEEE, 2015.

[186] Guanding Yu, Qimei Chen, and Rui Yin. Dual-threshold sleep mode control scheme for small cells. *IET communications*, 8(11):2008–2016, 2014.

[187] Rongpeng Li, Zhifeng Zhao, Xianfu Chen, and Honggang Zhang. Energy saving through a learning framework in greener cellular radio access networks. In *2012 IEEE Global Communications Conference (GLOBECOM)*, pages 1556–1561. IEEE, 2012.

[188] Xiaoying Gan, Luyang Wang, Xinxin Feng, Jing Liu, Hui Yu, Zhizhong Zhang, and Haitao Liu. Energy efficient switch policy for small cells. *China Communications*, 12(1):78–88, 2015.

[189] Marco Miozzo, Lorenza Giupponi, Michele Rossi, and Paolo Dini. Switch-on/off policies for energy harvesting small cells through distributed q-learning. In *2017 IEEE Wireless Communications and Networking Conference Workshops (WCNCW)*, pages 1–6. IEEE, 2017.

[190] Shaoshuai Fan, Hui Tian, and Cigdem Sengul. Self-optimized heterogeneous networks for energy efficiency. *EURASIP Journal on Wireless Communications and Networking*, 2015(1):21, 2015.

[191] Peng-Yong Kong and Dorin Panaitopol. Reinforcement learning approach to dynamic activation of base station resources in wireless networks. In *2013 IEEE 24th Annual International Symposium on Personal, Indoor, and Mobile Radio Communications (PIMRC)*, pages 3264–3268. IEEE, 2013.

[192] Haewoon Kwak, Changhyun Lee, Hosung Park, and Sue Moon. What is twitter, a social network or a news media? In *Proceedings of the 19th international conference on World wide web*, pages 591–600, 2010.

[193] Purti Beri and Sanjay Ojha. Comparative analysis of big data management for social networking sites. In *2016 3rd International Conference on Computing for Sustainable Global Development (INDIACom)*, pages 1196–1200. IEEE, 2016.

[194] Zhongying Zhao, Zheng Feng, Yong Zhang, Li Ning, Jiancong Fan, and Shengzhong Feng. Collecting, managing and analyzing social networking data effectively. In *2015 12th International Conference on Fuzzy Systems and Knowledge Discovery (FSKD)*, pages 1642–1646. IEEE, 2015.

[195] Weisi Guo and Jie Zhang. Uncovering wireless blackspots using twitter data. *Electronics Letters*, 53(12):814–816, 2017.

[196] Tapan K Sarkar, Zhong Ji, Kyungjung Kim, Abdellatif Medouri, and Magdalena Salazar-Palma. A survey of various propagation models for mobile communication. *IEEE Antennas and propagation Magazine*, 45(3):51–82, 2003.

[197] Zitian Zhang, Yue Wu, Xiaoli Chu, and Jie Zhang. Resource allocation and power control for d2d communications to prolong the overall system survival time of mobile cells. *IEEE Access*, 7:17111–17124, 2019.

[198] Yiwei Xu, Jin Chen, Ducheng Wu, and Wanru Xu. Toward 5g: a novel sleeping strategy for green distributed base stations in small cell networks. In *2016 12th International Conference on Mobile Ad-Hoc and Sensor Networks (MSN)*, pages 115–119. IEEE, 2016.

[199] R Draelos. Best use of train/val/test splits, with tips for medical data. *Glass Box: Artificial Intelligence+ Medicine. https://glassboxmedicine. com/2019/09/15/best-use-of-train-val-test-splits-with-tips-for-medical-data*, 2019.

[200] Yong Sheng Soh, Tony QS Quek, and Marios Kountouris. Dynamic sleep mode strategies in energy efficient cellular networks. In *2013 IEEE International Conference on Communications (ICC)*, pages 3131–3136. IEEE, 2013.

[201] Seonwook Kim, Sunghyun Choi, and Byeong Gi Lee. A joint algorithm for base station operation and user association in heterogeneous networks. *IEEE Communications Letters*, 17(8):1552–1555, 2013.

[202] Ali Yadavar Nikravesh, Samuel A Ajila, Chung-Horng Lung, and Wayne Ding. Mobile network traffic prediction using mlp, mlpwd, and svm. In *2016 IEEE International Congress on Big Data (BigData Congress)*, pages 402–409. IEEE, 2016.

[203] Yuan Gao, Ao Hong, Quan Zhou, Xiangyang Li, Shasha Liu, and Bingjia Shao. Prediction of traffic density and interest using real time mobile traffic data. In *2016 International Conference on Identification, Information and Knowledge in the Internet of Things (IIKI)*, pages 250–254. IEEE, 2016.

[204] Safaa Dawoud, Abdulbaki Uzun, Sebastian Göndör, and Axel Küpper. Optimizing the power consumption of mobile networks based on traffic prediction. In *2014 IEEE 38th Annual Computer Software and Applications Conference*, pages 279–288. IEEE, 2014.

[205] Kyunghan Lee, Seongik Hong, Seong Joon Kim, Injong Rhee, and Song Chong. Slaw: A new mobility model for human walks. In *IEEE INFOCOM 2009*, pages 855–863. IEEE, 2009.

[206] Minkyong Kim, David Kotz, and Songkuk Kim. Extracting a mobility model from real user traces. 2006.

[207] Kittisak Kerdprasop, Nittaya Kerdprasop, and Pairote Sattayatham. Weighted k-means for density-biased clustering. In *International Conference on Data Warehousing and Knowledge Discovery*, pages 488–497. Springer, 2005.

[208] Derya Birant and Alp Kut. St-dbscan: An algorithm for clustering spatial–temporal data. *Data & knowledge engineering*, 60(1):208–221, 2007.

[209] Flood Sung, Yongxin Yang, Li Zhang, Tao Xiang, Philip HS Torr, and Timothy M Hospedales. Learning to compare: Relation network for few-shot learning. In *Proceedings of the IEEE Conference on Computer Vision and Pattern Recognition*, pages 1199–1208, 2018.

[210] Syawal Gultom, S Sriadhi, M Martiano, and Janner Simarmata. Comparison analysis of k-means and k-medoid with ecluidience distance algorithm, chanberra distance, and chebyshev distance for big data clustering. In *IOP Conf. Ser., Mater. Sci. Eng.*, volume 420, 2018.

[211] Hieu V Nguyen and Li Bai. Cosine similarity metric learning for face verification. In *Asian conference on computer vision*, pages 709–720. Springer, 2010.

[212] Jacob Benesty, Jingdong Chen, Yiteng Huang, and Israel Cohen. Pearson correlation coefficient. In *Noise reduction in speech processing*, pages 1–4. Springer, 2009.

[213] Joram Walfisch and Henry L Bertoni. A theoretical model of uhf propagation in urban environments. *IEEE Transactions on antennas and propagation*, 36(12):1788–1796, 1988.

[214] Fumio Ikegami, Susumu Yoshida, Tsutomu Takeuchi, and Masahiro Umehira. Propagation factors controlling mean field strength on urban streets. *IEEE Transactions on Antennas and Propagation*, 32(8):822–829, 1984.

[215] Karl Low. Comparison of urban propagation models with cw-measurements. In *[1992 Proceedings] Vehicular Technology Society 42nd VTS Conference-Frontiers of Technology*, pages 936–942. IEEE, 1992.

[216] Syed A Ahson and Mohammad Ilyas. *WiMAX: standards and security*. CRC press, 2007.